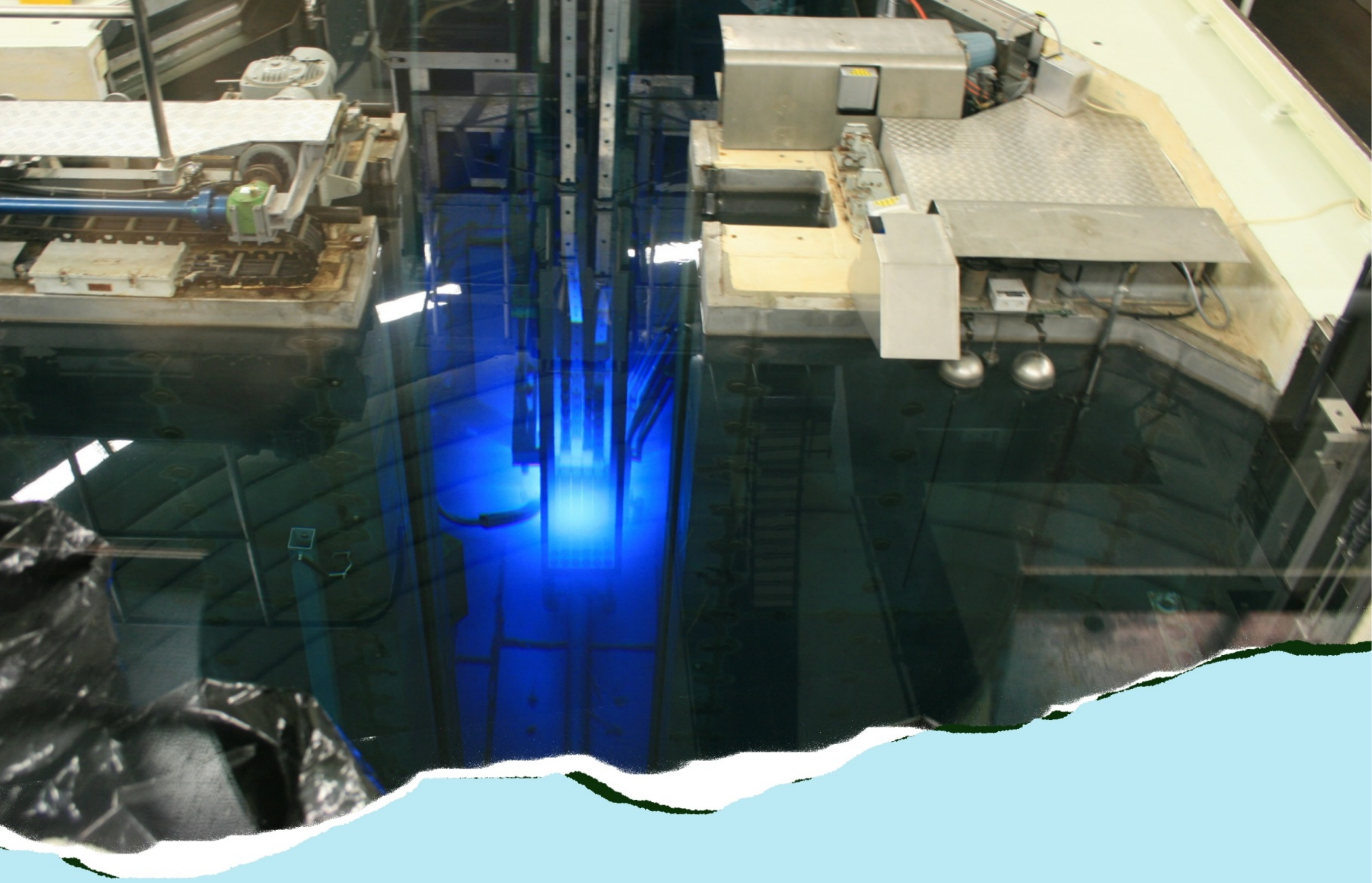

Proceedings of the 2nd Petrus-OPERA PhD and Early Stage Researcher Conference 2016

P.J. Vardon, D. Bykov (eds.)

Title: Proceedings of the 2nd Petrus-OPERA PhD and
early stage researcher conference 2016
Date: 27th June 2016
Editors: P.J. Vardon, D. Bykov
Publisher: Delft University of Technology
ISBN/EAN: 978-94-6186-669-1

Photo credits:
Front top: Delft Research Reactor, RID, TU Delft; Front bottom: HADES underground laboratory at SCK•CEN, P Vardon; Back: TU Delft campus, TU Delft.

Preface

This school and conference come from two different directions, a European project to develop methods of education in radioactive waste disposal (the PETRUS project) and the Dutch national research programme into radioactive waste disposal (OPERA). Both of us work in both education and research at TU Delft and in the OPERA project, therefore it was a good opportunity to host such a conference and school here in Delft.

We intend this conference, not to be a formal ‘show and tell’ of research, but to try to make a dynamic event, with aspects of schools, conferences, field trips and most importantly plenty of time and opportunity for discussion and networking. We hope that we have instigated an informal atmosphere for you to discuss work with experts in the field and for the experts to meet the next generation.

This event could not occur without a large amount of time, effort and enthusiasm being donated by the lecturers, programme committee and a large amount of time, effort and enthusiasm being spent by the participants. Moreover, this event could not be free to attend without support of the funders: the EU, COVRA, TU Delft and the lecturers companies.

We hope you enjoy the conference!

P.J. Vardon & D. Bykov (eds.)

Contents

Programme committee

Philip J. Vardon	Delft University of Technology
Denis M. Bykov	Delft University of Technology
Erika A.C Neeft	COVRA
Ewoud V. Verhoef	COVRA
Behrooz Bazargan-Sabet	Ecole des Mines de Nancy / Université de Lorraine

Projects and funders

This school and conference is grateful for the projects and partners via which it has been organised and the funders which have enabled the project to happen. Special thanks to:

- The European Commission via the PETRUS III project.
- COVRA and the OPERA research programme which they manage.
- Delft University of Technology for provision of facilities.
- SCK•CEN, COVRA and TU Delft for access to facilities for the field trips.

Funders:

Partners (PETRUS III project):

Programme

Locations

Registration, coffee breaks, drinks and snacks: Ground floor hall, Culture Centre TU Delft

Lectures and presentations: Theaterzaal, Culture Centre TU Delft

Poster session Day 3: Balletzaal (including extended lunch), Culture Centre TU Delft

Day 1 ***Introduction*** *Chair: D. Bykov*	0900 – 0930	------------Registration and coffee------------
	0930 – 0945	• Welcome • *Representative from OPERA/PETRUS/organising committee*
	0945 – 1030	• Origin of radioactive waste, classification, solutions. *Lecturer: Denis Bykov, TU Delft*
	1030 – 1115	• Principles of radioactive waste disposal *Lecturer: Monika Skrzeczkowska, IAEA*
	1115 – 1130	------------Coffee------------
	1130 – 1215	• Waste management, storage and disposal programme *Lecturer: Ewoud Verhoef, COVRA*
	1215 – 1300	• How to develop a source term for disposal of waste (waste families, inventory) *Lecturer: Erika Neeft, COVRA*
	1300 – 1400	------------Lunch------------
	1400 – 1630	***PhD/early stage researcher presentations (20mins each including questions)*** • **Thermal Treatment of UK Magnox Sludge:** Sean Barlow • **Dismantling of the graphite pile of Latina NPP: characterization and handling/removal equipment for single brick or multi-bricks**: Giuseppe Canzone • **Good practices in free release of materials:** Evelina Ionescu ------------Coffee------------ • **Radiological characterization of radioactive waste produced in particle accelerators:** Biagio Zaffora • **Multi-scale investigation of fracture apertures in clay rock subjected to desiccation:** Anne-Laure Fauchille • **Thermo-hydro-mechanical behaviour of compacted MX80 bentonite at 150°C:** Panagiotis Stratos
	1630 - 1800	------------Welcome drinks and snacks------------

Day 2 ***Field trip***	**<u>0630 start</u>** (Buses leave at 0645 sharp. We cannot wait for people who are late!)	• Storage facilities at COVRA (Central Organisation for Radioactive Waste) in Vlissingen, the Netherlands • The underground research laboratory HADES at SCK•CEN in Mol, Belgium **Travel by bus. Groups will be announced on the first day at registration. Due to pre-registration please ensure that you travel with the correct group.**

Day 3 ***Short-term behaviour*** *Chair: P. Vardon*	0815 – 0900	• Underground disposal: design, construction and mechanical behaviour *Lecturer: Phil Vardon, TU Delft*
	0900 – 0945	• Cementitious materials for repositories *Lecturer: Rob Wiegers, IBR Consult BV*
	0945 – 1000	------------Coffee------------
	1000 – 1045	• Microbes, barrier functions and nuclear safety cases *Lecturer: Karsten Pedersen, Microbial Analytics Sweden AB*
	1045 – 1130	• Why does heat matter in radioactive waste disposal? *Lecturer: Alex Bond, Quintessa and DECOVALEX*
	1130 – 1430	------------Extended lunch and poster session------------ 2 minute poster pitches starting at 1145
	1430 – 1630	• Visits to the Delft nuclear reactor **Groups and exact timings to be announced on the first day at registration. Due to pre-registration please ensure that you travel with the correct group.** **Due to technical reasons, these trips may be altered or cancelled at any time.**
	1930 – 2200	------------ Networking Dinner ------------ Location: Prinsenkelder, Delft

List of posters

1. **Radionuclide transport model of the near field and far field of geological repository**
   D. Barátová, V. Nečas
2. **Complexation and Adsorption of [^{152}Eu]Eu to Superplasticizers and Bentonite at Variable Salt Concentrations**
   M. Becker, H. Lippold
3. **Sorption properties of granitic rock from potential deep geological repository site in Czech Republic**
   V. Brynych, K. Kolomá, V. Havlová
4. **Coupled Thermo–Hydro–Mechanical Processes for the Dutch Radioactive Waste Repository**
   P.Buragohain, P.J. Vardon, M.A. Hicks
5. **Effect of open-gaps in nuclear spent fuel disposal containers storage**
   I.P. Damians, S. Olivella, X. Pintado
6. **Final disposal of SNF - solutions and trends**
   A.M. Dima
7. **Relationships between cracking, strains and proportions of clay matrix and rigid inclusions in Tournemire clay rock**
   A.-L. Fauchille, S. Hedan, V. Valle, D. Pret, J. Cabrera, P. Cosenza
8. **Intrinsic dissolution rate determination of vitrified high level waste**
   A.J. Fisher, C.L. Corkhill, R.J. Hand & N.C. Hyatt
9. **Numerical study of bentonite confined hydration**
   G.M. Ghiadistri
10. **Application of BIB–SEM technology to characterize microstructure and pores in mudstone at a range of scales**
    J. Klaver, J. Schmatz, G. Desbois, S. Hemes, J.L. Urai
11. **Experimental and digital characterisations of the hydro-mechanical behaviour of a heterogeneous powder/pellet bentonite material**
    A. Molinero Guerra, N. Mokni, Y.-J. Cui, A. M. Tang, P. Delage, P. Aimedieu, F. Bernier, M. Bornert
12. **Water transport across concrete studied by means of Neutron Imaging**
    A. Sabău, Y. Yigittop, D. Bykov, J. Plomp, L. van Eijck, J.L. Kloosterman
13. **Long term evaluation on the groundwater chemistry due to cement materials with numerical simulation**
    D. Sampietro, E. Abarca, M. Bayer, S. Jordana, J. Molinero, T. Tanaka, S. Hashimoto, T. Iwatsuki, H. Onoe
14. **Characterization of microbial communities in raw and homogenized bentonite samples**
    R. Shrestha, J. Steinová, L. Falteisek, D. Vlková, A. Ševců
15. **Experimental study of mechanical behaviour of compacted Czech Bentonite 75**
    H. Sun, D. Mašín, J. Boháč
16. **Sorption of Uranium on Polyamide and Graphen Oxide Composite Material**
    Z. Tomášová, V. Brynych, J. Pospěchová, P. Ecorchard, J. Tolasz
17. **Damage model contribution on shape and extension of failure zone in quasi-brittle rocks**
    A. Pouya, E. Trivellato, M. Ngoc Vu
18. **Radiological characterization of graphite from thermal column of VVR-S research reactor in view of intermediary storage**
    V. Fugaru, C. Postolache, C. Tuca, M. Dragusin, E. Ionescu and R. Deju
19. **Radiological characterization of radioactive waste produced in particle accelerators**
    B. Zaffora, M. Magistris

Day 4 ***Long-term behaviour*** *Chair: D. Bykov*	0900 – 0945	• The hydro-geological setting – present state and predictions of the future *Lecturer: Johan H. ten Veen, TNO – Geological Survey of the Netherlands*
	0945 – 1030	• Waste packaging and degradation *Lecturer: Guido Deissmann, Brenk Systemplanung GmbH*
	1030 – 1100	------------Coffee------------
	1100 – 1145	• Speciation of actinides during migration in argillaceous rocks *Lecturer: Tobias Reich, Johannes Gutenberg-Universität*
	1145 – 1230	• Radionuclide transport and retardation *Lecturer: Hans Meeussen, NRG*
	1230 – 1400	------------Lunch------------
	1400 – 1630	***PhD/early stage researcher presentations (20mins each including questions)*** • **Numerical study of bentonite confined hydration:** Giulia Ghiadistri • **Modelling the excavation damaged zone using a hydro-mechanical double-scale model:** Bram van den Eijnden • **Probabilistic performance assessment of a deep tunnel for a radioactive waste repository in French COx claystone:** Yajun Li ------------Coffee------------ • **Time-dependent mechanical and transport behaviors of Callovo-Oxfordian argillite:** Zaobao Liu • **Transient boundary conditions in the frame of high level radioactive waste disposal at deep geological repository:** Abhishek Rawat • **Application of BIB–SEM technology to characterize microstructure and pores in mudstone at a range of scales:** Jop Klaver • **Proposed method for semantic mapping of communities of practice in the nuclear industry for alignment of education:** Vincent Kuo

Day 5 ***Safety*** *Chair: P. Vardon*	0900 – 0945	• Natural Analogues *Lecturer: Ulrich Noseck, GRS*
	0945 – 1030	• Radioactive Waste Management and Geological Disposal: a long term socio-technical challenge *Lecturer: Anne Bergmans, University of Antwerp*
	1030 – 1045	------------Coffee------------
	1045 – 1130	• Role and purpose of the Safety Case *Lecturer: Lucy Bailey, RWM*
	1130 – 1215	• Modelling to underpin the Safety Case *Lecturer: Sarah Watson, Quintessa*
	1215 – 1300	• Confidence building in the presence of uncertainties *Lecturer: Klaus-Jurgen Rohlig, TU Claustal*
	1300 – 1330	• Prizes for best poster / presentation • Wrap-up discussion
	1330 – 1430	------------Lunch------------
	1430	------------ End of the event ------------

Lecturers

Lucy Bailey

Acting Head of Disposal System Assessment, RWM

Chair of the OECD-NEA Integration Group for the Safety Case (IGSC)

"I am currently Acting Head of Disposal System Assessment at RWM, the implementing body for geological disposal in the UK. I am responsible for developing the safety cases to support the implementation of a geological disposal facility for higher activity radioactive waste in the UK. I have more than 20 years' experience in the safety assessment of radioactive wastes, particularly specialising in the development of sound approaches to performance assessment and safety case development that aid communication. I have a long-standing involvement with the OECD-Nuclear Energy Agency (NEA) and am currently the Chair of the NEA's Integration Group for the Safety Case. I have also worked on a number of EC projects and am co-chairing an IAEA safety case project. I have been an expert reviewer of a number of international safety cases and have many publications in the safety case field, including the Overview report and Environmental Safety Case for the UK's Generic Disposal System Safety Case."

Anne Bergmans

Lecturer Faculties of Law and Social Sciences, University of Antwerp

Anne Bergmans is lecturer and senior researcher at the University of Antwerp's Faculties of Law and of Social Sciences. She holds a PhD in Sociology (UAntwerpen, May 2005). Her research interests are situated in the field of science and technology governance, environmental sociology and sociology of safety and risk, with an empirical focus on questions related to the long-term governance of radioactive waste.

Alex Bond

Principal Consultant, Quintessa Ltd, UK

Areas of work: Coupled Numerical Analysis and Radioactive Waste Safety Assessment.

Alex has an academic background covering physical natural sciences, hydrogeology and numerical analysis, and is professionally qualified as both a Chartered Scientist and Geologist. Through his wide-ranging consultancy work, Alex has gained considerable practical experience of modelling at all scales of interest required for understanding environmental systems, ranging from highly detailed coupled analysis to whole-system safety analysis techniques. Currently, Alex specialises in coupled numerical analysis of thermal-hydraulic mechanical systems primarily focussed on radioactive waste management, the geological storage of carbon dioxide and support to nuclear reactor safety cases. Complemented by his role as Technical Coordinator for the international research project DECOVALEX-2019, Alex has a keen insight into the state of the art of radioactive waste disposal in particular, and complex geological systems in general.

Denis Bykov

Postdoctoral Researcher, Delft University of Technology, Department of Radiation Science and Technology, Section Nuclear Energy and Radiation Applications (NERA)

Area of work: Radioactive waste immobilization and disposal.

Dr. Denis Bykov holds a PhD degree in inorganic chemistry from the State University of Nizhny Novgorod, Russia. His research interests include retention and transport properties of radionuclides in geological media and engineered barrier materials, as well as materials aspects of chemical forms for radioactive waste solidification.. He is responsible for the education on geological disposal at the RST department of TU Delft and teaches courses "Chemistry of the Nuclear Fuel Cycle" and "Chemistry and Physics of Actinides". He is supervising a number of student research projects on the nuclear waste disposal, both on bachelor and master levels.

Guido Deissmann

Senior Scientist, Forschungszentrum Jülich GmbH, Institute of Energy and Climate Research: Nuclear Waste Management and Reactor Safety (IEK-6)

Area of work: Geological disposal of nuclear wastes

PhD in Geochemistry from RWTH Aachen University, Germany. More than 20 years professional experience with issues related to radioactive waste disposal (LLW/ILW/HLW) such as the assessment of waste form durability and engineered barrier systems, evaluation and modelling of key processes governing radionuclide migration in the near and far field, and the development and evaluation of safety cases and performance assessments for geological disposal facilities. Further expertise comprises the assessment of problems related to NORM/TENORM in the mining industry, and the evaluation and modelling of acid mine drainage and radionuclide/contaminant mobilisation and migration at uranium mining and milling sites. After 17 years of scientific consulting work with Brenk Systemplanung, Aachen, Germany, he joined Forschungszentrum Jülich as Senior Scientist in 2013.

Hans Meeussen

Senior Researcher/Consultant, NRG Petten

Areas of work: Reactive transport processes in the context of geological waste disposal.

Hans Meeussen holds a PhD in soil chemistry, from Wageningen University. His main research interest are reactive transport processes, which is the exciting interdisciplinary area that is dominated by interaction between chemical, physical and biological processes. Reactive transport processes determine long term migration rates of radionuclides through clay and concrete, but also migration of nutrients from soil to plant roots. He is author of the ORCHESTRA modelling framework, a software tool that makes it possible to combine process models from different disciplines into combined simulation models. He has (co)authored more than 50 papers in this area.

Erika Neeft

Researcher, COVRA

Areas of work: geological disposal of radioactive waste.

Dr. Neeft is the technical coordinator of the Dutch research programme into geological disposal of radioactive waste at the waste management organisation COVRA. She holds a MSc degree in Earth Sciences from Utrecht University and a PhD in reactor physics (transmutation of nuclear waste) from Delft University of Technology.

Ulrich Noseck

Senior Scientist, Final Repository Safety Research Division, Gesellschaft für Anlagen- und Reaktorsicherheit (GRS) mbH

Professional experience for more than 20 years in development of methods for the safety case, safety assessments of repositories for radioactive wastes, groundwater and contaminant transport modelling and natural analogue studies. Project leader in many national and international projects.

Member of the NEA working group IGSC (Integrated Group for the Safety Case) and the German expert group on high level waste (Arbeitskreis HAW-Produkte).

Guest lecturer at University of Braunschweig on Waste Disposal in Deep Geological Formations

Karsten Pedersen

Senior Principle Scientist, Microbial Analytics Sweden AB

Areas of work: Microbiology in radioactive waste disposal

Karsten Pedersen obtained his PhD degree 1982 at Department of Microbiology, University of Gothenburg, Sweden with a thesis on microbial biofilms in seawater. His present affiliation is senior principal scientist at Microbial Analytics Sweden AB, www.micans.se. Pedersen has 30 years of experience of research and education regarding microbiology in radioactive waste disposal. He has presently published more than 100 papers, reviews and book chapters in peer-reviewed international scientific press and he has written many reports for national and international nuclear waste disposal organizations.

Tobias Reich

Managing Director of the Institute of Nuclear Chemistry, Professor for Nuclear Chemistry, Johannes Gutenberg University Mainz

Areas of work: Nuclear Chemistry, Actinide Chemistry, Spectroscopy, Analytics

Tobias Reich is the Managing Director of the Institute of Nuclear Chemistry at the University of Mainz. He holds a diploma from the University of Leipzig and carried out his doctoral research in the Russian Academy of Sciences in Moscow. Following this is was a postdoctoral fellow at the Lawrence Berkeley Laboratory moving then to the Research Center Rossendorf. Since 2002 he's been a professor at the University of Mainz and since 2009 has been the Managing Director of the Institute of Nuclear Chemistry. He serves on several scientific committees, was a member of the review committee for the Diamond Light Source facility and a member of the scientific advisory board of the European Network of Excellence ACTINET-I3 and TALISMAN.

Klaus-Jürgen Röhlig

University Professor, Institute of Disposal Research, Clausthal University of Technology

Areas of work: Long-term safety assessment, socio-technical issues

Klaus-Jürgen Röhlig holds a diploma (1985) and a PhD (1989) in Mathematics from TU Bergakademie Freiberg. From 1991 to 2007, he was employed by Gesellschaft für Anlagen- und Reaktorsicherheit (GRS) gGmbH. His work included research and technical advice to the German Federal Ministry for Environment, Nature Conservation and Nuclear Safety (BMU) in fields such as safety assessment and safety criteria for radioactive waste repositories, policy, regulatory and licensing issues. Since 2007, he is Professor for Repository Systems at the Institute of Disposal Research, Clausthal University of Technology. He performs research on safety case methodology, analytical assessment of repository systems as well as on socio-technical issues and lectures on radioactive waste management and safety assessment.

From 2010 to 2015, he served as Chair of the Integration Group for the Safety Case (IGSC) at OECD/NEA. He is a member of several advisory bodies, including the Radioactive Waste Management Commission (ESK), an advisory body to BMU (2008-2010 deputy chair and chair of its Committee on Final Disposal). He participated in international peer reviews of safety reports produced in France, Sweden, and in the UK.

Monika Skrzeczkowska

International Atomic Energy Agency (IAEA)

Monika Skrzeczkowska – geologist, MSc in geochemistry, mineralogy & petrology, focusing on drivers for long-term radionuclide dispersion in post-accident conditions (Chornobyl). Worked in National Atomic Energy Agency, (Polish nuclear regulatory authority), where among others, was involved in updates of legislative framework (focus on siting of nuclear facilities and radioactive waste disposal). Before joining IAEA worked at the Polish Geological Institute – geological survey of Poland, with focus on radioactive waste disposal (projects related to the existing surface repository, site selection & characterization for a new surface radioactive waste repository, desk studies for geological disposal). Member of team designated for preparation of National Radioactive Waste and Spent Nuclear Fuel Management Plan by the Minister of Economy (focus on geological disposal). Participated in a number of EIAs and strategic EIAs, including the Polish Nuclear Power Programme, as well as facilities or programs of European countries.

Philip Vardon

Assistant Professor, Delft University of Technology

Areas of work: Coupled numerical modelling, Thermo-Hydro-Mechanical processes.

"I am an Assistant Professor in Geo-Engineering at Delft University of Technology. My main interest is in the development of numerical models for coupled processes occurring in soils and rocks. This is when one process occurring affects another occurring at the same time.

Over the past 10 years I've applied this techniques to radioactive waste disposal, ground source heat, mine wastes and slopes. In the past few years I've been working on OPERA, the Dutch national research programme for radioactive waste disposal, on the technical feasibility of the proposed repository.

In education, I teach 'Numerical Modelling' and 'Soil Mechanics' and internationally I'm involved in the PETRUS European consortium which examines ways to provide education for radioactive waste disposal at a European level. This course is part of both the OPERA programme and the PETRUS consortium's work."

Johan H. ten Veen

Senior Geologist, TNO – Geological Survey of the Netherlands

Johan is senior research geoscientist at TNO-GSN where he works as a structural geologist on the construction and refinement of geomodels that reveal the structure and properties of the Dutch subsurface. In the role of principal investigator, he has initiated and supervised several research projects centred around characterization of un-, non- and conventional reservoirs and regional basin studies (NW Europe focus). Next to applied research he coaches junior staff, interns and master students and teaches (petroleum) geological university courses.

Ewoud Verhoef

Deputy Director, COVRA

Areas of work: management of radioactive waste management.

Dr. Ir. Ewoud Verhoef (1973) is deputy director of COVRA, the central organisation for radioactive waste in the Netherlands. COVRA collects, treats and stores all radioactive waste in the Netherlands for a period of at least 100 years.

Ewoud leads the Dutch national programme on geological disposal, is the acting chair of the ERDO working group on developing multinational waste management organisation in Europe, and is a member of the executive group of the European technology platform on the disposal of radioactive waste (IGD-TP). He is member of the board of Royal Netherlands Society of Engineers, section Nuclear technology, and the Netherlands Nuclear Society.

Ewoud studied chemical technology at Delft University of Technology, where he also received his PhD on research on the influence of policy and legislation on waste management processes in general and metal recycling in metallurgical processes in particular.

Sarah Watson

Principal Consultant, Quintessa Limited

Areas of work: Development of safety cases for the disposal of radioactive waste

Sarah is an experienced geoscientist who has, since the mid-1990s, worked on numerous safety assessments / performance assessments, mostly in the radioactive waste management sector. She specialises in integrating information from different technical areas (e.g. site characterisation, waste packaging, wasteform behaviour, performance of engineered barriers, biosphere) to develop safety arguments and explore the 'couplings' between different technical areas to build evidence based safety arguments that are broad-based and explore their potential long-term performance of disposal systems.

Rob Wiegers

Managing Director, IBR Consult

Areas of work: Material sciences with an emphasis on building materials and radioactive aspects of materials

Rob Wiegers studied at the TUE for building material engineer and worked for both institutes and industry, Since 1992 he is partner in IBR Consult bv which is specialized in building product development. Furthermore, Rob Wiegers is active in the field of the nuclear aspects of materials especially NORM materials and is involved in several national and international gremia on this subject as well as research projects amongst which the OPERA research project.

Abstracts

Abstracts are listed alphabetically by the presenting author's surname (underlined).

Radionuclide transport model of the near field and far field of geological repository

D. Barátová, V. Nečas

Slovak University of Technology in Bratislava,
Institute of Nuclear and Physical Engineering, Bratislava, Slovakia

Abstract

The results on the analysis of radionuclide release from the geosphere of hypothetical repository in crystalline rocks are presented. Radionuclides with poor retentive properties (C-14, I-129, Cl-36, Cs-135), represent the largest contribution to the total release rate from the geosphere. The release rates of radionuclides with low solubility limits can be significantly reduced. The presence of stable isotopes of the same element has the effect of reducing the solubility of safety relevant radionuclides. The calculations of release rates were carried out for one disposal container using the simulation software GoldSim.

Introduction

In Slovakia, a preferred alternative of long-term spent fuel management is a direct disposal of spent nuclear fuel which will be disposed together with radioactive waste which is not suitable for the National Radioactive Waste Repository in Mochovce (near-surface repository).

Within the deep geological repository development program in the Slovak Republic between years 1996 and 2001 were in a gradual site selection process selected five reconnaissance localities in the environment of crystalline and sedimentary rocks. Since 2010, company JAVYS, a.s. has become the implementer of deep geological disposal in the Slovak Republic and the deep geological repository program was renewed [1].

Disposal system

Spent fuel (from VVER-440 reactors) is considered to be disposed in containers made of stainless steel (inner part) and carbon steel (outer part). The disposal capacity of one container is 7 fuel assemblies [2].

Within this assessment the calculations were performed for the spent fuel with an initial average enrichment of 4.87 % of U-235 and burnup 60 MWd/kgU .The analysis was carried out for one disposal container (7 fuel assemblies). The storage time before the final disposal is 60 years. Disposal container is surrounded by a bentonite buffer with a wall thickness of 300 mm.

In Slovakia, there has not been selected a final locality for the geological disposal facility. Due to this fact, the assessment of long-term safety was performed for a hypothetical geological repository located in crystalline rocks and by using also the international research achievements (Czech Republic, Switzerland, Sweden, Japan). Transport pathways are in crystalline rocks represented by individual fractures.

Conceptual model

Spent fuel is a complex and heterogeneous system and therefore was within the model conceptually divided into the structural material, UO_2 matrix and instant release fraction. Instant release fraction is a fraction of inventory which is after water contact released rapidly, in the term of long-term safety instantaneously. Then the long-term release occurs congruently with the degradation of the fuel matrix and structural material.

After the disposal canister fails due to normal evolution processes (1000 years) and water comes into contact with the source term (fuel and structural material), released radionuclides start to migrate through the bentonite buffer, excavation disturbed zone (EDZ) and crystalline host rock. Concentrations of radionuclides in the void volume of the disposal container and in the bentonite buffer are limited by the solubility of each chemical element. The solubility limit is partitioned between stable and radioactive isotopes of the elements. Since it is considered that the buffer is fully water-saturated, nuclides migrate through the bentonite buffer by radial diffusion and are retarded by sorption on the buffer material.

Host rock is modelled like a fractured zone where each transport pathway has a different transmissivity. The variability in transmissivity of individual transport pathways is represented by using a log-normal distribution [3], [4]. The transport pathways have a length of 100 m and flow into the major water-conducting fault whose length is 300 m. In the individual fractures of the host rock as well as in the major-conducting fault, the one-dimensional advection, longitudinal dispersion, radioactive decay and ingrowth, diffusion of the nuclides into the adjacent rock and instantaneous and reversible sorption on mineral surfaces of the host rock are assumed in the conceptual model. The matrix diffusion takes place only in the direction perpendicular to the groundwater flow. No infill medium and no solubility limitation are considered in the individual transport pathways.

Results

The release rates from the major water-conducting fault for one disposal container containing 7 spent fuel assemblies were calculated and are illustrated in Figure 1. Modelling was carried out using the simulation software GoldSim which RT (Radionuclide Transport) module allows users to dynamically model mass transport within a complex system of engineering and natural barriers [5].

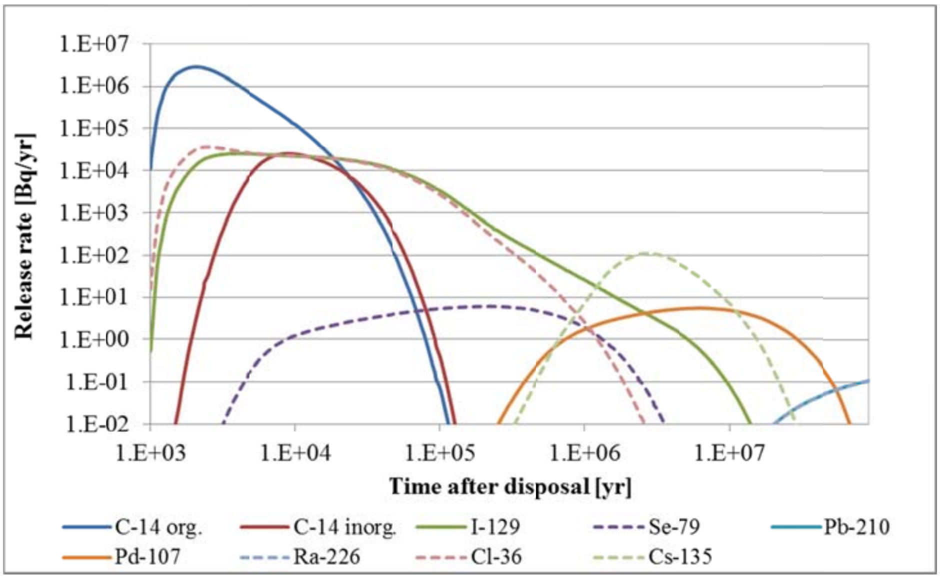

Figure 1: Release rates from the major water-conducting fault to the aquifer.

Transport of nuclides through the host rock and the major water-conducting fault considerably reduces the release rates of many nuclides. Actinides are relatively strongly sorbed on the bentonite as well as on the host rock matrix and therefore their release rates are very low. Based on the results it can be seen that activation and fission products like C-14, Cl-36, I-129, Se-79 and Cs-135 represent the largest contribution to the total release rate from the geosphere. Cl-36 and I-129 are assumed to have very poor retentive properties (high solubility limits and low distribution coefficients) and that is why these nuclides dominate the total release rate for a long period of time. Inventory of C-14 was divided between the structural material and UO_2 matrix. It was assumed that C-14 originated from the structural material is in an organic form and C-14 originated from UO_2 matrix is a part of inorganic compounds [6]. For C-14 organic, no solubility limitation and sorption is considered in the model (in the near field as well as in the far field) and its specific activity is relatively high in comparison with long-lived radionuclides. Because of that the release rate of this nuclide is the most significant in the early years of the analysis. It can be seen that the release rates are strongly dependent on the retentive properties of individual nuclides.

Nuclides precipitate when the concentration of released nuclides in the porewater exceeds their solubility limits. The elements which precipitate in the void volume of the disposal container are U, Pu, Np, Ra, Zr, Se, Tc, Pd and Sn. Elements as U and Ra precipitate also in the bentonite buffer. The effect of solubility limitation is showed in Figure 2. When the solubility limit is assumed in the calculations, the release rate of Ra-226 from the near field is significantly reduced.

The presence of radioactive or stable isotopes of the same element has the effect of reducing the solubility of safety relevant radionuclides. This is also illustated in Figure 2 when the isotopes (stable and Se-82) of Se-79 are and are not assumed in the model.

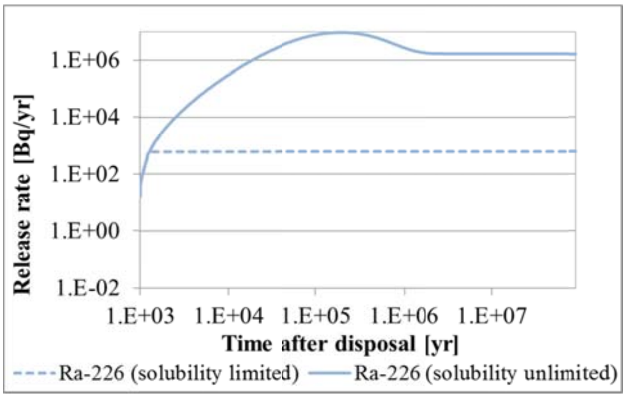

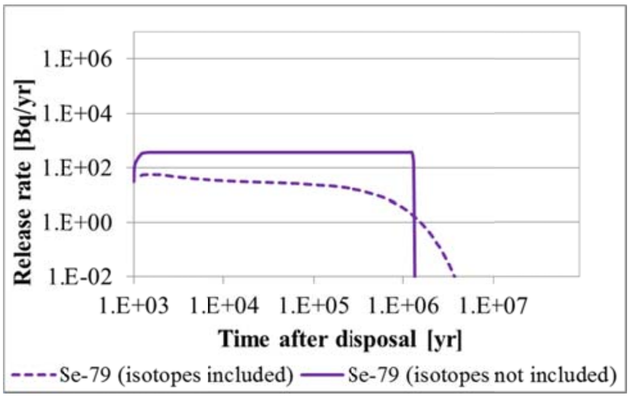

Figure 2: On the left - the effect of solubility limitation on the release rate of Ra-226 from the near field; on the right - the effect of sharing solubility between isotopes on the release rate of Se-79 from the near field.

Conclusion

The near field and far field model of hypothetical geological repository was developed. The results showed that many of nuclides are effectively sorbed on the bentonite buffer and host rock matrix. Based on the results it can be concluded that activation and fission products like C-14, Cl-36, I-129, Se-79 and Cs-135 represent the largest contribution to the total release rate from the geosphere. Cl-36 and I-129 are assumed to have high solubility limits and low distribution coefficients and that is why these nuclides dominate the total release rate for a long period of time. Nuclides precipitate when the concentration of released nuclides in the porewater exceeds their elemental solubility limits. The release rates of radionuclides which concentration is controlled by solubility are reduced in relation to their inventories and half-lives. The presence of isotopes of the same element has the effect of reducing the solubility of nuclides.

Acknowledgments

This project has been supported by the Slovak Grant Agency for Science through grant VEGA 1/0796/13.

References

[1] National Nuclear Fund for Decommissioning of the Nuclear Installations and for Handling of Spent Fuel and Radioactive Waste: The Strategy for the Final Stage of Peaceful Utilization of the Nuclear Energy in SR. January 2014.

[2] Radioactive Waste Repository Authority (RAWRA). Updated Reference Project of Geological Repository in a Hypothetical Locality. Czech Republic: RAWRA, 2012.

[3] Japan Nuclear Cycle Development Institute. H12: Project to Establish the Scientific and Technical Basis for HLW Disposal in Japan. Japan: JNC, April 2000.

[4] Japan Atomic Energy Agency (JAEA). Preliminary Assessment of Geological Disposal System for Spent Fuel in Japan: First Progress Report on Direct Disposal. Japan: JAEA, December 2015.

[5] GOLDSIM Technology Group LLC. GoldSim Contaminant Transport Module, User`s Guide. Washington, USA, 2014.

Thermal Treatment of UK Magnox Sludge

Sean T. Barlow[1]*, Martin C. Stennett[1], Russell J. Hand[1], Sean P. Morgan[2] & Neil C. Hyatt[1]

1. *Department of Materials Science & Engineering, The University of Sheffield, Sheffield S1 3JD, UK*
2. *Sellafield Ltd., Hinton House, Risley, Warrington WA3 6GR, UK*

Abstract

Magnox sludge waste is a major radiological hazard which needs containing. Vitrification is a viable alternative to the current baseline plan and is demonstrated here. Significant quantities of uranium and magnesium metal were successfully digested into glass melts and mostly amorphous material formed. Dissolution of the glass samples was found to be low in borosilicate samples but aluminosilicate samples deemed not as desirable due to higher melting temperatures and increased dissolution.

Introduction

Figure 1: The last Magnox nuclear power station to shutdown at Wylfa, Anglesey, UK [1]

The United Kingdom's first generation of nuclear power stations built at the dawn of the atomic age from 1953 were of the graphite moderated, gas cooled reactor design incorporating unenriched uranium metal fuel clad in a **mag**nesium **n**on-**ox**idising (Magnox) alloy [2] [3]. This type of reactor has operated successfully at stations such as Wylfa in Anglesey, North Wales for over 40 years (Figure 1).

The spent fuel from Magnox reactors across the UK was sent to the reprocessing plant at Sellafield to recycle uranium and plutonium. During the coal miners' strikes of the 1970s and 1980s, spent fuel for reprocessing built up at a quicker rate than predicted due to fuel elements being used more swiftly in power stations to generate the extra electricity needed to keep the country running. Spent fuel was stored for longer than anticipated in the open-air water filled cooling ponds causing corrosion of the magnesium based alloy cladding the fuel; forming a primarily magnesium hydroxide sludge covering the floor of the ponds [4]. The inclusion of uranium into some 3,148 m^3 of sludge in the First Generation Magnox Storage Ponds and Swarf Storage Silos is one of its biggest problems Sellafield is facing to date [5].

Magnox sludge is planned to be removed from the ponds and placed in a new engineered facility whilst awaiting encapsulation in a cement matrix, as with most intermediate level waste (ILW). Whilst being relatively cost effective in the short term, cementation increases the volume of the waste to be disposed by over 300% increasing the cost of final disposal in the UK's planned geological disposal facility (GDF). Vitrification technologies offer higher waste loadings, volume reduction and greater durability by chemically bonding waste into the structure of a glass.

Methods

Two bounding extremes for the waste found within the First Generation Magnox Storage Ponds were proposed, one with 80% corroded Magnox cladding [$Mg(OH)_2$], 10% corroded uranium [U_3O_8] and 10% metallic content (U & Mg) and the other composed of 80% metallic content and 20% corroded Magnox cladding, see Table 1.

Table 1: Waste Composition

	Mg	$Mg(OH)_2$	U	U_3O_8
Metallic waste	**12**	**20**	**68**	**0**
Corroded waste	**5**	**80**	**5**	**10**

Borosilicate and Aluminosilicate glass was created by adding glass formers SiO_2, B_2O_3, Al_2O_3 and network modifiers such as MgO and Na_2O to the waste stream in compositions based off the MgO-Al_2O_3-SiO_2 (MAS) and MgO-B_2O_3-SiO_2 (MBS) phase diagrams. Well mixed stoichiometric batches were melted in a muffle furnace for 3 hours at 1250 °C (borosilicate) or 5 hours at 1500 °C (aluminosilicate) before casting and annealing for 1 hour.

Characterisation was accomplished using a wide variety of techniques including X-ray diffraction (XRD) and scanning electron microscopy with energy dispersive X-rays detection (SEM-EDX) to identify phases present. X-ray absorption near edge structure analysis (XANES) was used to identify the uranium oxidation state and differential thermal analysis (DTA) used to find the glass transition point, any crystallisation temperatures and final melting point.

Long term durability of glass samples performed according to ASTM product consistency test B experiments (PCT-B) was ran at 90 °C for 28 days with sampling on days 1, 3, 7, 14, 21 and 28. Aliquots of solution from each sampling point were analysed on an inductively coupled plasma optical emission spectrometer (ICP-OES) to determine the amount of material transferred from glass into solution. Cross-sectional SEM on the altered glass particles was used to identify any alteration layers formed at the glass surface interface.

Results/Discussion

Borosilicate glass samples melted successfully at 1250 °C forming a very fluid melt that was easy to cast whilst aluminosilicate glass samples required heating to 1500 °C in order to form a fluid melt. Visual observations of glass batched with the high metallic waste showed phase separation and a high degree of crystallisation whereas glass created from the corroded waste stream appeared single phase with little to no crystallisation, confirmed by XRD (Figure 2).

Crystallisation in samples from the metallic waste stream was found to take the form of UO_2 and U_3O_8 which was also evident in SEM-EDX imaging in the form of fused and dendritic crystals, see Figure 3. These are likely to have formed during the melting process and allowed to grow during casting and annealing.

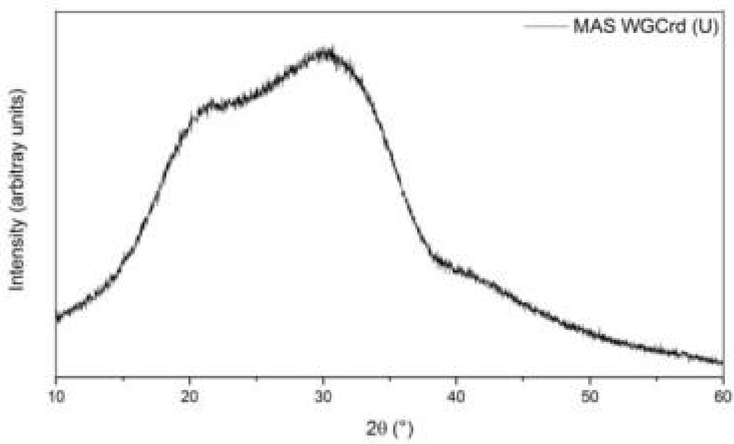

Figure 2: Diffuse scattering of X-rays, indicative of amorphous materials, from MAS corroded waste glass sample

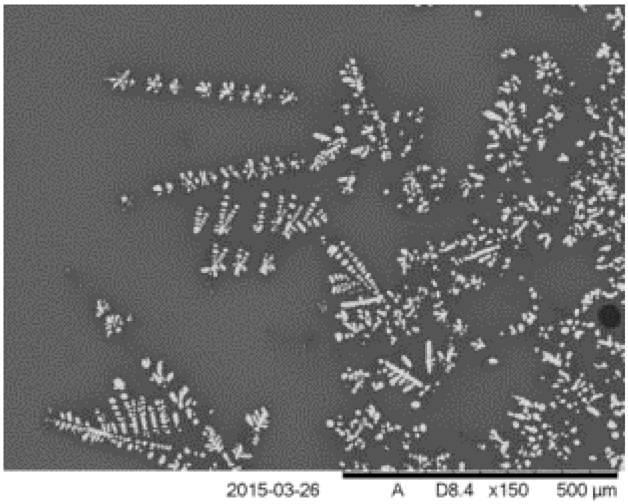

Figure 3: Dendritic UO_2 crystals found within MBS metallic waste glass

XANES on the U L_{III} edge compared to U (IV), (V) & (VI) reference samples proved U had been passively oxidised and digested in the glass with an oxidation state varying from 4.97 for the MBS metallic waste sample to 5.74 for the MAS corroded waste stream sample. Higher melting temperature and duration is the cause for the higher oxidation state in MAS samples. Glass transition occurs between 617 °C and 631 °C in MAS samples and from 672 °C in MBS samples with two distinct crystallisation points. The point at which the glass became a liquidus melt did not occur until 1420 °C in MAS samples and at between 1135 °C and 1153 °C for MBS samples. The lower melting point in the MBS system is attributed to the high (>21 mol%) boron content which acts as both a flux and a glass former. MAS samples have a higher content of Al_2O_3 acting as an intermediate glass former but also a refractory increasing the melt temperature significantly.

Dissolution of the MBS glass over 28 days was observed to be very low with little to no release of U into solution. The pH of the solution was buffered to 8.5 whilst MAS samples buffered the solution to above pH 12 causing higher rates of glass dissolution. Boron release rates were over three times higher in MAS samples compared with the MBS samples. U was detected from MAS samples in significant quantities rising sharply during the first 7 days before reaching a steady rate due to the formation of alteration layers that reduce further dissolution (Figure 4). SEM-EDX analysis of the 28 day altered samples confirms the presence of alteration layers on the surface extending for approximately 10 µm. The alteration layer is composed of Mg, Al and Si with trace amounts of Na and U at the glass-surface transition indicating these elements pass through the alteration layer. No U was detected in solution from MBS samples until day 28 and the rate is almost negligible, with no major alteration layers observable via SEM.

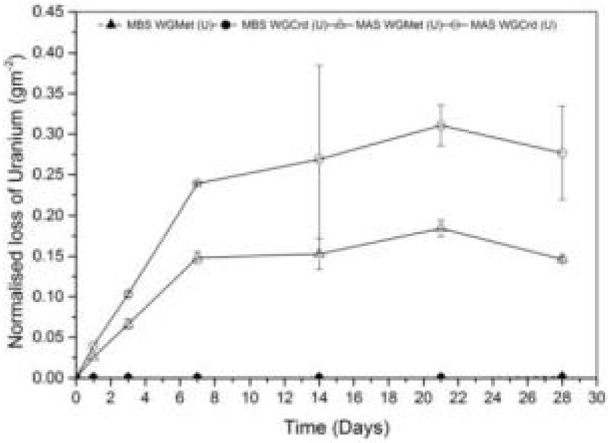

Figure 4: Normalised mass loss of uranium from all samples

Conclusion

Durable glass waste forms for the immobilisation of Magnox sludge ILW have been developed with the MBS glasses showing considerable promise. Homogeneous glass that can be melted over a reasonable composition range at temperatures below 1200 °C was created that provides flexibility with respect to this particular waste stream. MAS samples have proven to not be as successful due to the higher melting temperatures (~1500 °C) and the increased leaching of boron and uranium compared to the MBS system. This project has also demonstrated the passive oxidation and digestion of uranium and other metals into the melt without any mechanical aid which could be useful for the intended application. High leaching rates for boron and uranium in MAS samples was attributed to the composition and melting parameters as well as uranium oxidation state with alteration layers on the surface of the glass particles forming a protective barrier to further dissolution, evident in the steady-state stage of dissolution after approximately 7 days. Volume reduction achieved by vitrification of Magnox sludge could be as great as 80% compared to the current baseline plan with a cost saving of approximately £83 million for long term storage.

Acknowledgments

The authors would like to thank the EPSRC (Grant EP/G037140/1) for funding this research which was performed in part at the MIDAS Facility, at the University of Sheffield, which was established with support from the Department of Energy and Climate Change.

References and Citations

[1] Nuclear Decommissioning Authority, "Waste Inventory Data for Wylfa" 2015. [Online]. Available: http://www.nda.gov.uk/ukinventory/site/wlyfa/ [Accessed 23-Nov-2015]

[2] R. E. Hester and R. M. Harrison, Nuclear Power and the Environment, vol. 32, Royal Society of Chemistry Publishing, 2011

[3] D. G. Cacuci, Handbook of Nuclear Engineering- Volume 1 Nuclear Enginering Fundamentals, 1st ed. Springer US, 2010

[4] J. Cronin and N. Collier, “Corrosion and expansion of grouted Magnox,” *Mineral Mag.*, vol. 76, no. 8, pp. 2901–2909, Dec. 2012

[5] Nuclear Decommissioning Authority, “UK Radioactive Waste Inventory - 2D22, 2D24, 2D35 Consolidated Magnox fuel cladding and miscellaneous waste,” 2013.

Complexation and Adsorption of [^{152}Eu]Eu to Superplasticizers and Bentonite at Variable Salt Concentrations

M. Becker[1], H. Lippold[1]

[1]*Helmholtz-Zentrum Dresden-Rossendorf, Institute of Resource Ecology-, (Reactive Transport Division), Permoserstr. 15, 04318 Leipzig, Germany*

Abstract

The preferred method for the storage of spent nuclear fuel (HLW) is the disposal in deep geological formations. The repository will consist not only of the geological barrier but also of an engineered barrier and has to isolate the waste for at least 10^6 years from the biosphere [1]. In this barrier, several materials like concrete or bentonite are effective in retention of radionuclides. In modern concrete, several additives are used to improve the properties of the cement paste. Superplasticizers of the polycarboxylateether (PCE)-family are widely used for this purpose [2]. These organic materials might have an influence on the mobility of radionuclides. Hence, it is necessary to study their complexation and adsorption behaviour with radionuclides, cement-phases like C-S-H and buffer materials like bentonite considering a possible leaching of PCE from cement in consequence of water influx. In this study, the complexation and adsorption behaviour of the superplasticizer MasterGlenium® 51 was investigated by means of the radionuclide ^{152}Eu, which is an analogue for trivalent actinides such as Cm(III) or Am(III), at a fixed pH and variable salt concentrations (NaCl, $CaCl_2$). Complexation constant and loading capacity for the PCE with [^{152}Eu]Eu were determined on the basis of the Langmuir isotherm equation as well as of the charge neutralisation model [3]. Furthermore the adsorption behaviour of [^{152}Eu]Eu to bentonite with and without MasterGlenium51® in the presence of different background electrolytes was studied.

Introduction

Considering the situation of a deep geological repository for spent nuclear fuel, possible water intrusion and therefore the corrosion of the engineered barriers like the waste bearing canisters may take place in a few hundreds of years after inclosure of the waste. As a consequence, radionuclides may be released into the nearfield of the repository. The mobility of the radionuclides in presence of superplasticizers under alkaline conditions and high salinity up to 4 mol/L has to be investigated to evaluate the performance of the engineered barrier consisting of cement-phases like C-S-H and buffer materials such as bentonite. Complexation and adsorption of [^{152}Eu]Eu with MasterGlenium® 51 and bentonite were studied in batch experiments.

Methods

A stock solution of [^{152}Eu]$Eu(NO_3)_3$ was prepared with a concentration of $2 \cdot 10^{-4}$ mol/L and an activity of 0.3 MBq. The solution was adjusted to pH 3 to avoid formation of colloids and wall adsorption. For recording an isotherm of binding of Eu to the superplasticizer, solutions with different concentrations of $Eu(NO_3)_3$ were prepared ranging from 10^{-7} mol/L down to 10^{-2} mol/L spiked with ^{152}Eu at an activity of 0.6 kBq. Experiments on the effect of electrolytes (NaCl and $CaCl_2$ up to 4 M) on complexation were carried out at a fixed [^{152}Eu]Eu concentration of 10^{-6} M. The superplasticizer was added as last component, resulting in a concentration of 100 mg/L. Separation of bound and non-bound Eu was carried out after 24 hours of contact time by ultrafiltration with polyethersulfon-membrane centrifuge filters (Vivaspin, Sartorius) with an MWCO of 3kDa. Concentrations of Eu in the filtrate were determined relative to reference samples with a Perkin Elmer Wizard 1470 automatic γ-counter in an energy window of 0 - 2 keV. Wall adsorption during equilibration in 4 mL PP tubes was found to be negligible. The amount of [^{152}Eu]Eu complexed to the superplasticizer was calculated from the difference in the count rates between reference and filtrates. To determine the carboxyl-content of the superplasticizer a direct titration with 0.1 M NaOH was carried out in 0.1 M $NaClO_4$ under a N_2 atmosphere using a WTW inoLab 720 pH meter [4]. For batch adsorption experiments, two stock suspensions of 5.05 g/L bentonite without and with NaCl or $CaCl_2$ (4.5 mol/L) were mixed at variable ratios before adding [^{152}Eu]Eu and MasterGlenium® 51 at concentrations of 10^{-6} M and 100 mg/L, respectively. After 24 hours of end-over-end rotation at 20 rpm, the samples were centrifuged at 7000 rpm for 60 min. 3 mL of the supernatant solution where taken for analysis by γ-counting relative to reference solutions.

Results/Discussion

Titration of the superplasticizer MasterGlenium® 51 resulted in a carboxylgroup-content of (1.17 ± 0.01) meq/g, taken from an equivalence-point at pH 9.3. The isotherm of binding of [^{152}Eu]Eu to the organic material exhibits a linear range from 10^{-7} mol/L up to 10^{-4} mol/L with the Langmuir parameters Γ_{max} = (0.32 ± 0.01) mmol/g Eu and K_L = (15.59 ± 0.01) L/mmol at pH 5.8. According to the charge neutralization model the maximum loading Γ_{max} is expressed as a loading capacity (LC), which is normalized to the measured content of carboxyl groups. It represents the molar fraction of the maximum available complexing sites under the given setup of experimental conditions. The Langmuir constant K_L is normalized to the charge of the cation giving a stability constant β. A good agreement was obtained for the constants derived from the Langmuir isotherm equation and from charge neutralization model with LC = 0.827 ± 0.003 and β = (12.86 ± 0.01) L/mmol. Batch sorption experiments with bentonite, MasterGlenium® 51 and [^{152}Eu]Eu show a quantitative adsorption of Eu for all concentrations of NaCl, whereas for the $CaCl_2$ system, a pronounced decrease in adsorption was found for higher salt concentrations (down to 20 % of total Eu). The effect the superplasticizer is relatively small in both cases, resulting in an increase in Eu adsorption approximately 5 %.

Conclusion

For the first time, metal complexation with a polycarboxylateether (superplasticizer) was quantitatively investigated for the example of the system Eu / MasterGlenium® 51. Interaction parameters based on the Langmuir isotherm equation and the charge neutralisation model were shown to analogue. Competition effects of NaCl and $CaCl_2$ with respect to complexation and adsorption turned out to be very different. At the chosen pH of 5.8, the influence of the superplasticizer on adsorption of Eu onto bentonite is rather small, in spite of significant complexation. Further experiments are planned at alkaline conditions (pH 9 – 13), including the adsorption behaviour of the organic component, which will allow an eludication of its effect on Eu adsorption.

Acknowledgments

This work is funded by the German Federal Ministry for Economic Affairs and Energy (BMWi), support code 02E11415B, within the joined project GRaZ (“Geochemische Radionuklidrückhaltung an Zementalterationsphasen”).

References and citations

[1] Sellin, P. and O.X. Leupin, *The Use of Clay as an Engineered Barrier in Radioactive-Waste Management - A Review.* Clays and Clay Minerals, 2013. **61**(6): p. 477-498.
[2] Ferrari, L., et al., *Multi-method approach to study influence of superplasticizers on cement suspensions.* Cement and Concrete Research, 2011. **41**(10): p. 1058-1066.
[3] Kim, J.I. and K.R. Czerwinski, *Complexation of metal ions with humic acid: Metal ion charge neutralization model.* Radiochimica Acta, 1996. **73**(1): p. 5-10.
[4] Young, S.D., et al., *Analysis of the potentiometric titration of natural and synthetic polycarboxylates.* Journal of Soil Science, 1981. **32**(4): p. 579-592.

Sorption properties of granitic rock from potential deep geological repository site in Czech Republic

Vojtěch Brynych, Kateřina Kolomá, Václava Havlová

ÚJV Řež, a.s., Hlavní 130, Řež, 250 68 Husinec, Czech Republic

Abstract

Results of radionuclide batch sorption experiments for Czech rock samples will be present on the poster. Sorption of radionuclides, relevant for deep geological repository (DGR) safety (^{137}Cs, Se, U), will be studied on granitic rock material from DGR potential site.

Introduction

Granite is considered as a host rock for deep geological disposal of spent nuclear fuel and high radioactive waste in Czech Republic. The deep geological repository concept assumes that waste packages containing spent nuclear fuel (SNF) assemblies will be enclosed in steel-based canisters placed in vertical or horizontal boreholes at a depth of ~ 500 m below the earth's surface. The space between the canisters and the host crystalline rock will be backfilled with compacted bentonite which will make up the final engineered barrier. Seven sites have been pre-selected as potential ones for DGR sitting in Czech Republic.

DGR itself is constructed as a multibarrier system, aiming to fulfill the main safety function: *To provide protection to human and environment in such a way that even considering all the risk during operational and post-closure period the effective dose 0,25 mSv per year for critical group of inhabitant will be not exceeded* [1]. One of the host rock safety functions within the multibarrier system is *to restrict and delay radionuclide transport due to the effect of physical and chemical processes in the geosphere* [1]. One of the most important processes contributing to the function is radionuclide sorption on mineral phases. On the other hand, ^{137}Cs, ^{79}Se and U isotopes belong to the most relevant radionuclides, being present in spent nuclear waste that can potentially contribute significantly to the potential danger for human and biota.

Rock samples

The sites, preselected as potential ones for DGR sitting, are mostly located in granitic rock massifs. The only one, Kravi hora, is located within a metamorphosed rock massive. Sorption properties of potential site granitic rock materials will be studied within the Czech R&D project [2]. Horka site samples (marked as PZV1) were chosen for the first round of batch sorption experiments. Rock samples from PZV1 borehole were milled and sieved into defined fractions. Each fraction mineral composition was determined using XRD (see Tab. 1).

Table 1: Mineral composition of Horka site samples

Sample	Fraction (mm)	Quartz	Plagioclase	K-feldspar	Chlorite	Amphibole	Mica (biotite)
PZV1-A	<0.063	24	20	22.5	1	19.5	13
PZV1-B	0.125-0.063	23	21	22.5	-	20.5	13
PZV1-C	0.63-0.125	24.5	21	20	-	15	19.5
PZV1-D	0.8-0.63	25	24.5	26	-	14.5	10
PZV1-E	>0.8	20	29	30	-	13.5	7.5

Fractions C and D were chosen for further sorption studies.

Solution

Synthetic groundwater SGW2, based on Ca-HCO_3 groundwater from 600 m depth in Rozna mine (CZ), was proposed and prepared in [2]. The chemical composition is reported in Tab. 2. SGW2 was used then as a solution for tracer solution preparation. The salts of CsCl, Na_2SeO_3 (or Na_2SeO_4) and $UO_2(NO_3)_2$ were added to SGW2 in order to form solution with following concentrations $2\cdot10^{-5}$ mol/L (Cs), $2\cdot10^{-5}$ mol/L (SeIV or SeVI) and $2.6\cdot10^{-4}$ mol/L (U), respectively. The solution of CsCl was spiked with ^{137}Cs.

Table 2: Synthetic groundwater SGW2 chemical composition

	pH	Na^+	K^+	Ca^{2+}	Mg^{2+}	Cl^-	SO_4^{2-}	HCO_3^-
SGW2	8.2	16.5	2.1	34.6	8.3	3.3	21.0	168.7

Bath sorption experiments

The sorption on selected materials was studied by batch method. The batch method is based on the contact of solid material with tracer solution and measurement of tracer concentration (activity) decrease in solution. s/L ratio was 1 :10. Sorption experiments were carried out at 24 °C under atmospheric conditions and lasted 7 days. After the adsorption, the suspension was centrifuged and an aliquot of the supernatant was measured by different method for each sorbate. ^{137}Cs was measured on Perkin Elmer 1480 Wizard 3" Gamma counter (Wallac Oy, Finland). The Se was measured by ICP-MS (Inductively coupled plasma mass spectrometry), Elan DRC-e (Perkin Elmer, USA). U was measured on UV-Vis spectrometer Uvi Light PC 2, (Secoma) with Arsenazo III disodium salt which gives marked colour reactions with uranium. Finally the value of sorption distribution coefficient K_d was calculated.

Results/Discussion

The results of the batch sorption experiments will be presented on the poster.

The kinetics of Cs, Se and U sorption on the rock samples for one week period will be reported. Resulting K_d values will be compared with batch sorption experiments (Czech granites, Grimsel test site samples, Aspo Hard Rock laboratory samples).

Conclusion

Description of sorption kinetics is the first step in determination of radionuclide sorption process. Sorption isotherms will be determined in the next step for studied radionuclides and rock material. The identical studies for rock material from further DGR sites will then follow.

Acknowledgments

The research within the Scientific support of DGR safety assessment project have been funded by SURAO.

The poster can be downloaded here: https://goo.gl/NjwCya

References and Citations

[1] Vokál A. et al. “Actualisation of the DGR Reference Project for Hypothetical Site”,*C.2 Long term assessment*, ÚJV Rez, a.s. report, pp. 172, 2011.

[2] Scientific support of DGR safety assessment (2014 - 2018). SURAO funded project.

Coupled Thermo–Hydro–Mechanical Processes for the Dutch Radioactive Waste Repository

P.Buragohain[1], P.J. Vardon [2], M.A. Hicks[3],

P.Buragohain@tudelft.nl / P.J.Vardon@tudelft.nl / M.A.Hicks@tudelft.nl

[1,2,3] Section of Geo-Engineering, Delft University of Technology
P.O. Box 5048, 2600 GA Delft, The Netherlands

[1]Post-Doctoral researcher. [2]Assistant Professor, [3]Professor

Abstract

Disposal of spent nuclear fuel and long lived radioactive waste in deep clay geological formations is one of the promising options worldwide. In this concept of the geological disposal system, the Boom Clay is considered as a potential host rock when designing a generic waste repository in the Netherlands. For design and evaluation of a repository for geologic disposal of nuclear wastes one of its principal concern is the thermal loading. High-level radioactive waste and spent fuel generate considerable amounts of heat. When those waste types are disposed in a geological repository the elevated thermal effect on the behaviour of soils surrounding nuclear waste disposal give rise to change in hydraulic and mechanical properties is a significant factor for repository design. Understanding these time-dependent phenomena processes in relation to both the effects of pore water dissipation and of the thermal expansion is essential for reliably assessing repository performance and evaluating the safety case. This paper presents some of the investigation on the thermal processes with emphasis on the coupled Thermo-Hydro-Mechanical (THM) processes for the disposal concept of a radioactive waste disposal facility, in Boom Clay at a depth of about 500m.

Keywords: radioactive waste, disposal, Boom clay, thermal, thermo-hydro-mechanical behaviour.

Introduction

Deep geological disposal of high level radioactive waste and spent fuel is considered the safest and most sustainable option long term nuclear waste containment and isolation. The Boom Clay is considered as a potential host rock when designing a generic waste repository in the Netherlands. As a starting point in the third Dutch research programme OPERA, in a Dutch disposal concept, a geological disposal facility is assumed to be constructed in bedrock 500 meters depth and with a stratum thickness of about 100m. As the high level nuclear waste generates a great amount of heat it needs to be temporarily stored for some years before disposal. For Netherlands the interim storage period is for 100 years. However even after this, the residual heat production is expected to produce a raise of temperature in the near as well as the far field. Various coupled mechanical (M), hydraulic (H) and thermal (T) perturbations will be induced in the surrounding clay host rocks and create a disturbed zone, during the various stages of the repository evolution: the excavation, construction, emplacement and post-closure. Of particular importance in such a clay rock is the zone surrounding the disposal galleries, which will have plastic deformations, influencing the stability of the tunnel and the hydraulic conductivity of the rock. The prediction of the evolution of various changes in properties within this zone are major issues especially in the context of underground nuclear waste disposal. To further planning and design the Boom Clay response for coupled THM is terms of performance and safety functions, as well as financial and engineering feasibility is addressed in this paper.

Methods

A 2D plane strain model was utilised, as the disposal tunnels are designed to be 50 m in length. An elasto-plastic hardening material model, the Hardening Soil (HS) model, was previously calibrated for Boom Clay behaviour [1] from limited experimental data and these parameters are utilised here. An initial mechanical and thermal assessment, taking into account the uncertainties in the material behaviour is presented in [1] and this paper extends that work to consider the thermo-hydro-mechanical (THM) coupled behaviour. The major THM coupled processes are first presented and then a numerical simulation utilising a commercial geotechnical numerical model [2] for this specific case is presented. The model incorporated the excavation, construction and post-closure stages of the repository.

The domain of the numerical model was 80 × 160m, discretised using 15-node triangular elements and refined in the close vicinity of the tunnel, excavated at a 500 m depth and with a 1.6 m radius, in the Boom Clay layer. The initial vertical effective stress in the domain was set to increase with depth (10 kPa/m) with a total vertical stress of 4.2 MPa applied along the top boundary, the pore pressure was initially hydrostatic and the initial temperature set to 295 K. The bottom mechanical boundary was fixed, the left-side and right-side boundaries were fixed in the horizontal direction (due to symmetry) and free in the vertical direction. The analysis was conducted in 3 stages: (i) a K0 stage, where the horizontal stresses were calculated, (ii) an excavation and construction stage, where the tunnel lining was included and contracted representing rock relaxation, and (iii) a heating THM stage, where a heat flux representing the flux from the emplaced waste was applied to the tunnel boundary. An initial heat flux of 11 W/m^2 was applied and reduced over time, based upon the expected radioactive decay.

Results and Discussions

Figure 1 presents contour plots of the drained response showing the variation of (a) the pore pressures at the end of 30 years, (b) the temperatures at the end of 30 years when the temperature is at its peak, and (c) the plastic and failure points of the model after construction and after 30 years. The results are presented in terms of the pore pressures changes, the stress/strain response, the temperature and the plastic zone development. The simulated results indicated a rapid increase in pore water pressure during the first few decades in conjunction with temperature increase, followed by stabilisation and decay of both. This sharp initial increase in pore water pressure and the occurrence of thermal consolidation at the beginning is explained to the slower water dissipation rate of the Boom Clay. This is followed by a rapid increase in pore water pressure.

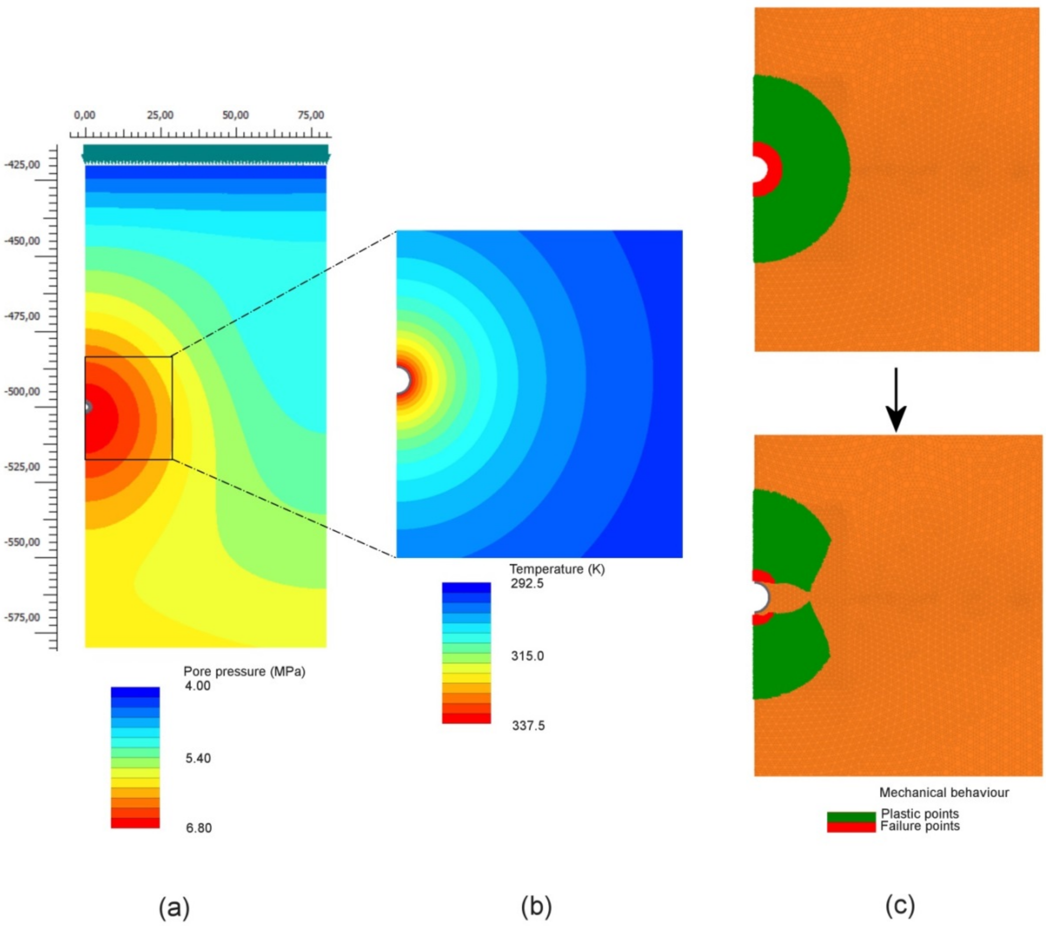

Figure 1. Contour plots of (a) pore water pressure at 30 years, (b) temperature at 30 years, and (c) plastic zone after construction and at 30 years

The study indicated that the magnitude of the excessive pore pressure depends not only on the temperature increase, but is sensitive to the hydraulic conductivity. It can be seen that at 30 years the extent of the hardening zone (plastic points) increases negligibly in the vertical direction and decreases in the horizontal direction. This reduction in the plastic zone is due to the thermal expansion of the liner and an increase in the confining pressure. This pore pressure increase causes a decrease in the mean effective stress, albeit with the impact reduced by an increase in confining pressures by the thermal expansion of the tunnel lining. This leads to an increase in the plastic shear deformation and the extent of the plastic zone and an increase in total stresses on the liner. The hydraulic conductivity plays a critical role in the development of the plastic zone, as this controls how easily the thermally induced excess pore pressures are dissipated.

Conclusion

The stability of the performance and safety assessment during operation and post-closure stage was addressed in this study. Coupled Thermo-hydro-mechanical behaviour of the boom clay was utilised as well as studies related to peak temperature, thermally induced pressurization of boom clay pore water, on the repository design was analysed***.*** The modelling results demonstrated there exists a strong coupling between the thermal, mechanical hardening behaviour and the hydraulic response The results showed that while the temperatures reached in this disposal concept are not of concern, the additional mechanical load should be considered. For safety assessment, a low hydraulic conductivity is favoured to reduce the possibility of advective flow, which causes an additional mechanical load on the liner.

Acknowledgments

The research leading to these results has received funding from the Dutch research programme on geological disposal, OPERA. OPERA is financed by the Dutch Ministry of Economic Affairs and the public limited liability company Elektriciteits-Produktiemaatschappij Zuid-Nederland (EPZ), and is coordinated by COVRA.

References and Citations

[1] P. Arnold, P.J.Vardon, M.A. Hicks, J. Fokkens, P.A. Fokker, " A numerical and reliability-based investigation into the technical feasibility of a Dutch radioactive waste repository in Boom Clay." Report no. OPERA-PU-TUD311. COVRA. 2015, pp. 316. (available http://www.covra.nl/cms-file/get/iFileId/2844)

[2] Plaxis, *PLAXIS 2D Anniversary Edition - Reference Manual*. Plaxis bv: Delft, 2014.

Dismantling of the graphite pile of Latina NPP: characterization and handling/removal equipment for single brick or multi-bricks

Giuseppe Canzone[a], Rosa Lo Frano[b], Marco Sumini[c], Francesco Troiani[a]

[a] *Sogin Spa- Roma, Italy*

[b] *Department of Industrial and Civil Engineering (DICI) – University of Pisa, Italy*

[c] *Department of Industrial Engineering, University of Bologna, Italy*

Abstract

This work describes the issues related to the dismantling of the graphite pile of the 1st generation gas cooled reactor of Latina NPP (Italy). The retrieval of the graphite is a strategic matter for the decommissioning of this type of plant: the aim of this study is to describe and analyse the current approaches used to access the core and to perform the remote and dry extraction of graphite bricks from the top. The outcomes of this study could be useful to plan the removal of Latina NPP graphite: the extraction of the graphite would be carried out layer by layer by means of a dedicated remote controlled handling systems; this equipment would be duly designed according to the nuclear, physical and mechanical constraints of the graphite piles in core. Thus, the issues regarding the irradiated graphite have been analysed by FEM code, especially those related to the core geometry and the proposed technique of hooking the graphite bricks by a ‘gripper’ tool inside the axial channel. Data on fresh nuclear grade and irradiated graphite, used for the numerical simulations, have been obtained by means of theoretical models and experimental tests, carried out on samples extracted from the reactor. The results obtained could support the final design of proper lifting, gripper tools and handling equipment, for single brick or multi-bricks, and could implement graphite waste management strategy.

Introduction

When dealing with the decommissioning of gas-cooled graphite-moderated reactors, concerns arise due to the large amount of radwaste in the form of graphite stack fragments that was generated during the reactor lifetime (on average 1500-2000 tons per reactor, as evaluated by the IAEA). The most obvious source of irradiated graphite is from reactor moderators and reflectors. In this study, the current approach for the management of radioactive graphite, and specifically the procedure adopted for the remote and dry extraction of graphite from the Latina reactor will be described and analysed.

Decommissioning strategy of Latina NPP

The Latina plant is a Magnox reactor type, definitively shut down in November 1986. During its 23 years of operation, the plant really produced 4200 Equivalent Full Power Days (EFPD). Since 90’s Sogin S.p.A (Italian State Owned Company appointed for Nuclear Decommissioning and Radioactive waste management) is managing the plant, with specific regard to decommissioning activities.

In Fig.1, it is shown synthetically the general decommissioning approach considered for Latina plant: the dismantling of reactor foresees firstly the empting of reactor pit and then the removal of graphite, to be obtained disassembling or demolishing/tearing down the core bricks[1-2].

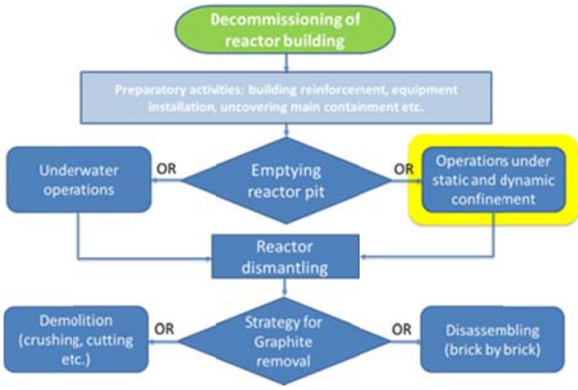

Figure 1: Decommissioning approach taken into account for Latina NPP[2]

The removal of the graphite from the core is a concern mainly because of the material changes caused by the irradiation effects. In consideration of that and of the possible aging effects several techniques for the removal of irradiated graphite have been examined: by critically reviewing the state of art acquired over the past years the 'in-air' dismantling seems the more reasonable and possible solution for a direct demolition or a retrieval 'brick-by brick' retrieval. The carried out feasibility study concerning the disassembling of the graphite stack brick also showed that the mechanical retrieval, the lifting and, in general, the mechanical handling of the bricks are possible avoiding or limiting/minimizing the number of brick breaks.

Graphite behaviour

The Latina reactor graphite used as moderator and reflector has a high anisotropy; for that reason they are called respectively Pile Grade A (PGA) and Pile Grade B (PGB). Both two were manufactured in UK at the end of the 50s to be used in the early Magnox reactors.

Figure 2 show the single '4-sides' and '8-sides' brick scheme and the arrangements used to combine and assemble together these prismatic bricks. As it is possible to observe they are restrained each other with mechanical tying that allow to avoid in plane deflection and accommodate thermal expansion without any significant increase of stress state.

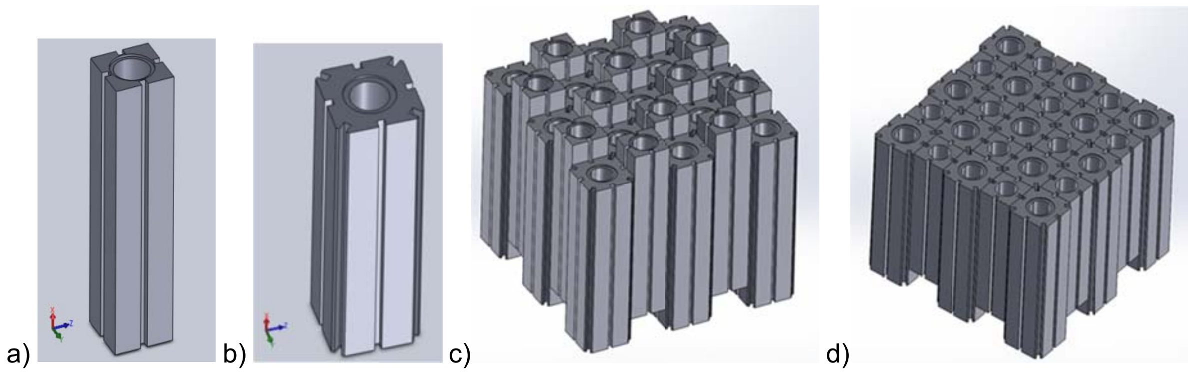

Figure 2: Graphite a) '4-sides' brick, and b) '8-sides' brick c) Graphite network for a generic arrangement of the moderator (9 layers) and for d) the upper reflector layer.

Numerical Modelling and Results

The removal of irradiated graphite is indeed depending on the feasibility of the gripping and the lifting system to be used to manage bricks. In this study a part from the graphite characterization that allowed to obtain useful information of material behaviour and potential damages it suffered over the lifeplant, is focused on the evaluation of the reliability of such systems that should be able to remove graphite bricks from the reactor vessel without breaks. In doing that, numerical investigation has been also performed to account the effects caused by the extraction force in terms of bearing load capacity of graphite brick.

Moreover to qualify and support this assessment, experimental results, which were obtained from the experimental investigation of nuclear grade graphite, not irradiated and without considering core restraints, have been taken into account (this study is part of a feasibility study aiming at the definition of an appropriate procedure to extract graphite bricks from the core configuration of Latina reactor without/minimizing the risk of fragmentation or rupture of the bricks themselves) [3].

A (3D) FEM model (Figure 3) has been thus set up and implemented assuming that the material behaves as anisotropic only along the extrusion direction of the brick[4-5], whereas in the remaining directions isotropic conditions have been imposed. A representation of the stress distribution caused by the retrieval/lifting is given in Figure 4 for the '4-side brick'. It is, in fact, possible to observe that the brick extraction results in an increase of stress applied thoroughly the brick itself. The mostly stressed area is at the annular step of the down base for both two '4-sides' and '8-sides' brick. Moreover it resulted that for a lifting force of 3 kN, the Von Mises stress did not overcome, in the transversal and longitudinal direction of the brick, the allowed limit value of nuclear-grade graphite. As a consequence of that it is possible to conclude that no rupture of the brick would occur during retrieval operation.

a) 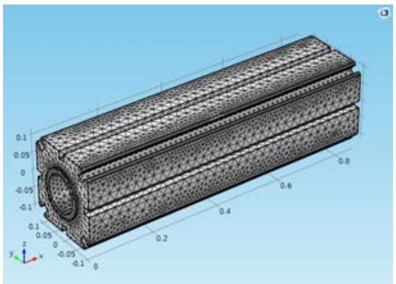 b) 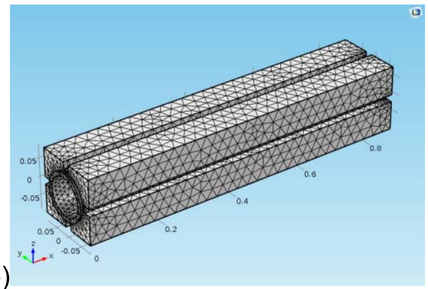

Figure 3: FEM of the single graphite element for a)'4-sides' brick, and b) '8-sides' brick.

a) 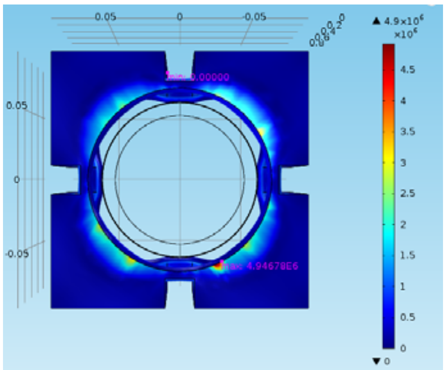 b) 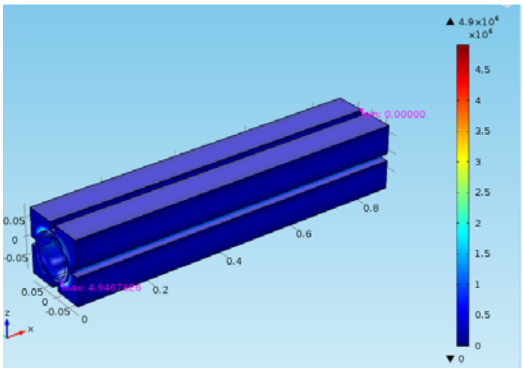

Figure 4: Maximum Von Mises stress due to lifting of '4-sides'brick.

Conclusion

Finally, although preliminary, modelling could be considered as a valuable technique in supporting the selected tool for retrieval operations of graphite bricks from the stack of the Latina NPP avoiding breaks. Further study seems necessary for a complete assessment of the technical solution presented in this paper, such as the investigation of material properties of the i-graphite, the effects of the cumulative damage of the graphite in the reactor, etc.

Acknowledgments

The authors would like to thank SOGIN Latina NPP Management for giving technical and historical support.

References and Citations

[1] EPRI, *Graphite Decommissioning Options for Graphite Treatment, Recycling, or Disposal, including a discussion of Safety-Related Issues*, Final Report, March 2006.

[2] IAEA, *Progress in Radioactive Graphite Waste Management*, IAEA-TECDOC-1647, 2010.

[3] SOGIN LTGR00070– *Prove fisico meccaniche su campioni di grafite irraggiata*.

[4] COMSOL 5.0, *Structural Mechanics Module User's Guide*, October 2014

[5] D.K.L. Tsang and B.J. Marsden, *Constitutive material model for the prediction of stresses in irradiated anisotropic graphite components*, J. Nuclear Material, 381, 129-136, 2008.

Effect of open-gaps in nuclear spent fuel disposal containers storage

I.P. Damians [1], S. Olivella [1], X. Pintado [2]

[1] Universitat Politècnica de Catalunya-BarcelonaTech; [2] B+Tech Oy

Abstract

The KBS-3H alternative is composed by horizontally placed supercontainers comprising the canisters with the nuclear spent fuel surrounded by compacted bentonite blocks (buffer) enclosed in a perforated metal shell. The gaps between the supercontainers and blocks and the host rock have direct effects on the buffer behaviour. This paper presents a Thermo-Hydraulic 3D numerical model generated in order to analyse a particular geometry assuming two different gap state conditions and providing results of the degree of saturation evolution.

Introduction

Nuclear spent fuel management is done in a way that is not harmful to organic nature. Posiva Oy is an expert organization responsible for the final disposal of nuclear spent fuel in Finland and it is constructing the final disposal in Onkalo [1]. The current paper presents some results from a TH 3D numerical model generated in order to analyse the degree of saturation evolution of a nuclear spent fuel disposal with a sequential emplacement of canisters in a drift, assuming two different gap state conditions between the buffer blocks and the supercontainer shell and the host rock in KBS-3H design alternative [2].

Model geometry and material properties

The drift was assumed to be placed at 425 m-depth. The model was built assuming 100 m vertical separation of host rock above and below the drift (i.e., distance to boundaries; which was determined to be far enough in order to assure the proper temperature dissipation [3]). After 1 year with empty tunnel and atmospheric pressure imposed at internal drift surfaces, eight canisters (and related components) were assumed to be serially distributed and horizontally arranged (with 2º tilt longitudinally), and the separation between parallel tunnels was fixed to be 25 m (see Figure 1a). The total length of the tunnel is about 107 m, and supercontainers separation is variable due to rock fractures presence (e.g., from 3.5 m up to 16 m distance for the longest case). Description about how to deal with intersecting fractures is described in [2].

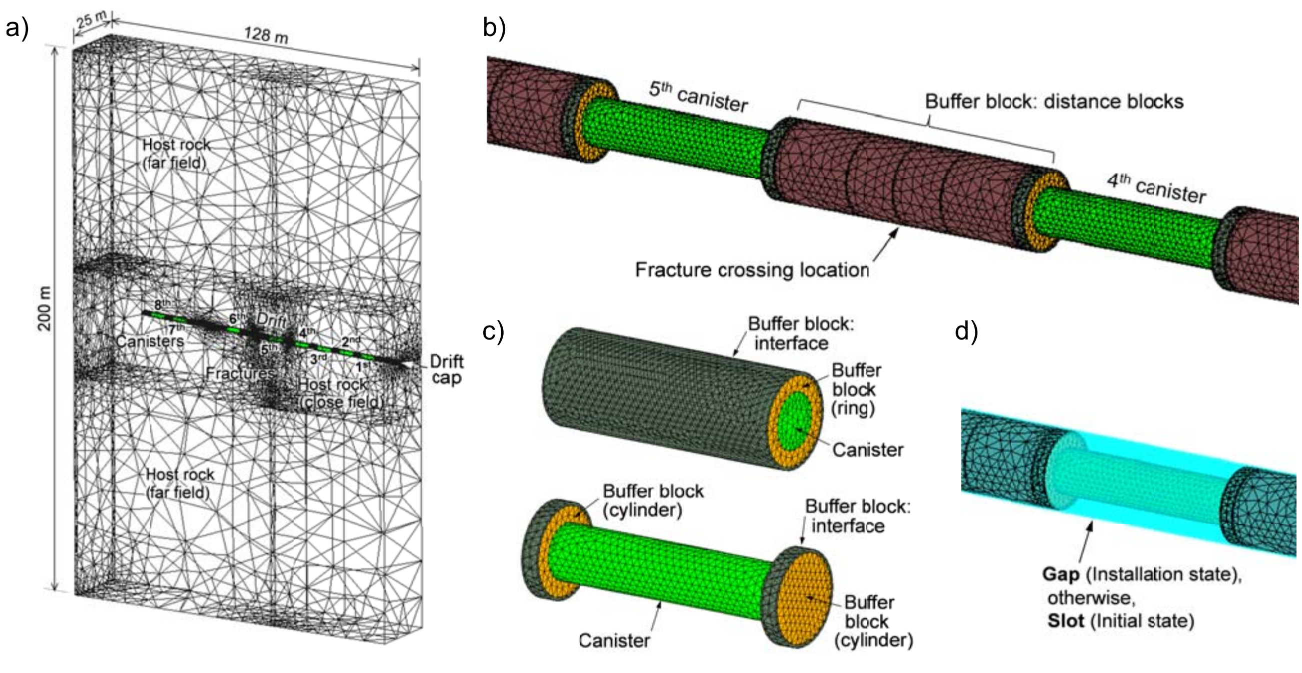

Figure 1: Entire drift 3D model mesh and main geometry dimensions (a), canister-to-canister mesh detail (b), super-container components (c), and gap/slot detail (d).

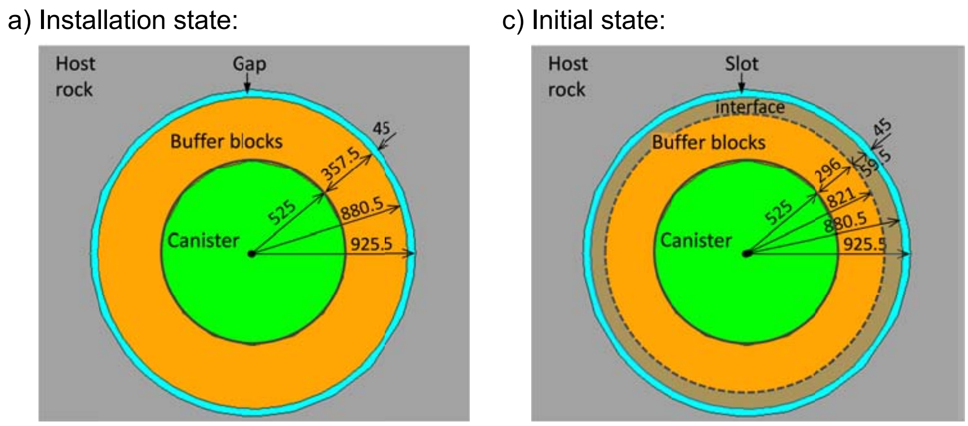

Figure 2: Super container cross-section geometry: Installation (a), and Initial (b) states.

Bentonite buffer blocks separate both containers and the host rock and containers themselves (see Figure 1b-c). A gap of 45 mm-thick was assumed between the buffer blocks and the host rock, which performs the actual "gap" at Installation state, otherwise "slot" due to buffer block swelling at Initial state (see Figure 1d and Figure 2). To perform this buffer block swelling effect and gap closure at Initial state, a certain thickness of block is defined as "interface" material, which shares properties with closed gap (now called "slot") with equivalent properties from block swelling). Calculations at this "Initial state" assume that the bentonite has flowed out from the supercontainer and the material which fills the gap (slot) can be considered as a solid. Part of the material inside the supercontainer (interface) has the same properties the material at the slot and the rest of the blocks remain unchanged. This is a simplification because the gap filling process cannot be simulated. Table 1 presents the material properties at initial conditions for both Installation and Initial states. Table 2 presents the buffer blocks drift components for these states.

Table 1. Material properties at starting conditions:

Parameters:		Host rock	Fractures	Buffer blocks	Gap / Slot	Canister
Porosity [-]		0.005	0.005	(Table 2)	(Table 2)	0.01
Intrinsic permeability [m^2]		1.52e-19 at close field, 1.52e-17 at far field [(a)]	1e-15	k_0 = 5.59e-21 [(b)]	Initial state: k_0 = 5.59e-21 [(b)] Installation: 1e-16 (fixed)	1e-24
Water retention curve [(c)]	**P_0 [MPa]**	1.5	1.5	31.25	0.05	31.25
	λ [-]	0.3	0.3	0.5	0.3	0.5
Relative permeability [(d)] [n-power]		3	3	3	3	3
Dry thermal conductivity [W/mK]		2.82	2.82	0.22	Initial: 0.22 Installation: 0.02	390
Saturated thermal conductivity [W/mK]		2.82	2.82	1.25	Initial: 1.25 Installation: 0.6	390
Solid unit weight [kg/m^3]		2743	-	2780	Initial: 2780 Installation: 0	8930
Solid phase specific heat [J/kgK]		746	-	830	1000	390
Initial liquid pressure [MPa]		hydrost.[(e)]	hydrost.[(e)]	(Table 2)	(Table 2)	-20
Initial Temperature [ºC]		10.5	10.5	10.5	10.5	50

Notes: [(a)] Higher value of permeability at far-field rock material (i.e., from 20 m up to 100 m above and below the tunnel) to take into account the network fracture capacity to keep the pressure almost constant at 20 m from the axis drift; [(b)] Intrinsic permeability defined as per the following exponential law: $k_{ii} = k_0 \exp\{b(\phi - \phi_0)\}$, which returns k_0 =5.59e-21 (for b =15 and ϕ_0 =0.438); [(c)] Water retention curve according to Van Genuchten model (λ: shape function); [(d)] Relative permeability $k_{rl} = (S_r)^n$, where S_r: degree of saturation; [(e)] Hydrostatic-linear law from 3.25 MPa (top) to 5.25 MPa (bottom boundary).

Table 2. Installation and Initial states starting porosity (ϕ), degree of saturation (S_r), and liquid pressure (P_l) for buffer block drift components:

	Buffer block: Cylinder			Buffer block: Ring			Distance block		
Installation:	**block**	**interface**	**gap**	**block**	**interface**	**gap**	**block**	**interface**	**gap**
ϕ [-]	0.369		0.99	0.322		0.99	0.384		0.99
S_r [-]	0.807		1	0.644		1	0.936		1
P_l [MPa]	-23		0.1	-37		0.1	-11.7		0.1
Initial:	**block**	**interface**	**slot**	**block**	**interface**	**slot**	**block**	**interface**	**slot**
ϕ [-]	0.369	0.689		0.322	0.689		0.384	0.664	
S_r [-]	0.807	0.861		0.644	0.805		0.936	0.961	
P_l [MPa]	-23	-18.5	0.1	-37	-23	0.1	-11.7	-9	0.1

Results

Figure 3 shows the evolution of the degree of saturation at several points around 5th canister. Despite the trends and minimum degree of saturation are approximately the same at points 4 and 5, slowed saturation process was done in points 1, 2 and 3. At Point 1 saturation is reached 4 years faster at Initial state.

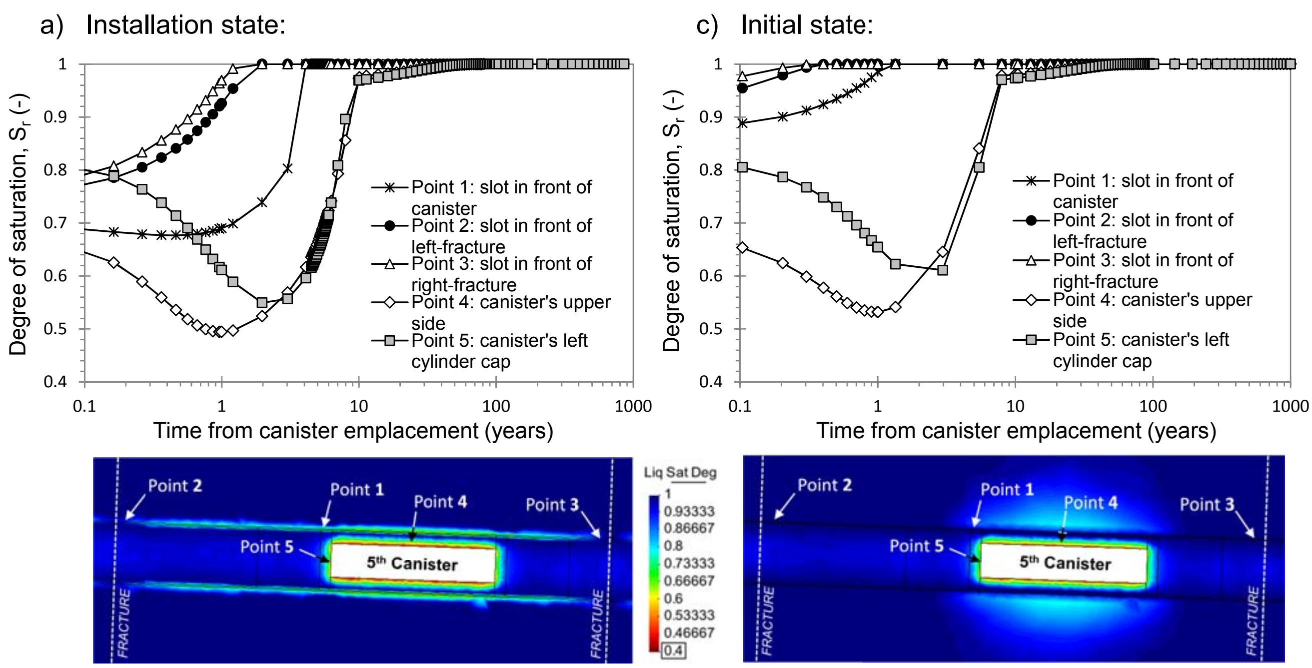

Figure 3: Degree of saturation evolution at several points around 5th canister: Installation (a), and Initial (b) states. Figure results after 1 year from canister emplacement.

Conclusions

The numerical TH 3D model for studying nuclear spent fuel disposal looks promising for further sensitivity analyses. In the current study, the presence of actual gap condition between the buffer blocks and the host rock resulted in direct effect on KBS-3H design alternative behaviour.

Acknowledgements

This work was financed by B+Tech Oy (Finland) under a POSIVA Oy project.

References and Citations

[1] Posiva Oy, *Olkiluoto Site Description 2008*, Posiva Report 2009-01, Eurajoki, Finland, 2009.

[2] Posiva Oy, *KHS-3H Complementary Studies 2008-2010*, Posiva Report 2013-3, Eurajoki, Finland, 2013.

[3] E. Toprak, N. Mokni, S. Olivella, and X. Pintado, *Thermo-Hydro-Mechanical Modelling of Buffer, Synthesis Report*, Posiva Report 2012-47, Eurajoki, Findland, 2013.

Modelling the excavation damaged zone using a hydro-mechanical double-scale model

A.P. van den Eijnden[1], P. Bésuelle[2,3], F. Collin[4], R. Chambon[2], J. Desrues[2]

[1]*Delft University of Technology, Section of Geo-Engineering, Delft, Netherlands*

[2]*Univ. Grenoble Alpes, 3SR, 38000 Grenoble, France*
[3]*CNRS, 3SR, 38000 Grenoble, France*
[4]*ArGEnCo dept, Univ. of Liège, 4000 Liège, Belgium*

Abstract

The principle of deep geological repositories for the disposal of radioactive waste relies among others on the low permeability of the host rock. As the permeability is influenced by mechanical damage of the material, the coupling between hydraulic and mechanical behaviour of the host rock is of importance in the study of radioactive waste repositories. In this context an approach is investigated for the modelling hydro-mechanical coupled behaviour of Callovo-Oxfordian claystone, a potential host rock for repositories in France. The presented approach is a double-scale finite element method (FE^2) using a representative elementary volume (REV) to model the material behaviour at the micro-scale. The global response of this REV serves as a homogenised numerical constitutive law for the macro-scale, to be used in the modelling of the excavation damaged zone (EDZ) around the repository galleries.

The double-scale model

On the macro-scale, a poro-mechanical continuum is defined with fully coupled hydro-mechanical behaviour. Boundary value problems (BVP) are solved using the finite element method, regularized using a local second gradient model [1].

On the micro-scale, the microstructure of the material in the REV contains elastic deformable solids separated by cohesive interfaces, thereby allowing material softening with deformation. Additionally, the interfaces form a porous network allowing fluid transport prescribed by the variation in interface opening. With fluid pressure acting on the solid parts, this gives a coupled hydro-mechanical system at the micro level.

The two scales are linked in the framework of computational homogenization [4,2]. This technique provides a consistent scale transition, taking into account the homogenization of a granular microstructure to a macroscale continuum (Figure 1).

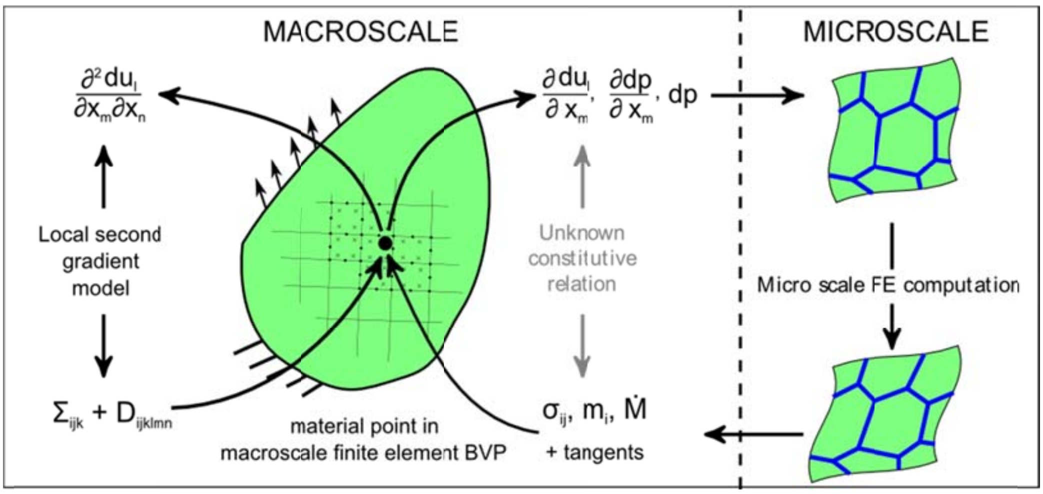

Figure 1: Outline of the double-scale model for hydro-mechanical coupling in the framework of computational homogenization with a poro-mechanical continuum at the macroscale and a granular microstructure with pore channels at the microscale [2].

Modelling approach to the benchmark exercise

The double scale approach was applied on the modelling of a modelling benchmark exercise related to the excavation damaged zone around [5]. Modelling the excavation process in 2D by means of unloading the gallery wall in the numerical model over a period of 28 days. The boundary conditions for unloading correspond to the in-situ conditions during excavation of a gallery in Callovo-Oxfordian claystone, characteristic for the Underground Research Laboratory (URL) in Bure, Marne/Haute-Meuse, France. The time-dependent response to this unloading is modelled for a period of 100 years.

The microstructure in the REV is used to model the behaviour of the claystone at the level of inclusions embedded in the clay matrix. Microstructure geometries and constitutive behaviour are calibrated against microstructural experimental results and laboratory tests. The double-scale modelling is then used to predict the full-field, macroscopic distribution of fluid pressures, deformations and material properties such as permeability.

Results

The presented results cover the first 1,5 years of excavation, during which most of the response to excavation takes place in the numerical simulation. A comparative study between modelling results and in-situ measurements with respect to gallery convergence, pore pressure response and the enhancement of permeability is made. This comparison is used to evaluate the capabilities of the double-scale model in capturing the behaviour of the excavation damaged zone around galleries during and after excavation.

The influence of the microstructure is studied in term of onset and pattern of strain localisation. Figure 2 shows an example of displacements and pore pressures to excavation, demonstrating the distribution of strain localization. The specific pattern of active strain localization bands is demonstrated to be related to the anisotropy introduced by the microstructure.

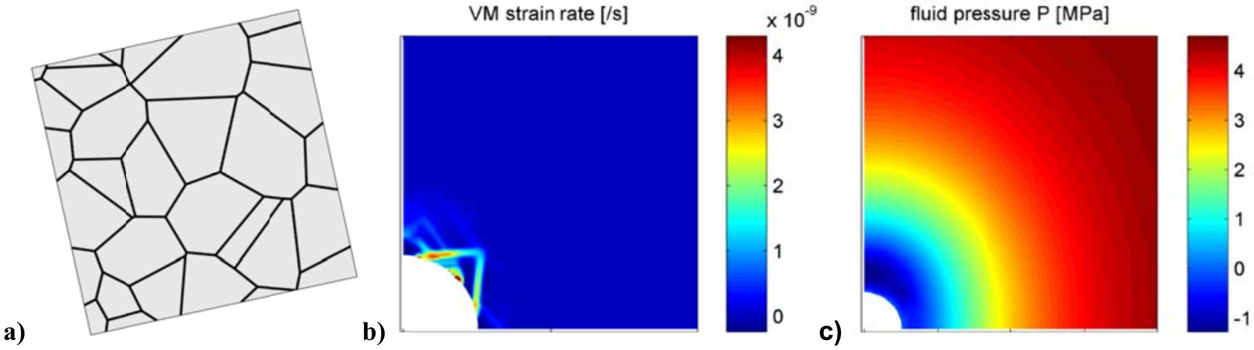

Figure 2: a) The initial microstructure. b) The Von-Mises equivalent strain rate 1,5 years after excavation. c) The pore pressure distribution 1,5 years after excavation [3].

Conclusion

The newly developed double-scale model proves applicable in engineering problems such as the benchmark project. Qualitative comparison with in-situ measurements of gallery convergence demonstrates that the method is able to capture different aspects of the hydro-mechanical behaviour of claystone and provides a tool for deriving complex material response from micromechanical behaviour with a reduced complexity. The model is able to make predictions for both deformations and pore pressure distributions, taking into account evolution of anisotropy in strength, stiffness and hydraulic conductivity.

Acknowledgments

The support of the French nuclear waste management agency (ANDRA) to this research is gratefully acknowledged.

References

[1] F. Collin, R. Chambon,R. Charlier, 2006. “A finite element method for poro mechanical modelling of geotechnical problems using local second gradient models” *International Journal for Numerical Methods in Engineering*, 65 (11), 1749–1772.

[2] A.P. van den Eijnden, “Multiscale modelling of the hydromechanical behaviour of argillaceous rocks”, *PhD Thesis*, Université Grenoble Alpes, France**,** 2015.

[3] A.P. van den Eijnden, P. Bésuelle, F. Collin, J. Desrues, “Modeling the strain localization around an underground gallery with a hydro-mechanical double scale model; effect of anisotropy”, *under review*

[4] V. Kouznetsova, W.A.M. Brekelmans, F.P.T. Baaijens, 2001. “An approach to micro-macro modeling of heterogeneous materials”. *Computational Mechanics* 27 (1), 37–48.

[5] D. Seyedi, G. Armand, A. Noiret, 2016. “’Transverse action’ - a model benchmark exercise for numerical analysis of the Callovo-Oxfordian clay-stone hydromechanical response to excavation operations”, *under review*

Multi-scale investigation of fracture apertures in clay rock subjected to desiccation

Anne-Laure Fauchille[1], Stephen Hedan[1*], Valery Valle[2], Dimitri Pret[1], Justo Cabrera[3], Philippe Cosenza[1]

[1] Université de Poitiers, CNRS UMR 7285 IC2MP, HydrASA, Ecole Nationale Supérieure d'Ingénieurs de POITIERS, Bât B27 - TSA 51106, 4, rue Michel Brunet 86073 Poitiers Cedex 9, France.

[2] Université de Poitiers, CNRS UPR 3346 Institut PPRIME, S.P. 2 M.I., Bd. M. et P. Curie, Téléport 2, B.P. 30179, 86962 Futuroscope Chasseneuil Cedex, France.

[3] DEI-SARG Department, Institute for Radiological Protection and Nuclear Safety, B.P. 17, 92262 Fontenay aux-Roses Cedex, France.

Abstract

In the laboratory, the desiccation fracture apertures in Tournemire clay rock were investigated at different scales (millimetre and centimetre) and compared to the variations of the average water content and mean strains of the sample. The induced hydric strains and desiccation fractures were monitored by digital image correlation (H-DIC). At the centimetre scale, the results revealed the fracture aperture kinematics were separated into a first phase of opening and closure, and a second phase of only gradual closure. Closure of the cracks was only observed at the millimetre scale, revealing that the kinematics of cracks depends on the scale observed. The interpretation of the entire dataset emphasizes the need for a multi-scale approach to understand and model desiccation cracking mechanisms and their associated hydric strains in clay rocks.

Introduction

Clay rocks have been considered as potential repositories for high-level radioactive wastes at great depth in several countries, because of their mechanical and microstructural properties. Nevertheless, a significant cracking due to a desaturation process of the argillaceous medium is observed on the gallery walls in several underground research laboratories, such as the experimental platform of Tournemire in France [1,2]. This desiccation cracking takes part in the so called excavation damaged zone (EDZ). The initiation and extension of the EDZ are governed by a range of parameters including the material anisotropy, the initial stress field, the geometry of the gallery and the mineralogy [3,4]. In the Underground Laboratory at Tournemire, the desiccation cracking at the decimetre scale is organised in a network of sub-horizontal cracks separated by 64-100mm and lying parallel to the bedding planes [1,5,6], and a vertical network which shows more complex orientations. The mean crack aperture of these cracks is correlated with the relative humidity in the gallery [5,7]. At a much lower scale, some desiccation fractures with apertures of 1 µm were observed under ESEM on Callovo-Oxfordian clays rocks from Bure laboratory (France) [8,9]. However, these observations were obtained at very different spatial scales, and the phenomenological links or causal relationships between the two scales of fracture network are unclear. Consequently, the main objective of this laboratory investigation was to provide new correlations between hydric strains, desiccation crack apertures and state variables (relative humidity (RH) and water content) at the millimeter and centimeter scales, which are rarely compared in the context of clay rocks. The methodology is based on the combination of a new experimental setup and a new DIC algorithm H-DIC [6] in order to allow the measurement of the kinematic field and patterns for the two considered scales to improve the identification of the micromechanisms governing desiccation cracking [10,11].

Material and Methods

A 20x20x20mm^3 cube of Tournemire clay rock (Aveyron, France) was used as the sample in this study. The sample was extracted from the FD90 drill core in the East 96 gallery, at a depth of 4.20-4.40 meters, where the rock is considered to be saturated and outside of the EDZ. The clay rock has a mineralogical composition of 20-50wt% clay minerals, 10-20wt% quartz, 10-30wt% carbonates and 2-7wt% sulphides [1].

The experimental setup is composed of an impermeable cell in which humidity and temperature are controlled by saline solutions and an air-conditioning unit at 22°C, respectively. Two cameras image a small zone of 5.5x4.1 mm on one face of the sample every two minutes at the millimetre scale (images of 2560x1980 pixels with a resolution of 2.2 µm^2.pixel^{-1}), and a large zone of 20x20 mm on another face (images of 2560x1980 pixels with a resolution of 10 µm.pixel^{-1}). The bedding planes are perpendicular to the camera planes. The sample was placed on Teflon© slices on a precision balance to obtain its average water content <ΔW>. The DIC software (X-Correl [6]) was used to calculate the mean plane strain ε_{is} (as a qualitative indicator of the volume) and fracture apertures [14,15] on these zones during a fast desiccation from 98 to 33% relative humidity (over 10 days), in free deformation conditions.

Results and Discussion

During desiccation, different types of fractures were defined as a function of the scale, their orientation relative to the sample bedding planes and their continuity in the zones at the beginning of the test (**Table 1**).

Type of fracture	Number of fractures analyzed	Zone	Orientation relative to Bedding planes	Continuity
I	2 *(I-1 and I-2)*	Large zone (centimetre scale)	parallel	Crossing the large zone
II	3 *(II-1, II-2 and I-3)*			Not crossing the large zone
III	1 *(III-1)*		perpendicular	Connected to types I and II
IV	3 *(IV-1, IV-2 and IV-3)*	Small zone (millimetre scale)	parallel	Crossing the small zone

Table 1 : Definition of the different types of desiccation fractures.

Figure 1 shows the crack aperture as a function of compared to the average water content and the mean strain of the sample during the desiccation process (**Figure 1**).

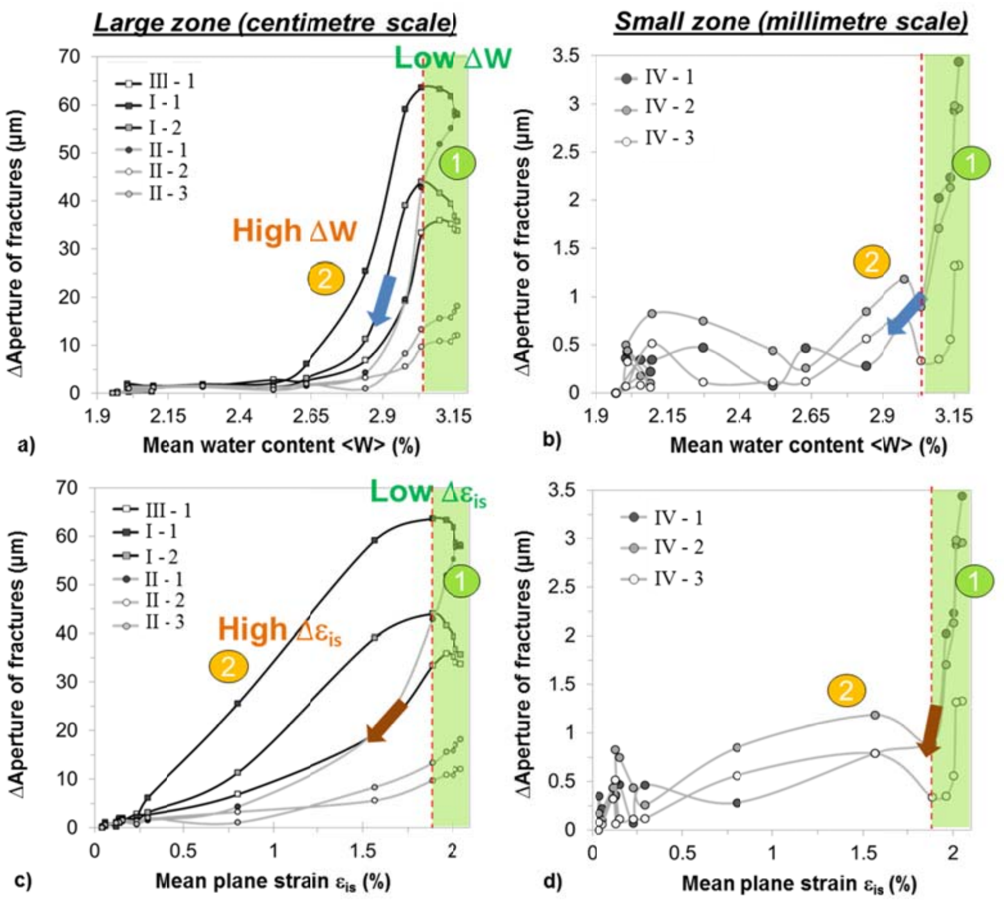

Figure 1 : Variation of the fracture apertures as a function of a) <ΔW> on the large zone, b) <ΔW> on the small zone, c) ε_{is} on the large zone and d) ε_{is} on the small zone, during desiccation and for different types of fractures [10,11].

The desiccation of the sample is divided in two important steps (Figure 1). At the centimetre scale, Step 1 is characterised by the simultaneous opening of types I and III and the closure of type II, whereas all fractures are closing at the millimetre scale (type IV). The loss of water content is very low (3.16 to 3.00%), as is the mean strain reduction (2.1 to 1.8%). This step was interpreted as a desiccation only on the surface of the sample. The fracture opening and closure cause opposing deformation from the shrinkage of the solid matrix, leading to the low reduction of the mean strain [10,11].

At both scales, Step 2 is characterised by an important closure of all cracks, with large reduction in water content and mean strain. This step is interpreted as desiccation deep inside the sample, causing a global shrinkage.

Conclusion

During a fast desiccation process from 98 to 33% relative humidity, the apertures of different types of fractures were quantitatively compared to the average water content and the mean plane strain of a Tournemire clay rock sample. In free conditions of deformation, the results highlight two important steps of desiccation: a first step of simultaneous opening and closure of cracks, and a second step with closure of all fractures. These two steps correspond to the progression of the desiccation from the surface to the centre of the sample. These results were compared to other scales and desiccation processes [10,11], and the microstructure of the sample was mapped over the entire small zone allowing quantitative comparison between the local strains and the proportion of rigid inclusions and clay matrix [11].

Acknowledgments

The authors acknowledge the NEEDS-MIPOR program (Nucléaire, Energie, Environnement, Déchets, Société-MIlieux POReux) and the French Institute for Nuclear Safety and Radioprotection (IRSN) for supporting and funding this work. The authors are also grateful to P.Touvenet, P.Rogeon, C.Laforest, F.Limousin and M.Chandler for technical assistance.

References and Citations

[1] J.Cabrera, C.Beaucaire, G.Bruno, L.De Windt, A.Genty, N.Ramambasoa, A.Rejeb, S.Savoye, P.Volant. *Projet Tournemire : Synthèse des Résultats des Programmes de Recherche 1995/1999*, IRSN Report, 2001.

[2] J.M.Matray, S.Savoye, J.Cabrera. *Desaturation and structure relationships around drifts excavated in the well-compacted Tournemire's argillite (Aveyron, France).* Eng. Geol. 90, 1-16, 2007.

[3] P.Bossard, M.P.Meier, A.Moeri, T.Trick, J.C.Major. *Geological and hydraulic characterisation of the excavation disturbed zone in the Opalinus Clay of the Mont Terri Rock Laboratory*, Eng. Geol. 66 (1-2), 19-38, 2002.

[4] C.F.Tsang, F.Bernier, C.Davies. *Geohydromechanical processes in the Excavation Damaged Zone in crystalline rock, rock salt, and indurated and plastic clays - In the context of radioactive waste disposal*. Int. J. of Rock Mech. and Min. Sci. 42(1), 109-125, 2005.

[5] S.Hedan, A.L.Fauchille, V.Valle, J.Cabrera, P.Cosenza. *One-year monitoring of desiccation cracks in Tournemire argillite using digital image correlation*, Int. J. Rock Mech. Min. Sci., 68, 22-35, 2014.

[6] V.Valle, S.Hedan, P.Cosenza, M.Berdjane, A.L.Fauchille, *Digital Image Correlation Development for the Study of Materials Including Multiple Crossing Cracks*, Experimental Mechanics 55, 379-391, 2015.

[7] D.Bailly, J.M.Matray, R.Ababou. *Temporal behavior of a ventilated claystone at the Tournemire URL: Cross-spectral analyses focused on daily harmonics*. Engineering Geology 183, 137-158, 2014.

[8] L.Wang, M.Bornert, S.Chanchole, D.S.Yang, E.Héripré, A.Tanguy, D.Caldemaison. *Microscale experimental investigation of the swelling anisotropy of the Callovo-Oxfordian argillaceous rock*, Clay Minerals 48, 391-402, 2013.

[9] L.Wang, M.Bornert, E.Héripré, D.S.Yang, S.Chanchole. *Irreversible deformation and damage in argillaceous rocks induced by wetting and drying*, Journal of Applied Geophysics 107, 108-118, 2014.

[10] A.L.Fauchille, S.Hedan, V.Valle, D.Pret, J.Cabrera, P.Cosenza. *Multi-scale study on the deformation and fracture evolution of clay rock sample subjected to desiccation,* Accepted for publication in Applied Clay Science, 2016.

[11] A.L.Fauchille. Déterminismes microstructuraux et minéralogiques de la fissuration hydrique dans les argilites de Tournemire : apports couples de la pétrographie quantitative et de la corrélation d'images numériques, PhD thesis of the University of Poitiers (France), 2015.

Relationships between cracking, strains and proportions of clay matrix and rigid inclusions in Tournemire clay rock

Anne-Laure Fauchille[1], Stephen Hedan[1*], Valery Valle[2], Dimitri Pret[1], Justo Cabrera[3], Philippe Cosenza[1]

[1] *Université de Poitiers, CNRS UMR 7285 IC2MP, HydrASA, Ecole Nationale Supérieure d'Ingénieurs de POITIERS, Bât B27 - TSA 51106, 4, rue Michel Brunet 86073 Poitiers Cedex 9, FRANCE.*

[2] *Université de Poitiers, CNRS UPR 3346 Institut PPRIME, S.P. 2 M.I., Bd. M. et P. Curie, Téléport 2, B.P. 30179, 86962 Futuroscope Chasseneuil Cedex, France.*

[3] *DEI-SARG Department, Institute for Radiological Protection and Nuclear Safety, B.P. 17, 92262 Fontenay aux-Roses Cedex, France.*

Abstract

A clay rock sample from the Tournemire Underground Research Laboratory (Averyon, France) was subjected to a fast desiccation in the laboratory, from 98 to 33% relative humidity. At the millimetre scale, fracture locations were identified and desiccation strains and fracture apertures were calculated by digital image correlation on a surface of 5.5x4.1 mm^2. After the desiccation, the microstructure of this surface was mapped under scanning electron microscopy by a large mosaic of back scattered electron images in high resolution. The aim of the study is a quantitative comparison between local strains and crack apertures to the local proportion of clay matrix and rigid inclusions of the sample, in order to understand better the role of microstructure in desiccation mechanisms in clay rocks. The results have shown that: a) the crack apertures are heterogeneous and seem to be higher at some interfaces between rigid inclusions and matrix, and b) the strains are heterogeneous and their intensity is not directly related to the proportion of clay matrix at the millimetre scale. The interpretation of the dataset emphasizes the need for a microstructural approach to understand and model desiccation deformation and cracking mechanisms in clay rocks.

Introduction

Clay-rocks are of interest as a medium for nuclear waste disposal at great depth because of their mechanical and microstructural properties. Significant cracking due to desaturation of the argillaceous medium is observed on the gallery walls of the Underground Laboratory of Tournemire (Aveyron, France). This important cracking takes part in the so called excavation damaged zone (EDZ). The initiation and extension of the EDZ are governed by different parameters such as the material anisotropy, the initial stress field, the geometry of the gallery and the mineralogy [1-3]. The desiccation cracking is oriented in a network of sub-horizontal cracks separated by 14-60 mm and lying parallel to the bedding planes [4,5] as well as a vertical network which shows more complex orientations. The mean crack aperture of these fractures is correlated with the relative humidity in the gallery [5], and with the average water content in the laboratory at the centimetre and millimetre scales [6]. In the laboratory, the sub-horizontal desiccation cracks are located in the clay matrix adjacent to hard grain heterogeneities such as a high local proportion of coarse grains or a high concentration of large quartz or carbonate grains [7]. At each scale, the majority of desiccation cracks are in the same orientation as the bedding planes. Moreover, the desiccation deformation of clay rocks is often significantly higher perpendicular to the bedding planes [8-11], which demonstrates a close relationship between the deformation and cracking behaviour of the rock, and the microstructure. During desiccation, some authors [11,12] interpret the high deformations of clay rocks as corresponding to high proportions of clay matrix, and the low deformations by high proportions of coarse grains. However, these observations were qualitative. The aim of this paper is to study the relationship between the deformation and cracking behaviour and the microstructure using a quantitative approach [7,14].

Material and Methods

The sample used in this study is a 20x20x20 mm^3 cube of Tournemire clay rock (Aveyron, France) extracted from the FD90 drill-core in the East 96 gallery, at a depth of 4.20-4.40 meters where the rock is considered to be saturated and outside of the EDZ. The rock has a mineralogical composition of 20-50wt% clay minerals, 10-20wt% quartz, 10-30wt% carbonates and 2-7wt% sulphides [4]. The experimental setup consists of an impermeable box in which humidity and temperature conditions are controlled by saline solutions and an air-conditioning unit at 22°C, respectively. One camera images a 5.5x4.1mm^2 surface (2560x1980 pixels with a resolution of 2.2 µm.pixel^{-1}) every two minutes at the millimetre scale. The bedding planes are perpendicular to the surface. The DIC software (X-Correl [13]) was used to calculate the fracture aperture and strains during a fast desiccation between 98 to 33% relative humidity (over 10 days), in free deformation conditions. After desiccation, the microstructure of the sample surface was mapped by a mosaic of 153 back-scattered electron images (1024x768 pixels, with a resolution of 0.625 µm.pixel^{-1}) under a scanning electron microscope. The electron beam was quantified in terms of displacement, deformation, rotation and grey levels to assemble the images [14] and segment the clay matrix and rigid inclusions [15].

Results and Discussion

Comparison between the local crack aperture and the proportion of clay matrix

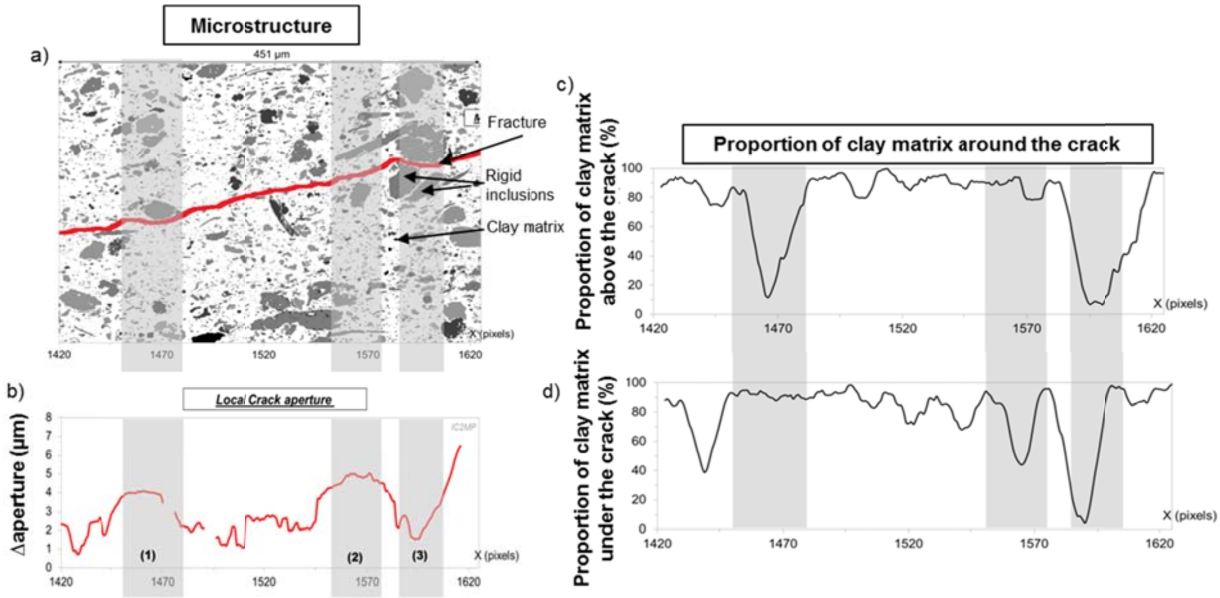

Figure 1 : a) Extract of the map of the microstructure, b) Profile of the crack aperture variations between the beginning and end of the desiccation corresponding to image a), c) Proportion of clay matrix above the crack, d) Proportion of clay matrix under the crack, vs. X coordinates [14].

The local crack aperture was compared to the local proportion of clay matrix along a desiccation crack of 205 pixels length (451µm) (Figure 1). The clay matrix proportion is calculated on each side of the crack, in successive areas of 90 pixels (22x19.8µm^2) along the crack. Other sizes of successive areas and other zones of cracks were tested [14]. The local crack aperture and the proportion of clay matrix around the crack are heterogeneous at the study scale with values between 0.5 to 7 µm, and. The proportion of clay matrix is also heterogeneous above and beneath the crack (Figure 1c to d). In two domains (Figure 1b, (1) X=1455-1480, and (2) X=1555-1580 pixels), the local crack aperture increases significantly where there is an interface between a clay-rich zone and a hard grain zone. For the first domain, such an interface is characterized by a clay matrix proportion of 13% above the crack and 92% beneath the crack. For the second domain, the clay matrix proportions are respectively 88% and 45% above and beneath the crack. In a third domain (Figure 1b, (3) X=1585-1610), the crack aperture is very narrow with a minimum of 1.5µm. Large hard grains are adjacent to the crack (Figure 1a) so the clay matrix proportion is very low on both sides of the crack with values up to 8% above the crack and 6.5% beneath the crack (Figures 1c and d). This interface between large coarse grains could obstruct the crack opening during the desiccation process. Nevertheless, the crack analysed here also presents other narrow apertures, such as between X=1480-1510 or for X<1430 pixels, whereas the proportion of clay matrix is higher than 80% on either sides of the crack. In this case, the relationship between the clay proportion and the crack aperture is not entirely well-understood.

Comparison between the strains and the proportion of clay matrix and rigid inclusions

In the same surface, the local principal strains were superimposed onto the local proportion of rigid inclusions. Our results demonstrate a high variability of strain values from -0.04 to 0.20 with a significant concentration of values between 0.02 and 0.04. At the millimetre scale, a low proportion of rigid inclusions (from 8 to 40%, with a high proportion of clay matrix, (from 60% to 98%) are not seen to correspond to high strains but to very variable strains. At the microscopic scale, [11,12] the different desiccation strain intensities of clay rocks are explained by different proportions of clay matrix and hard grains. A high proportion of clays causes larger deformations. In our experimental conditions, our study suggests that there is not an objective relationship between the intensity of strains and the proportion of hard grains and clay matrix at the millimetre scale.

Conclusion

The crack apertures and the strains were quantitatively compared to the microstructure during a desiccation process in the laboratory. At the mesoscopic scale, a simple relationship between the desiccation crack aperture, the strain intensity and the microstructure is not obvious. Contrary to the literature, the results obtained in this study focused on the fact that a high proportion of clay matrix is not correlated to a high deformation or a high crack aperture and vice versa. However, the interface between clayey and rich hard grain zone seems to be correlated to a local crack opening because of an important incompatibility of local deformation.

Acknowledgments

The authors would like to express their acknowledgment to the NEEDS-MIPOR program (Nucléaire, Energie, Environnement, Déchets, Société-MIlieux POReux) and to the French Institute for Nuclear Safety and Radioprotection (IRSN) for supporting and funding this work. They are also grateful to M. Pascal Touvenet, M. Pascal Rogeon, M. Claude Laforest, M. Frédéric Limousin and M.Chandler for their technical help.

References

[1] P.Bossard, M.P.Meier, A.Moeri, T.Trick, J.C.Major. *Geological and hydraulic characterisation of the excavation disturbed zone in the Opalinus Clay of the Mont Terri Rock Laboratory*, Eng. Geol. 66 (1-2), 19-38, 2002.

[2] D.Charpentier, R.Mosser-Ruck, M.Cathelineau, D.Guillaume. *Oxidation of Mudstone in a Tunnel (Tournemire, France): Consequences for the Mineralogy and Chemistry of Clays Minerals.* Clay Minerals 39, 135-149, 2004.

[3] P.Blüming, F.Bernier, P.Lebon, C.D.Martin. *The Excavation-Damaged Zone in clay formations - Time-dependent behaviour and influence on performance assessment*. Phys. Chem. Earth 32, 588-599, 2007.

[4] J.Cabrera, C.Beaucaire, G.Bruno, L.De Windt, A.Genty, N.Ramambasoa, A.Rejeb, S.Savoye, P.Volant. *Projet Tournemire : Synthèse des Résultats des Programmes de Recherche 1995/1999*, IRSN Report, 2001.

[5] S.Hedan, A.L.Fauchille, V.Valle, J.Cabrera, P.Cosenza. *One-year monitoring of desiccation cracks in Tournemire argillite using digital image correlation*, Int. J. Rock Mech. Min. Sci., 68, 22-35, 2014.

[6] A.L.Fauchille, S.Hedan, V.Valle, D.Pret, J.Cabrera, P.Cosenza. *Multi-scale study on the deformation and fracture evolution of clay rock sample subjected to desiccation,* Accepted for publication in Applied Clay Science, 2016.

[7] A.L.Fauchille, S.Hedan, D.Prêt, V.Valle, J.Cabrera, P.Cosenza. *Relationships between desiccation cracking behavior and microstructure of the Tournemire clay rock by coupling DIC and SEM methods.* Proceedings of IS-Cambridge, Geomechanics from Micro to Macro 1-3 Sept. 2014, (2), 1421-1424, 2014.

[8] F.Valès, D.Nguyen Minh, H.Gharbi, A.Rejeb. *Experimental study of the influence of the degree of saturation on physical and mechanical properties in Tournemire shale (France)*. App. Clay Sci. 26, 197-207, 2004.

[9] Q.T.Pham, F.Vales, L.Malinsky, M.D.Nguyen, H. Gharbi. *Effets of desaturation-resaturation on mudstone*, Physics and Chemistry of the Earth 32, p646-655, 2007.

[10] T.Guillon, R.Giot, A.Giraud, G. Armand. *Response of Callovo-Oxfordian claystone during drying tests : unsaturated hydromechanical behavior*, Acta Geotechnica 7, p313-332, 2012.

[11] L.Wang. *Micromechanical experimental investigation and modeling of strain and damage of argillaceous rocks under combined hydric and mechanical loads*, PhD thesis of Ecole Polytechnique (France), 2012.

[12] G.Montes-H. Etude experimentale de la sorption d'eau et du gonfle;ent des argiles par microscopie electronique a balayage environnementale (ESEM) et l'analyse digitale d'images, PhD thesis of the University of Strasbourg, France

[13] V.Valle, S.Hedan, P.Cosenza, M.Berdjane, A.L.Fauchille, *Digital Image Correlation Development for the Study of Materials Including Multiple Crossing Cracks*, Experimental Mechanics 55, 379-391, 2015.

[14] A.L.Fauchille. Déterminismes microstructuraux et minéralogiques de la fissuration hydrique dans les argilites de Tournemire : apports couples de la pétrographie quantitative et de la corrélation d'images numériques, PhD thesis of the University of Poitiers (France), 2015.

[15] D.Prêt D., S.Sammartino, D.Beaufort, A.Meunier, L.Michot. *A new method for quantitative petrography based on image processing of chemical element maps: I. Mineral mapping applied to compacted bentonites*, American Mineralogist, 95, p1379-1388, 2010a.

Intrinsic dissolution rate determination of vitrified high level waste

Adam J. Fisher, Claire L. Corkhill, Russell J. Hand & Neil C. Hyatt

Department of Materials Science & Engineering, The University of Sheffield, Mappin Street, Sheffield S1 3JD, United Kingdom

Abstract

We present the results of an investigation of a kinetic analysis of the dissolution of the International Simple Glass (ISG), a reference high level waste (HLW) simulant base glass used by a collaborative group of nations interested in the advancement of glass dissolution knowledge. Using the Single-Pass-Flow-Through (SPFT) method we have determined the surface area to flow-rate dependence of ISG dissolution at 40 ^{o}C and pH 9, in preparation for an analysis of the temperature and pH dependence of dissolution in the range 40 – 80 ^{o}C and pH 7 to 11. Through application of the Transition State Theory, we will be able to extract the fundamental parameters necessary to model the dissolution kinetics; activation energy (E_a), pH power law coefficient (η) and the intrinsic rate constant (k_0). These results are discussed in comparison with those obtained on the same glass using the micro-channel flow through method [1] and also with those for a UK simulant nuclear waste glass [2].

Introduction

The UK's vitrified HLW from the reprocessing of spent nuclear fuel is destined for final disposal in a geological disposal facility. In this scenario, the release of radionuclides to the geo-sphere and bio-sphere will be controlled by the dissolution of the glass matrix. Developing an understanding of glass dissolution is therefore critical to building a robust safety case for geological disposal. In particular, an assessment of the kinetics of glass dissolution is required as a function of the long-term conditions expected within the repository, e.g. under relevant temperature and groundwater pH environments.

Attempting to model the dissolution kinetics (through the application of Transition State Theory) and to predict the fate of radionuclides in a disposal setting requires obtaining fundamental parameters of the glass under investigation; activation energy (E_a), pH power law coefficient (η) and the intrinsic rate constant (k_0). Accessing such parameters is only achievable by measuring the forward (intrinsic) dissolution rate, which is the maximum rate at which glass can dissolve under non-saturated conditions. Dynamic SPFT, described in Figures 1 & 2, is the primary method for gleaning such information.

The motivation for this study was to extract the inherent dissolution parameters from the ISG (a six-component, non-active alumino-borosilicate reference glass for nations collaborating on HLW dissolution [3], see Figure 3) which will be used as a baseline comparison for simulant UK HLW.

Figure 1: The SPFT set-up at The MIDAS facility at the Immobilisation Science Laboratory at The University of Sheffield, UK.

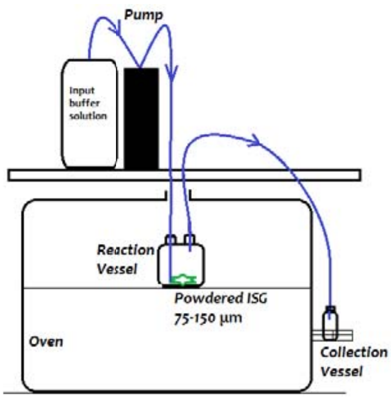

Figure 2: A schematic of the SPFT set-up. Solution flows at a constant rate throughout.

Figure 3: The International Simple Glass used by nations collaborating on HLW glass dissolution studies: France, USA, Japan, Belgium, UK and Germany. In mol %: SiO_2 45.4, B_2O_3 24.1, Na_2O 19.1, Al_2O_3 5.8, CaO 4.3, ZrO_2 1.3.

Methods

A suite of three syringe pumps connected to four reactor vessels containing powdered ISG (75 -150 µm sized particles) were used (see Figures 1 & 2). Reactor vessels were placed inside ovens. A variety of flow-rates were dispensed by the pumps (from 10 ml/d – 80 ml/d) in order to influence the chemical potential between the glass and solution. Exploring combinations of three temperatures (40, 60 and 80 ^{o}C) and three pH units (7, 9, and 11) provide forward dissolution rate measurements, which then allow for the determination of the fundamental parameters required to model the dissolution kinetics.

Samples were collected every two days per flow-rate applied, for a total period of 30 days and were analysed by Inductive Coupled Plasma - Optical Emission Spectroscopy (ICP-OES) to determine solution concentrations of Si, B and Na. From these values, dissolution rates at steady-state conditions (i.e. when glass dissolution becomes invariant with respect to time) were derived.

Results/Discussion

Steady-state conditions were met between 15-20 days (see Figure 4 for an example at a flow-rate of 40 ml/d).

Steady-state dissolution rates are expected to be constant at higher flow-rates, therefore signifying the forward dissolution rate i.e. the maximum dissolution rate (seen as a plateau on a plot of dissolution rate vs flow-rate). Hence, this shows the importance of obtaining steady-state dissolution rates over a range of flow-rates (see Figure 5).

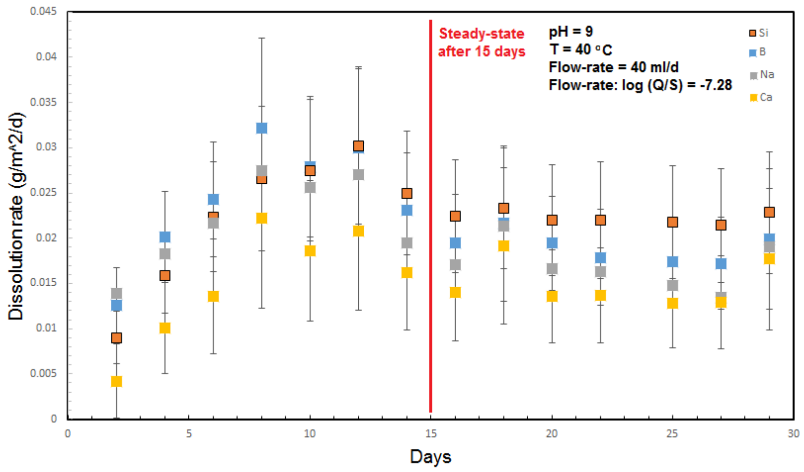

Figure 4: Plot of dissolution rate (based on Si, B, Na and Ca release) versus days for a sample subject to a mid solution flow-rate (40 ml/d). The dissolution rate obtained is likely to be that of the forward dissolution rate (see flow-rate Log Q/S = -7.28 in Figure 5). Steady-state dissolution rates were congruently observed after 15 days.

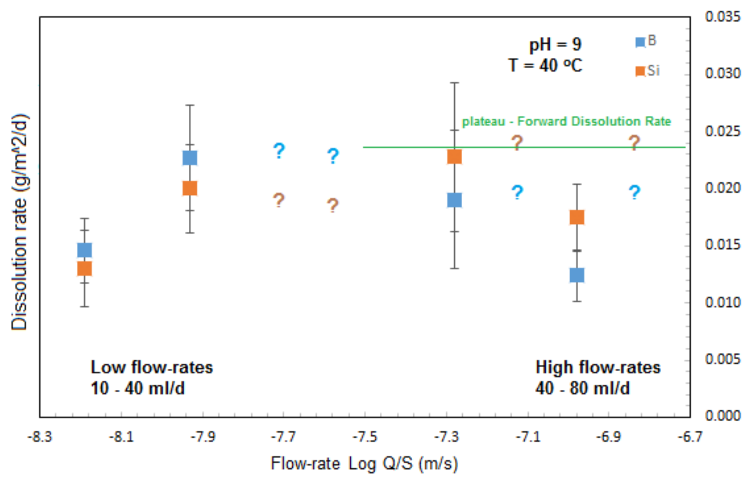

Figure 5: Plot of dissolution rate (based on B and Si release) versus flow-rate in units of m/s. The plateau represents the expected forward dissolution rate. Question marks denotes flow-rates currently under investigation.

Conclusion

The forward dissolution rate of a model simulant high level waste glass under a variety of conditions (pH and temperatures) relevant to the geological disposal of nuclear waste is under investigation. The fundamental parameters necessary to model the dissolution kinetics based on Transition State Theory (activation energy (E_a), pH power law coefficient (η) and the intrinsic rate constant (k_0)) will be obtained. In the future, this approach will be used on Zn/Ca-bearing UK HLW simulant glasses to strengthen the safety case for a geological disposal facility in the UK by reducing the uncertainty associated with the dissolution rate of these materials and by modelling and predicting the radionuclide release rate under a variety of conditions potentially expected upon final disposal, in an as yet undecided location.

Acknowledgements

Thanks to the funders of this project: Engineering and Physical Science Research Council (EPSRC), Radioactive Waste Management (RWM), Next Generation Nuclear Centre for Doctoral Training.

References and Citations

[1] Inagaki *et al*. "Initial dissolution rate of the international simple glass as a function of pH and temperature measured using the microchannel flow-through test method", *International Journal of Applied Glass Science* 4 [4] 317-327, 2013.

[2] Cassingham *et al*. "The initial dissolution rate of simulated UK Magnox-THORP blend nuclear waste glass as a function of pH, temperature and waste loading", *Mineralogical Magazine* 79 [6] 1529-1542, 2015.

[3] S. Gin *et al*, "An international initiative on long-term behaviour of high-level nuclear waste glass", *Materials Today*, Vol. 16, No. 6, pp. 243-248, 2013.

Numerical study of bentonite confined hydration

Giulia M. Ghiadistri

Department of Civil & Environmental Engineering, Imperial College London

Abstract

A numerical study of MX-80 bentonite confined hydration has been carried out. The results have been analysed in the light of the limits of applicability of the constitutive model used, a modified Barcelona Basic Model, and the available experimental data to characterise the material.

Introduction

Studying bentonite re-saturation is a challenging task, as it involves swelling upon wetting from groundwater in the host formation and shrinkage induced by heat coming from the energy generated by the nuclear waste in the container. Nevertheless, a good understanding of the phenomenology involved is important to build confidence in modelling the long-term behaviour of the Engineered Barriers Systems (EBS) for nuclear waste disposal.

One of the disposal concepts being considered in the UK is to dispose of High Level Waste (HLW) and Spent Fuel in containers surrounded by a buffer material consisting of bentonite. Bentonite's capacity to swell provides a low hydraulic conductivity barrier and protection of the container.

Hence, it is of paramount importance to understand and be able to reproduce numerically the hydro-mechanical (HM) interaction as a key to the swelling of the buffer. As a first step, this study aims at reproducing a column re-saturation test (Marcial et al., 2008).

Methods

For the investigation of the behaviour of unsaturated soils, a commonly adopted HM constitutive model is the Barcelona Basic Model (BBM) (Alonso et al., 1990). A modified BBM version (Georgiadis et al., 2005 and Tsiampousi et al., 2013) is currently implemented in the Imperial College Finite Elements Program (ICFEP, Potts & Zdravkovic, 1999), which is the main research tool of the current research project. Despite being widely used for modelling unsaturated soils, the BBM-type framework was not conceived for highly expansive materials: therefore its use for the analysis of bentonite behaviour is preceded by an extensive calibration against various sets of oedometric studies in order to somewhat foresee the possible shortcomings of the analyses.

Results/Discussion

Calibration of the BBM is carried out by exploiting laboratory data on bentonite, obtained from different experimental set-ups in order to evaluate the material behaviour under different boundary conditions and suction ranges. The outcomes from calibration provide insights for the interpretation of the column infiltration analysis (Marcial et al., 2008).

Calibration

From the analysed data, the results from Tang et al. (2008) and Villar (2005) are presented hereafter: the former studies the laterally unconfined swelling of a sample of MX-80 bentonite under low nominal vertical load, followed by a loading phase at a constant and relatively high suction; the latter shows the laterally confined wetting followed by loading at constant and very low suction.

The analyses have yielded the following results:

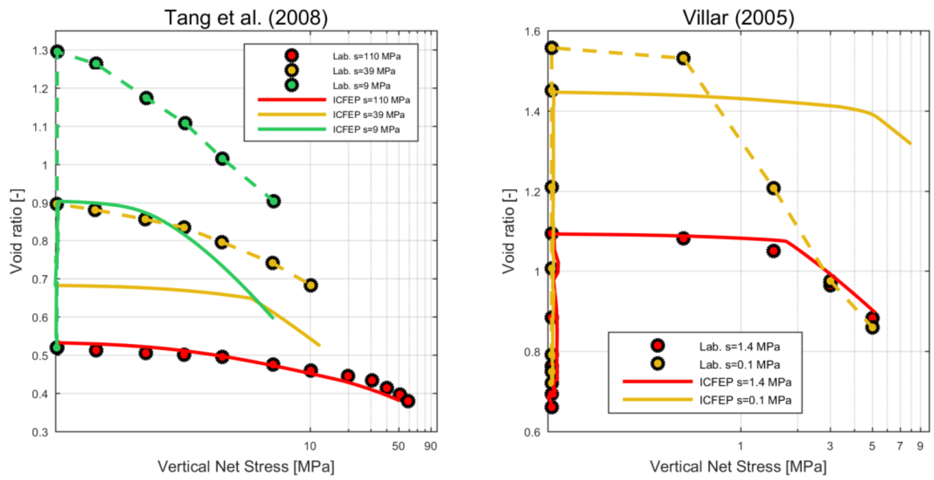

Figure 1: Results from Tang et al. (2008) on the left; from Villar (2005) on the right.

Figure 1, showing the evolution of void ratio in the sample with increasing vertical net stress, highlights two critical points: (i) under laterally unconfined boundary conditions the model does not capture well the amount of volumetric expansion of the material during the wetting phase; (ii) the rate of increase of swelling strains with suction becomes larger when the lower values of suction are reached (Gens et al., 1992).

Column re-saturation

This infiltration test by Marcial et al. (2008) was performed under constant volume conditions on compacted MX80 bentonite at initial suction of $103\ MPa$. The saturation has continued for 7 months. Selected results from the analysis are reported below:

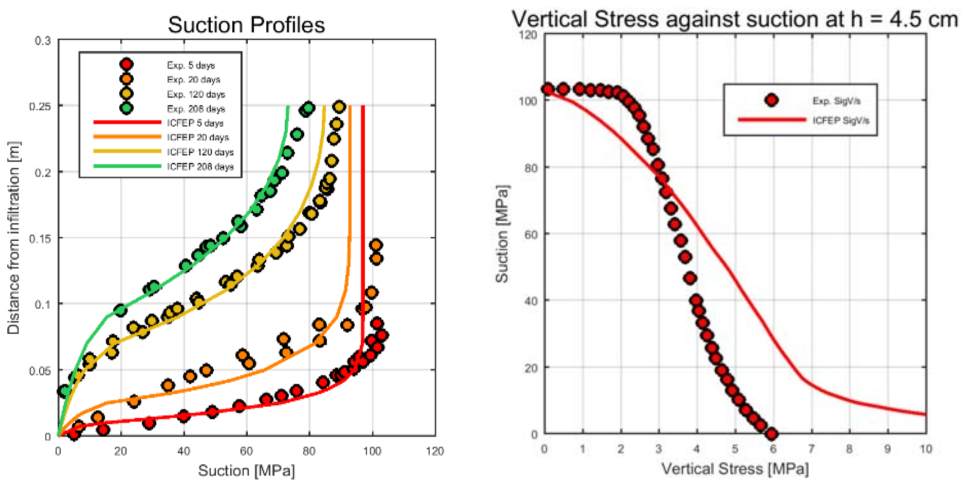

Figure 2: Suction profiles along vertical sections of the sample at different times, on the left; vertical stress against suction in a horizontal section of the sample, on the right.

The suction profiles show how the advancement of the water front throughout the sample is well reproduced in time: the hydraulic aspect of the test seems therefore well simulated. Nevertheless, the mechanical problem raises concern since the swelling pressures are considerably overestimated, especially at low suctions.

The causes of mismatch

Among the probable causes of the stress overestimation, there is the inability of the model to properly capture the volumetric expansion of the material, hence its plastic strains. Capturing these strains more accurately may come from applying two improvements:

(i) The BBM-type formulations suffer from limitations in modelling the behaviour of very expansive soils (such as bentonite). Consequently, the Barcelona Expansive Model (BExM) was conceptually introduced (Gens &

Alonso, 1992) and then fully developed (Alonso et al., 1999) to enable the modelling of such soils. BExM improves on its predecessor by taking into account a double porosity microstructure, typical of expansive soils, by considering two levels of structure interacting. A one-way interaction between these two levels constitutes an additional plastic mechanism that adds to the plastic macro-strains computation.

(ii) The input data for the model may present shortcomings. Whereas elastic strains are governed by elastic compressibility coefficient obtained from the observed oedometric studies, plastic strains are computed from the derivatives of the yield surface and the plastic potential. Their shapes can be investigated through triaxial tests, which are not often performed in experimental studies of bentonite. In the modified BBM implemented in ICFEP two fitting parameters for the shape of the yield surface and the plastic potential could be calibrated, nevertheless the lack of available data leads to assuming an associated Modified Cam Clay ellipse. This could be an unrealistic assumption and a source of error that spreads, throughout the constitutive relationships and hardening law, from the strains to the stresses.

Conclusions

A numerical study of MX-80 bentonite confined hydration has been carried out. Results have been satisfying in terms of hydraulic, but not accurate for the mechanical aspect of behaviour, as the swelling pressures are overestimated. Given the expansive nature of the material, the constitutive model employed, a modified Barcelona Basic Model, has been used outside its limits of applicability. Hence the results can be improved by updating the framework to a form of a BExM-type model that takes into account the double porosity structure of swelling clays. However additional improvement could also come from refining the model calibration with more laboratory data, especially triaxial tests that would help to better define the yield surface shape.

Acknowledgments

The author is grateful to Prof. Lidjia Zdravkovic, Prof. David Potts and Dr. Katerina Tsiampousi for their guidance and help on this project. The financial support of Amec Foster Wheeler and RWM UK is greatly appreciated.

References and Citations

[1] E.E. Alonso, A. Gens and A. Josa, “A constitutive model for partially saturated soils”. *Géotechnique*, Vol. 40, No. 3, pp. 405–430, 1990.

[2] E.E. Alonso, J. Vaunat, and A. Gens, “Modelling the mechanical behaviour of expansive clays”, *Engineering Geology,* Vol. 54, No.1-2, pp.173-183, 1999.

[3] A. Gens. and E.E. Alonso, “A framework for the behaviour of unsaturated expansive clays”, *Canadian Geotechnical Journal,* Vol. 29, No. 6, pp.1013-1032, 1992.

[4] K. Georgiadis, D.M.Potts and L. Zdravkovic, “Three-dimensional constitutive model for partially and fully saturated soils”, *Int J Geomech*, Vol. 5, No. 3, pp. 244–55, 2005.

[5] D. Marcial, P. Delage and Y. J. Cui, “*Hydromechanical couplings in confined MX80 bentonite during hydration*”. 1st European Conference on Unsaturated Soils, E-UNSAT 2008, 249-255. CRC Press, Durham, United kingdom, 2008.

[6] D.M. Potts and L. Zdravkovic, “*Finite element analysis in geotechnical engineering: theory*”, London: Thomas Telford; 1999.

[7] A.M.Tang, Y.J. Cui and N. Barnel, ”Thermo-mechanical behaviour of a compacted swelling clay”, *Géotechnique* Vol. 58, No. 1, pp. 45–54, 2008.

[8] A. Tsiampousi, L. Zdravkovic, and D.M. Potts, “A new Hvorslev surface for critical state type unsaturated and saturated constitutive models”, *Computers and Geotechnics,* Vol. 48, pp. 156–166, 2013.

[9] Villar, M.V, “*MX-80 Bentonite. Thermo-Hydro-Mechanical characterisation performed at CIEMAT in the context of the Prototype Project*”, CIEMAT Technical Report: CIEMAT/DIAE/54540/2/04, 2005.

Good practices in free release of materials resulting from the decommissioning of the VVR-S reactor

E. Ionescu, C. Tuca, D. Stanga, R. Deju and M. Dragusin

National Institute for Physics and Nuclear Engineering "Horia Hulubei", 30, Reactorului str., RO-077125, P.O.Box: MG-6, Magurele (Ilfov), Romania,

E-mail: eionescu@nipne.ro

Abstract

The paper aims to present the methodology used for free release of the materials arising from the VVR-S reactor decommissioning, as well as some practical examples for this methodology.

From decommissioning process of a nuclear reactor are arising important quantities of materials which are potential radioactive wastes. The role of the free release of materials from regulatory control is to demonstrate that the radioactivity contained in a large part of these materials is below the norm limits.

Introduction

The Magurele (Romania) VVR-S nuclear reactor is a research reactor with a maximum thermal power of 2MW, and distilled light water as moderator, coolant and reflector. After 40 years (1957-1997) of successful operation, the reactor was starting in 2010 the first stage of decommissioning. Between 1997-2010 years the reactor was kept in conservation process. Based on the radiological characterization of the reactor block [1] we can appreciate that more than 80% of these materials can be released.

International recommendations

The international organizations provide special care to free release of materials from regulatory control by following a set of recommendations and guidelines, based on radiological risks, and special dedicated to this process. Both, International Atomic Energy Agency (IAEA) and European Union (EU) standards and guides [2][3][4][5][6][7][8][9][10][11][12], are periodically updated in order to reduce the radiological risks of public environment and workers.

Free release Romanian Norms

The National Commission for Nuclear Activities Control (CNCAN) is the national authority competent in exercising the regulatory activity, authorization and controlling the nuclear field. The CNCAN's norms [13][14] for free release of the material are complying with the international recommendations.

Methodology for free release of the materials resulting from reactor

The free release of materials is conducted within an appropriate program of quality assurance in order to demonstrate the compliance with the release levels specified in Norms for release from regulatory control of materials within nuclear authorized practices (NDR-02) [14].The radionuclide inventory of reactor contains neutron activated materials and surface or bulk contaminated materials.

Neutron activated materials

Gamma spectrometry or gross gamma activity measurements are usually performed for measuring the specific activity of activated materials. High resolution gamma spectroscopy (HRGS) analysis and low resolution gamma spectroscopy (LRGS) is done.

For gross gamma counting measurements is used a CCM grind box monitor with plastic scintillation detectors. The monitor use Cobalt Coincidence Method spatially focusing and has no cross-sensitivity against interference from ambient dose rate.

Surface and bulk contaminated materials

Surface contamination surveys are performed using both scans and static direct measurements. Smear samples can also be used for non-fixed contamination indirect measurements.

Alpha and beta radiation measurements are mainly performed using scintillation detectors, proportional and Geiger-Muller counters. In some case, where large concrete surfaces or soils have to be monitored to low levels for unrestricted release, gamma spectrometry might be performed. Gamma gross counting can be performed with plastic scintillators or an inorganic scintillator such as NaI(Tl).

The methodology used for free release of materials includes three stages [15].

Preliminary stage consisting in:

(i) physical description of materials;
(ii) collecting and evaluating information concerning the materials location and operating history;
(iii) evaluating and documenting the contamination or activation potential and the nature of contamination.

The purpose of this stage is the material classification according to U.S. Nuclear Regulatory Commission NUREG 1761 [16] in one of the three classes of potential contamination or/and activation.

Decision stage – take into account previously classification having the following tasks:

(i) selecting of monitoring techniques;
(ii) selecting the instrumentation;
(iii) data analysis and interpretation;
(iv) comparison with legal limits.

Regulatory body reporting stage - consist in documentation preparing and obtaining of approval from regulatory body for those materials that meet the criteria stipulated in Radiological Safety Fundamentals Norms (NSR-01) and NDR-02.

Practical examples

To illustrate the methodology used for free release of the materials arising from the decommissioning of the VVR-S reactor are selected three practical examples:

Materials with high potential of surface contamination – cast iron lids of the reactor block.

Materials with high potential of bulk contamination - concrete result from scarifying the floor of the pump room.

Material with high potential of activation and surface contamination - experimental horizontal channel discs.

Conclusion

Free release methodology applied to nuclear decommissioning of the VVR-S Magurele reactor, complies with Romanian standards and international recommendations that regulate the nuclear industry.

Take into account that materials resulted from decommissioning process of a nuclear reactor are potential radioactive wastes, it is very important to demonstrate that the global activity of a large part of these materials is below the limits and are free released from regulatory control. Until now almost 300 tons of materials were released from regulatory control.

References and Citations

[1] E. Ionescu, D. Gurau, D. Stanga, O. G.Duliu “Decommissioning of the VVR-S research reactor – radiological characterization of the reactor block”, Romanian Reportsin Physics Vol. 64, No 2 pp 387-398, 2013.

[2] IAEA, International Basic Safety Standards for Protection against Ionizing Radiation and for the Safety of Radiation Sources (BSS) Safety Series No. 115, Vienna, 1996.

[3] IAEA, General Safety Requirements Part 3, No. GSR Part 3, Vienna, 2014.

[4] IAEA, Application of the Concepts of Exclusion, Exemption and Clearance, IAEA Safety Standards Series No. RS-G-1.7, Vienna, 2004.

[5] IAEA, Derivation of Activity Concentration Values for Exclusion, Exemption and Clearance, Safety Reports Series No. 44, Vienna, 2005.

[6] IAEA, Monitoring for Compliance with Exemption and Clearance Levels, Safety Reports Series No. 67, Vienna, 2012.

[7] IAEA, Safety Glossary, Terminology Used in Nuclear Safety and Radiation Protection, 2007.

[8] COUNCIL OF THE EUROPEAN UNION, Council Directive 96/29/EURATOM of 13 May 1996 laying down basic safety standards for the protection of the health of workers and the general public against the dangers arising from ionizing radiation, OJ no. L 159,1-114, 1996.

[9] EUROPEAN COMMISSION, Recommended radiological protection criteria for the recycling of metals from the dismantling of nuclear installations, Radiation Protection No. 89, Luxemburg, 1998.

[10] EUROPEAN COMMISSION, Recommended radiological protection criteria for the clearance of buildings and building rubble from the dismantling of nuclear installations, Recommendations of the group of experts setup under the terms of Article 31 of the Euratom Treaty, RP 113, 2000.

[11] EUROPEAN COMMISSION, Practical use of the concepts of clearance and exemption Part I: Guidance on General Clearance Levels for Practices; Recommendations of Group of Experts established under the terms of Article 31 of the Euratom Treaty, RP no.122, Luxemburg, 2000.

[12] EUROPEAN COMMISSION, Comparative Study of EC and IAEA Guidance on Exemption and Clearance Levels, RP no.157, 2010.

[13] CNCAN, NSR 01, Radiological Safety Fundamentals Norms, approved by order of the president of CNCAN no. 14/2000 and published in the Official Bulletin of Romania no. 404 bis/29th of August, (2000).

[14] CNCAN, NDR-02, Norms for release from regulatory control of materials within nuclear authorized practices, approved by CNCAN President Order No. 62/31.03.2004, (2004).

[15] E. Ionescu, D. Stanga, O. G. Duliu "The free release of the materials resulting from the decommissioning of the VVR-S research reactor" Romanian Reports in Physics, Vol. 65, No. 1,pp. 133–146, 2013.

[16] U.S. Nuclear Regulatory Commission, NUREG 1761, Radiological surveys for controlling release of solid materials, Washington, JULY, 2002.

Application of BIB–SEM technology to characterize microstructure and pores in mudstone at a range of scales

J. Klaver, J. Schmatz, G. Desbois, S. Hemes, J.L. Urai

Structural Geology, Tectonics and Geomechanics, Energy & Mineral Resources Group, RWTH Aachen University, Germany

Abstract

Characterization of the microstructure and pores in fine-grained geo-materials like mudstones is challenging because of their heterogeneity and small pore sizes. Combining Broad Ion Beam (BIB) polishing and Scanning Electron Microscopy (SEM) enables the visualization of microstructure and pores from millimetres down to a few nanometres in size. In the SEM, the BIB-polished section is mapped at high magnification with various detectors and the different features are segmented and quantified using image processing algorithms. This technology is applied on undeformed and naturally or experimentally deformed rock samples to analyse the strain behaviour of potential host rock formations of nuclear waste such as the Boom Clay and Callovian-Oxfordian Clay. Application of BIB-SEM in combination with Wood's Metal Injection allowed imaging the connected pore space in fine-grained rocks like the Boom Clay and Ypresian Clay. The in-situ fluid distribution of saturated rocks can be imaged by applying BIB-SEM at cryogenic conditions. These applications aim to increase understanding in deformation mechanisms, sealing capacity and transport properties of fine-grained materials.

Introduction

Fine-grained geo-materials like clays are considered as potential host rock formations since they have a high sealing capacity due to their fine grain size and small pores, typically below the micrometre. The microstructure and pore space morphology control to a large extent the deformation mechanisms and the storage and sealing capacity. For a comprehensive understanding of this relationship, and also of complementary bulk porosity and permeability measurements, accurate characterization of the microstructure and pores by imaging is required. Moreover, artefacts like (micro-) cracks due to core damage, sampling, storage, preparation and drying influence these measurements and should be corrected [1]. Due to the high variability of the mineral fabric and the small pore sizes, advanced imaging techniques need to be considered. Micro–Computed Tomography (µCT) is a valuable tool to image the 3D distribution and morphology of grains and large pores (typically above the micrometre) but cannot image the small pore bodies and throats (see Belgium paper). Focused Ion Beam (FIB) milling and Scanning Electron Microscopy (SEM) tomography visualizes the 3D microstructure and pores but the sampled volumes are often not representative and imaging the nanoscale pore throats remains a challenge. Here, Broad Ion Beam (BIB) polishing followed by SEM imaging allows imaging a sample size comparable to µCT at the same resolution as FIB-SEM; hence BIB-SEM links these two complementary techniques to each other. Moreover, by using Wood's Metal Injection (WMI) followed by BIB-SEM the connectivity of the pore space can be deduced over a relatively large sample area of several millimetres [2]. In this contribution we present applications of BIB-SEM with the aim to improve deformation and transport models in fine-grained rocks.

Methods

Broken or mechanically polished surfaces show too much topography or artefacts that complicate the interpretation of the microstructure and the pores (Fig. 1a). To avoid this problem BIB polishing is used. Subsamples of up to a several centimetres in size from cores, deformation or WMI experiments are prepared for the BIB polishing by keeping the orientation of the bedding in mind. During BIB polishing the samples are bombarded with Argon ions, either at low angle, known as surface polishing or at high angle, known as slope cutting. Surface polishing removes a thin layer of material of about a few micrometres over an area of several cm^2. Slope cutting removes about 100 micrometre of material but the polished area is smaller, typically 1-4 mm^2. The BIB polishing leaves a flat, planar and damage free cross-section that can be imaged in the SEM (Fig.1b). Fresh, saturated samples can be prepared and imaged by applying Cryo-BIB-SEM [3]. This technology is not limited to rocks only, but can also be applied on for example cement or salt (Fig. 1c and d).

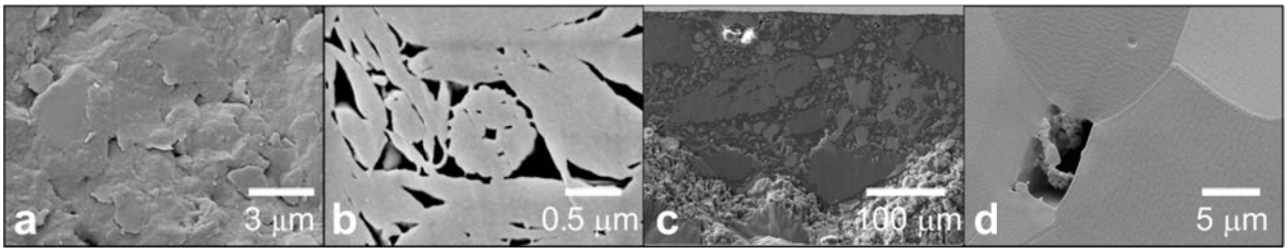

Figure 1: SE2 image of an unpolished clay shear surface (a). High resolution (100kx) SEM image of a BIB-polished clay cross-section (b). BSE image of saturated Portlland cement using Cryo-BIB-SEM (c). SE2 image of a macropore and grain boundaries in salt (d).

Microstructures in experimentally deformed Callovian-Oxfordian and Boom Clay

A normally consolidated sample from the Callovian-Oxfordian Clay (COx) was deformed in a tri-axial cell with a confining pressure of 2 MPa. After BIB polishing, the sub-sample was imaged in the SEM to study the microstructures. Fig. 2a shows grain fracturing of coccoliths fossil grains indicative of early cataclastic process. The Boom Clay sample, deformed at a confining pressure of 0.375 MPa, shows no indication of cataclastic processes but ductile behaviour like grain boundary sliding, rotation and grain bending within the damaged zone (Fig. 2b).

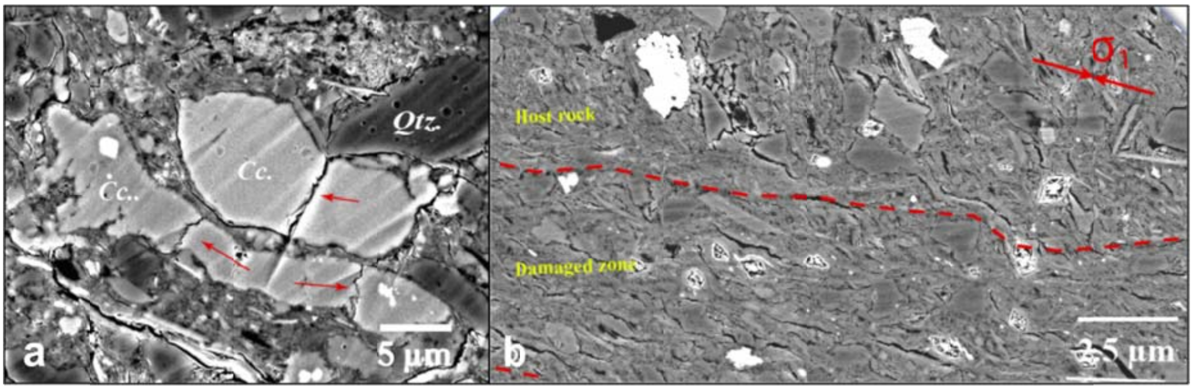

Figure 2: Microstructures in COx Clay (a) and Boom Clay (b).

Evaluation of pore connectivity in Boom Clay and Ypresian Clay samples

Oven dried sub-samples of Boom Clay and Ypresian Clay were injected with liquid Wood's Metal (WM) up to a pressure of 300 and 150 MPa, respectively. Once the desired pressures were reached, the heating was turned off, by keeping the sample under pressure, and the alloy solidified in the filled pore space. After cooling of the pressure vessel, the WM-injected samples were released and prepared for the BIB-polishing and SEM imaging. The Boom Clay sample showed WM virtually throughout the sample (Fig. 3a) except for some clay-rich regions that were partly filled with WM [2]. For the Ypresian Clay virtually all the interparticle pores are accessible for the WM at pressure of 150 MPa (Fig. 3b), equivalent to a pore throat diameter of about 10 nanometre [4].

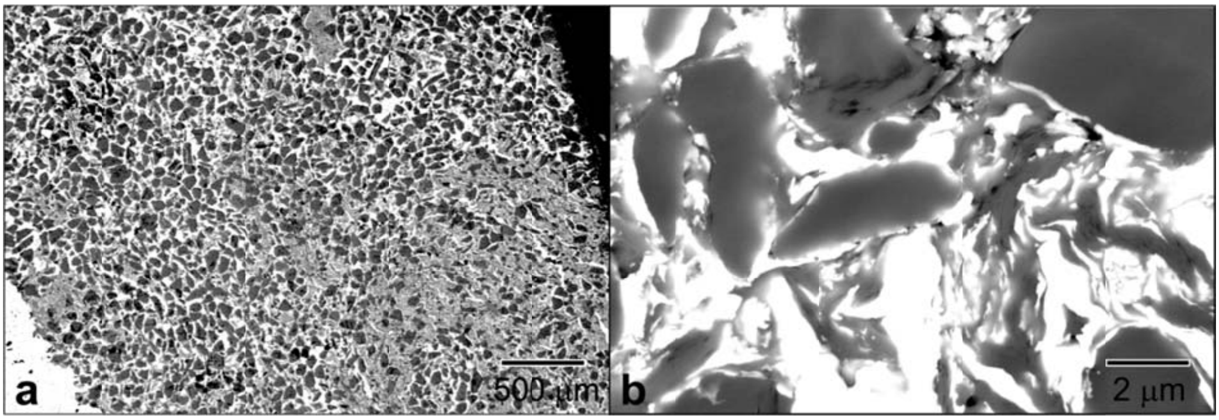

Figure 3: Connected porosity in a Boom Clay (a) and a Ypresian Clay sample. The WM appears very bright because of its relative high density.

Conclusion

BIB-SEM improves the understanding of microstructure at multiple scales and enables to link the microstructure to deformation mechanisms in a range of materials. Moreover, (WMI-) BIB-SEM allows quantification of the pore space geometries and evaluation of the connected pore space. These methods were initiated and are further developed and employed at the chair of Structural Geology, Tectonics and Geomechanics, RWTH Aachen University. Next steps are for example to link the microstructures of naturally deformed samples to deformation mechanisms and investigate the effect of the deformation on fluid flow properties.

Acknowledgments

The author would like to acknowledge EXIST Forschungstransfer (BMWi, Germany) for financial support. SCK-CEN is thanked for the sample material.

References

[1] G. Desbois, J.L. Urai, S. Hemes, S. Brassinnes, M. De Craen and X. Sillen, “Nanometer-scale pore fluid distribution and drying damage in preserved clay cores from Belgian clay formations inferred by BIB-cryo-SEM”, *Engineering Geology*, Vol. 179,: pp. 117-131, 2014.

[2] J. Klaver, S. Hemes, M. Houben, G. Desbois, Z. Radi and J.L. Urai, “The connectivity of pore space in mudstones: insights from high pressure Wood's Metal Injection, BIB-SEM imaging and Mercury Intrusion Porosimetry”, *Geofluids*, Vol. 15: p. 577-591, 2015.

[3] J. Schmatz, J.L. Urai, S. Berg and H. Ott, “Nanoscale imaging of pore-scale fluid-fluid-solid contacts in sandstone”, *Geophysical Research Letters*, Vol. 42, No 7, pp. 2189-2195, 2015.

[4] S. Hemes, G. Desbois, J. Klaver and J.L. Urai, “Microstructural characterisation of the Ypresian clays (Kallo-1) at nanometer resolution, using broad-ion beam milling and scanning electron microscopy”, *Netherlands Journal of Geosciences*, Accepted.

Proposed method for semantic mapping of communities of practice in the nuclear industry for alignment of education

V. Kuo

Aalto University, Doctoral Researcher

Abstract

There are great challenges gauging the relevance of knowledge, skills and competences (KSCs) provided in nuclear education and that of the industry needs. This is amplified by the difficulties within industry to efficiently identify the KSC typology depicted by the professional communities of practice (CoPs) within organizations. This study proposes a method using machine learning techniques, namely textual latent semantic analysis and hierarchical clustering, to visualize typologies of CoPs. This enables the efficacy of learning outcomes to be better assessed with respect to industry KSC requirements inherent within the industry CoPs.

Introduction

Nuclear educational organizations play a cardinal role in the development knowledge, skills and competences (KSCs), first-hand through the provision of relevant and effective learning outcomes. However, due to the divide between academia and industry, there has been great challenges to consistently assess the relevance of learning outcomes and need for adjustments, for instance, due to learning outcomes that may no longer serve a purpose, or new and emerging knowledge fields that are becoming more pertinent than before. Great challenges also involve the nuclear industry's ability to effectively and systematically identify and represent their KSC constituents, and thus requirements from education, amid the human resources of professional organizations, notwithstanding the difficulties in processing textual data in which KSCs are typically represented.

Nuclear industry organizations are vastly knowledge-driven and value is created through different domain knowledge communities within the organization known as communities of practice (CoPs), where continual developments in expert learning occurs among its members. The CoP perspective was introduced by Lave and Wenger [1] who proposes the situated nature of learning, in which individuals acquire professional expertise, leading to membership in a group of people sharing common knowledge, skills and competences. CoPs are inherent amid human interactions in organizations and may not even be evident at all to its members, because a CoP "need not be reified as such in the discourse of its participants" [2], are not stable or static entities, and evolve over time as new members join and others leave [3]. This definition underlines the dynamic nature of CoPs and thus the difficulties in mapping them, which is fundamental for assessing the alignment of KSCs provided in education, according to industry needs.

This paper describes a proposed method to map KSCs of CoPs using latent semantic textual processing techniques and hierarchical clustering. The results are visualized for ease of interpretation. In this short paper, a simple example is given to illustrate the logic.

Methodology: Latent Semantic Analysis

Latent semantic analysis (LSA) is an automatic statistical technique for extracting and inferring relations of expected contextual usage of words/terms in passages of discourse. It uses no humanly constructed dictionaries, knowledge bases, semantic networks, grammars, syntactic parsers, or morphologies and takes input from raw text parsed into words (terms) and separated into meaningful passages (documents).

Textual parsing and term-document matrix

The example from Kuo (2015) is provided again, this time, each of the passage of text represents the descriptions of the KSC pertaining to one expert practitioner in an organization (Figure 1). The example is thus a semantic representation of KSCs of 11 experts as 11 documents. Such input data can be abundantly acquired and aggregated from organizational documentation/databases (such as CVs, emails, project records, timesheets, human resource repositories etc.). Note that the one-sentence representations of each expert's KSC is only for sake of simple illustration – the document/text for each expert can indeed be any length, or can be labelled with existing classifications if any.

Nr	Documents	Terms
D1	The behaviour of barriers in the geological disposal of spent nuclear fuel	behaviour, barrier, geological, disposal, spent, nuclear, fuel
D2	Nuclear emergency response planning based on decision analysis	nuclear, emergency, response, planning, decision, analysis
D3	Ageing of concrete structures in Finnish rock caverns as application facilities for nuclear waste	ageing, concrete, structures, Finnish, rock, caverns, application, facilities, nuclear, waste
D4	Solute transport modelling of geological multi-barrier disposal system	solute, transport, model, geological, multi, barrier, disposal, system,
D5	Fire simulation models for radiative heat transfer and probabilistic risk assessment	fire, simulation, model, radiative, heat, transfer, probabilistic, risk, assessment,
D6	User interface for supporting operators' awareness in nuclear power plant control rooms	user, interface, support, operator, awareness, nuclear, power, plant, control, room
D7	Systems usability concept for control room design	system, usability, concept, control, room, design
D8	Interactive multi-criteria decision support - tools for practical applications	interactive, multi, criteria, decision, support, tool, practical, application, ,
D9	Fuel performance modelling in nuclear power plant	fuel, performance, model, nuclear, power, plant
D10	Code for Nuclear Fuel Cycle Analysis	code, nuclear, fuel, cycle, analysis
D11	Nuclear power plant procurement contracting in risky projects	nuclear, power, plant, procurement, contract, risk, project

Figure 1: 11 Expert documents parsed into 56 unique terms

Each "document" is parsed into "terms" (Figure 1) and a term-document matrix (*i*x*j*) is set up, containing the number of times term *i* appears in document *j*.

Singular value decomposition, Dimensionality Reduction and Cosine Similarity

The term-document matrix undergoes Singular Value Decomposition (SVD), to infer the patterns within the matrix. SVD is a linear algebra function where a matrix ***A*** of dimensions *nxm* is decomposed into the product of three other component matrices ***U*** *(nxn)*, ***S*** *(nxm)* and V^T*(mxm)*. The middle ***S*** matrix is a diagonal matrix containing scaling values in descending order along the diagonal of the matrix and the ***U*** and ***V*** matrices are thus regarded as all the constituent patterns that determine the original matrix ***A***. The columns in ***U*** and ***V*** are orthonormal vectors arranged in descending order of significance from left to right.

Dimensionality reduction is carried out to remove noise (small irrelevant patterns) inherent in natural language. This step is done by removing column vectors from ***U*** and ***V*** starting from the least significance. This corresponds also to the same number of diagonals retained in the ***S*** matrix. The number of dimensions to keep can be determined by plotting the singular values of the ***S*** matrix against the number of dimensions [5]. One may choose the number of dimensions where the singular values decrease substantially (an elbow of a plot) indicating the point where the patterns become insignificant.

The reduced ***U*** and ***V*** row vectors represent the semantic space of the terms and documents. Thus a similarity function can be used to measure semantic correlations between term-term, document-document, and term-document relationships. The cosine similarity function works well empirically [6] and is widely used for vector matching in many applications. Cosine similarity is denoted by the cosine of the angle between two vectors *a* and *b* and can be calculated by dividing the dot product of *a* and *b* by the product of their magnitudes. The cosine similarity between vectors of the reduced ***U*** and ***V*** matrices equates to semantic similarity between them. Since this process is automated, it allows the system to calculate similarities upon query and retrieve similar terms and and/or documents from the database.

Results/Discussion

The results of the latent semantic analysis allow each document and term to be represented as one semantic vector of the same dimension. Therefore, the relationships between vectors can be determined based on their semantic similarities. In this particular use case, it is of interest to see the relationship between different documents, representing the KSC profiles of each expert in relation to another, thus revealing the CoPs on different levels of abstraction. Visualization as a cosine similarity matrix is useful for quick inspection (Figure 2 left). Figure 2 (middle) shows the same matrix rearranged after undergoing hierarchical clustering to reveal possible communities of documents placed adjacent to one another, therefore representing the typology of CoPs, qualified by the semantic similarity of the textual descriptions of each expert's KSCs. Figure 2 (right) shows the same results of the hierarchical clustering visualized as a dendrogram, where the vertical axis indicates the semantic distance between the documents, or groups of documents, they connect. Simple inspection of the rearranged matrix can show evident communities (broken lines in Figure 2 middle) on the lowest level of abstraction formed by D2 and D10; D9 and D11; or D10, D1 and D9. On a slightly higher level D2, D10, D1, D9, and D11 can form one community, with D6, D3, D5, D4, D7, D8 remaining relatively independent. The dendrogram plot shows the same, though with easier interpretation given the clear semantic distances between the documents indicated by the length of vertical lines that connect them. For instance, it indicates weak (even negligible) relationship between D3 and D5; D4 and D7 etc. Drawing a horizontal line at a specific level of the dendrogram indicates the number of clusters at that specific level of abstraction (e.g. at 1.2 on the dendrogram vertical axis, 8 clusters are evident, while at 1.4 on a slightly higher level of abstraction, 7 clusters are evident).

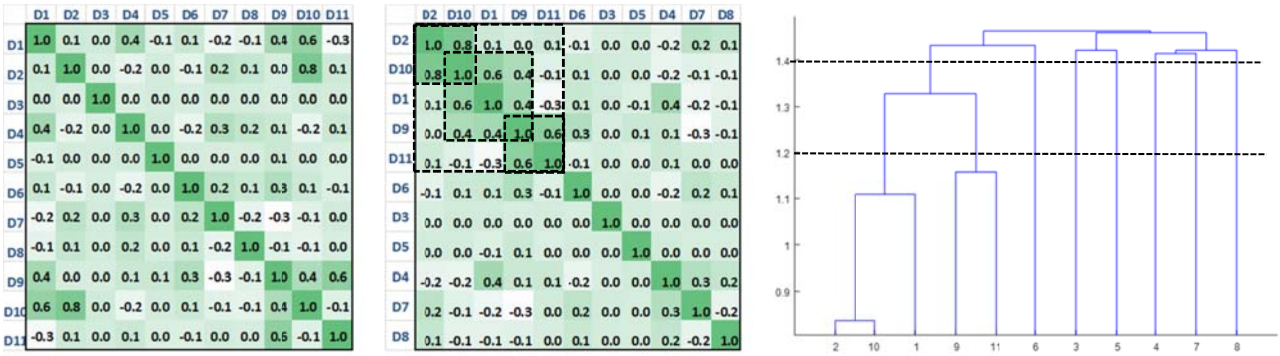

Figure 2: (left) Cosine similarity matrix of the 11 experts' KSCs; (middle) the rearranged matrix using hierarchical clustering, and (right) same clustered data visualized as a dendrogram

The extent of semantic similarity between texts, or where weak relationships are considered negligible becomes a philosophical question. For instance, one may argue that D9 should be more related to D10 than D11 (Figure 1), pertaining to the concept of "fuel", but the analysis shows otherwise, due to the other terms and concepts within the documents that are related. This may suggest that D9 and D11 are more related in another way, e.g. both pertaining to "nuclear power plant" explicitly and further qualified by more semantically related terms occurring in the documents. Therefore, even though "unintuitive" results can possibly be regarded as a result of an inadvertent pattern in the text (especially with small datasets such as this example), it can also be interpreted as hidden associations, which links the documents in ways not clearly evident first-hand to human interpretation. Either way, such issues are typically addressed with larger datasets where the distribution of terms and concepts more truthfully describe the semantic structures intuitively. Given the automated nature of the data mining and processing method, the knowledge typology of CoPs can be systematically represented in this way with large datasets.

Conclusion and future work

This paper addresses the problem of assessing the topic distribution/spectrum of learning outcomes provided in nuclear education with respect to KSC needs of industry, which are most accurately represented by the typography of CoPs. The latent semantic approach is proposed in order to effectively map industry KSCs underpinned by the dynamic CoPs, to allow alignment of education to meet industry needs.

References and Citations

[1] J. Lave and E. Wenger, *Situated learning: legitimate peripheral participation*. New York, New York, USA, 1991.

[2] E. Wenger, *Communities of Practice: Learning, Meaning, and Identity*. Cambridge: Cambridge Universeity Press, 1999.

[3] J. Roberts, "Limits to communities of practice," *J. Manag. Stud.*, vol. 43, no. 3, pp. 623–639, 2006.

[4] V. Kuo, "Proposed Artificial Intelligence Method to Improve the Discoverability of Semantic Links Between ECVET and ECTS in the Nuclear Industry Sector," in *1st PETRUS (Programme for Education, Training and Research on Underground Storage) PhD Conference*, 2015.

[5] A. Sidorova, N. Evangelopoulos, J. S. Valacich, and T. Ramakrishnan, "Uncovering the Intellectual Core of the Information Systems Discipline," *MIS Q.*, vol. 32, no. 3, pp. 467–A20, 2008.

[6] T. K. Landauer, P. W. Foltz, and D. Laham, "An introduction to latent semantic analysis," *Discourse Processes*, vol. 25, no. 2–3. pp. 259–284, 1998.

[7] M. W. Berry, S. T. Dumais, and G. W. O'Brien, "Using Linear Algebra for Intelligent Information Retrieval," *SIAM Review*, vol. 37, no. 4. pp. 573–595, 1995.

Probabilistic performance assessment of a deep tunnel for a radioactive waste repository in French COx claystone

Y. Li, P.J. Vardon, and M.A. Hicks

Geo-Engineering Section, Delft University of Technology

Abstract

A preliminary probabilistic study of the stability of a circular drift excavated for a radioactive waste repository in the French Callovo-Oxfordian claystone is presented and discussed. An analytical mechanical model assuming isotropic elastic behaviour and linear plastic softening was used. Particular emphasis here is placed on the uncertainty of mechanical property values. The test results from several laboratories showed considerably variable property values and they have been interpreted statistically in this investigation. The obtained statistical results were used in a Monte Carlo framework. The performance of the drift was evaluated in terms of the probability of threshold exceedance in the extent of the plastic zone.

Introduction

One of the main objectives of research programs for feasibility studies for deep geological repository of radioactive waste is the performance and safety assessment of disposal tunnels. In the case of variable material property values of the host rock, probabilistic calculations can be carried out to determine the probability of unsatisfactory performance. For example, Arnold et al. [1] implemented a simplified probabilistic framework based on an analytical Drucker-Prager softening model and investigated the probability of exceedance of a certain plastic limit around the proposed disposal drifts in the Dutch Boom Clay. This paper seeks to gain more confidence in the proposed analytical model when applied in a preliminary tunnel stability assessment, by first comparing the predicted radial displacement with the measurements that are available in the French disposal drifts at the Meuse/Haute-Marne (MHM) URL. To this end, the variability in the mechanical and deformation properties in the COx claystone was first characterised by reinterpreting the test results from various laboratories. Then, the results are used as input in the reliability-based framework to assess the performance of a disposal drift in terms of the probability of having a plastic zone.

Probabilistic interpretation of the test results

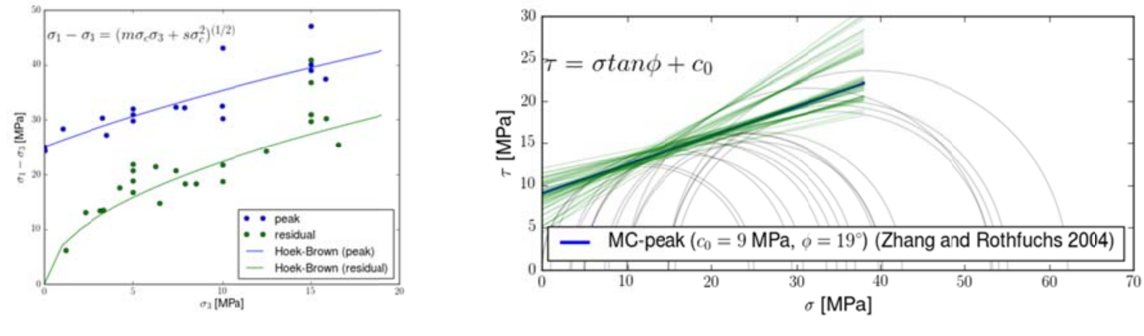

Figure 1: Peak and residual strength of the Callovo-Oxfordian argillite at MHM-URL (After [2]) (left) and Mohr circles (grey) and failure envelops (green) reinterpreted from left figure (right)

The data from different laboratories showed considerable variabilities. This has been interpreted probabilistically in this section to obtain point statistics used in the Monte Carlo simulation in the next section. Figure 1 (left) shows the peak and residual strength of the COx clay at MHM URL from ANDRA and GRS [2]. Based on the values σ_1 and σ_3 in the left figure, the Mohr circles are first plotted pair by pair. Then a straight line that is tangential to the two circles is defined (i.e. the failure envelope defining c_0 and ϕ). In this way, multiple envelop lines can be defined, resulting in a range of values for c_0 and ϕ. The same procedure was repeated for the data points at residual state. The distributions of ϕ, c_0 and c_r are shown in Figure 2 in terms of mean (μ), standard deviation (σ) and the coefficient of variation (cov). A normal distribution is seen to fit to the data reasonably well. Note that the distance between the circle centres is set to be larger than 10MPa to ensure reliable failure envelopes.

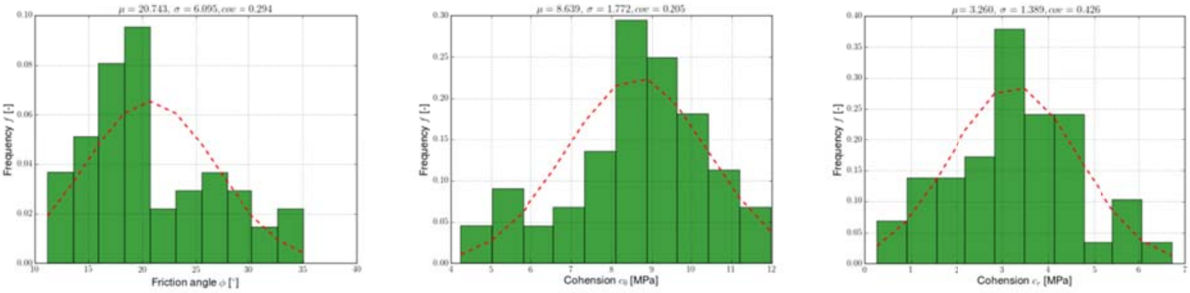

Figure 2: Normalised histograms and fitted probability density functions (pdf) for variables ϕ, c_0 and c_r.

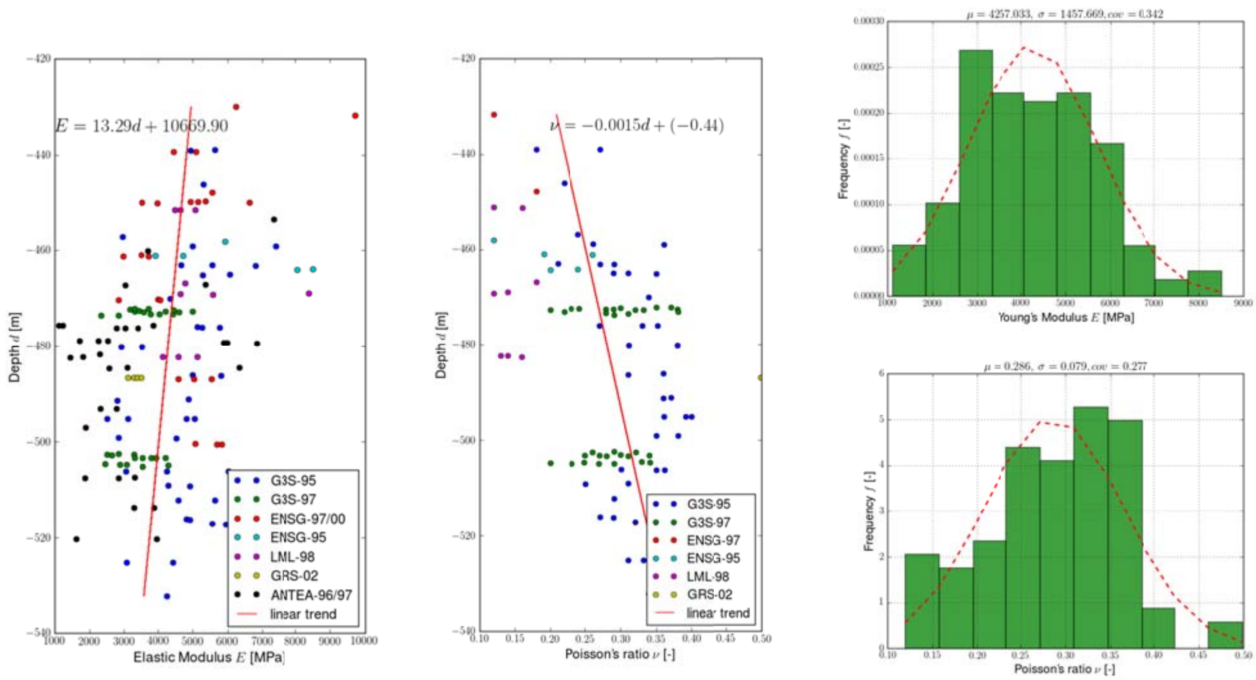

Figure 3: Elastic modulus and Poisson's ratio versus depth for COx claystones from different laboratories (digitised from [3], linear trend line added) (left and middle) and normalised histograms and fitted probability density functions (pdf) for variables *E* and ν (right).

Table 1: Point statistics describing the properties of COx claystones at MHM URL

Variable X	Symbol	Unit	μ_X	$cov(X) = \sigma_X/\mu_X$	Distribution type
Initial cohesion	c_0	MPa	8.6	0.21	Normal
Residual cohesion	c_r	MPa	3.3	0.43	Normal
Friction angle	ϕ	°	20.7	0.29	Normal
Young's modulus	E	MPa	4257	0.34	Normal
Tangent modulus	E_t	MPa	2100	0.34	Normal
Poisson's ratio	ν	-	0.29	0.28	Normal

The elastic modulus and Poisson's ratio versus depth data for COx claystones from different laboratories (G3S, ENSG, LML, GRS, ANTEA) are shown in Figure 3 (left and middle) [3]. These data have also been processed probabilistically to define the point statistics for *E* and ν (Figure 3 right). A summary of the point statistics describing the properties of COx claystones at MHM URL is shown in Table 1. Note that the mean of the tangential modulus is assumed to be approximately half that of elastic modulus and the COV is assumed to be the same, as little data is available about the tangential modulus.

Monte Carlo simulation

The GCS drift has been analysed in this section. It has a circular section with a radius of 2.6 m. As it was excavated with a road header, an over excavation (overcut) of 15 mm is used in the simulation. The support (fibre shotcrete) was 21 cm thick [4]. The drift was parallel to σ_H, and the initial in situ stress state was quasi-isotropic (σ_H = 16.12 MPa, σ_h = σ_v = 12.4 MPa) [5]. A pore water pressure of $u_{w,0}$ = 4.5 MPa was used at a depth of -490 m. The statistics in Table 1 were used in the MC simulation, assuming truncated normal distributions. The results are shown in Figure 4 and the radial displacements (Figure 4 left) are compared to the measurements [6].

Results/Discussion

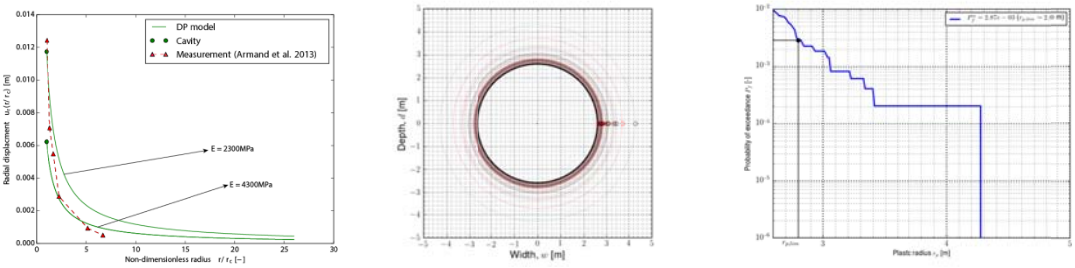

Figure 4: Deterministic radial displacement (left), plastic radius around the tunnel opening (middle, plastic softening zone in grey and plastic residual zone in red) and probability of exceedance (P_f) of a plastic zone limit ($r_{p,lim}$) (right)

Conclusion

The preliminary assessment compares favourably well with radial displacement measurements. The proposed probabilistic framework provides a way to assess the probability of unsatisfactory performance in terms of the exceedance of a certain plastic limit. However, the idealised isotropic DP model is not able to predict the anisotropic convergence measurements.

Acknowledgments

The research leading to these results has received funding from the Dutch research programme on geological disposal, OPERA. OPERA is financed by the Dutch Ministry of Economic Affairs and the public limited liability company Elektriciteits-Produktiemaatschappij Zuid-Nederland (EPZ), and is coordinated by COVRA.

References

[1] Arnold, P., Vardon, P.J. and Hicks, M.A., 2015. Preliminary Assessment of Tunnel Stability for a Radioactive Waste Repository in Boom Clay. In Engineering Geology for Society and Territory-Volume 6 (pp. 545-549). Springer International Publishing.

[2] Zhang, C. and Rothfuchs, T., 2004. Experimental study of the hydro-mechanical behaviour of the Callovo-Oxfordian argillite. Applied Clay Science, 26(1), pp.325-336.

[3] Miehe, B. 2004. Modelisation de la zone endommagee induite par le creusement du puits d'acces au laboratoire souterrain de Meuse/Haute-Marne (argilites de l'Est). Applied geology. Ecole Nationale Superieure des Mines de Paris. In French.

[4] Guayacán-Carrillo, L.M., Sulem, J., Seyedi, D.M., Ghabezloo, S., Noiret, A. and Armand, G., 2016. Analysis of Long-Term Anisotropic Convergence in Drifts Excavated in Callovo-Oxfordian Claystone. Rock Mechanics and Rock Engineering, 49(1), pp.97-114.

[5] Martín, L.B., Hadj-Hassen, F., Tijani, M. and Armand, G., 2011. New numerical modelling of the mechanical long-term behaviour of the GMR gallery in ANDRA's Underground Research Laboratory. Physics and Chemistry of the Earth, Parts A/B/C, 36(17), pp.1872-1877.

[6] Armand, G., Noiret, A., Zghondi, J. and Seyedi, D.M., 2013. Short-and long-term behaviors of drifts in the Callovo-Oxfordian claystone at the Meuse/Haute-Marne Underground Research Laboratory. Journal of Rock Mechanics and Geotechnical Engineering, 5(3), pp.221-230.

Time-dependent mechanical and transport behaviors of Callovo-Oxfordian argillite

Zaobao Liu, Jianfu Shao, Yanchun Tang

University of Lille -Science and Technologies, 59650 Villeneuve d'Ascq France

Abstract

An experimental study was carried out on the time-dependent mechanical and transport behaviors of the Callovo-Oxfordian (Cox) argillite, the geological barriers for high-level radioactive waste disposal in France. Six coupled one-step creep tests under the same confining pressure 6MPa and different deviatoric stresses were proposed to investigate the effect of deviatoric stress on the evolution of creep deformation and gas permeability in creep process. Another three multi-step creep tests under confining pressure (Pc) of 2, 6 and 12MPa were carried out to investigate the effect of confining pressure (mean stress). The results show that the creep strains can be enhanced by both the deviatoric and mean stress. The mean stress can reduce importantly the permeability of the Cox argillite but the deviatoric stress shows no evident effect. The gas permeability of the Cox argillite keeps decreasing when deviatoric stress is smaller than 84% of its peak strength at confining pressure of 6MPa. The structural anisotropic effect is also discussed according to the experimental results.

Introduction

Callovo-Oxfordian (Cox) argillite has been confirmed to be used as the geological barriers for the high-level radioactive waste disposal in Bure of France after two decades of investigations. This type of claystone is constituted mainly of quartz, calcite and clay minerals such as illite, smectite and illite/smectite[1, 2]. The porosity of the Cox claystone is at the range of 14%-18% and its water content in situ is about 6%-8% in the excavated formations[3, 4]. Due to the long-term requirements of the underground radioactive waste repositories, it is necessary to investigate the time-dependent mechanical and transport behaviors of the Cox claystone. The present study introduces the experimental results of a series of coupled triaxial creep tests on the Cox claystone with gas permeability measured in concurrence of the time-dependent deformations.

Methods

The coupled tests were carried out in an autonomous and auto-compensated hydromechanical testing system designed at the Laboratory of Mechanics of Lille (LML). The testing system[5] consists of three independent components, respectively for deviatoric stress loading, confining pressure application and interstitial pressure generation and monitoring, which are assembled around a triaxial cell.

The coupled creep experiments were carried out in the following steps:

(a) Check the testing system to make sure its functionality and install the sample at the base with a filter paper and a filter plate at each sample end, and then seal the sample in a plastic jacket from the pressure chamber of the triaxial cell; (b) Apply the confining pressure at the rate 0.5 MPa/min to a given level such as 6MPa and maintain it; (c) Inject the inert Nitrogen gas to keep both inlet and outlet pressure as 0.9MPa; (d) Augment 0.95MPa of the confining pressure to allow the effective confining pressure as i.g.6.0MPa in the process of gas permeability measurement; (e) Make the sample saturated in gas with constant pressure 0.9MPa to allow the gas pressure of the inlet and outlet reservoir in equilibrium at 0.9MPa; (f) Close the valve between the upstream and downstream reservoirs, and then inject a pressure pulse 0.1MPa at the upstream reservoir and cut off the nitrogen gas supply. The initial upstream pressure is thus 1.0MPa; (g) Wait till the upstream and downstream gas pressure to be in a new equilibrium state (Pressure in final equilibrium) which allows the calculation of the gas permeability by pressure decay method, and then go on to the next measurement; (h) Augment the confining pressure to another planned value, and repeat step (e) to (g) to measure the corresponding permeability for each planned confining stress; (i) Load the deviatoric stress to the expected creep level and then maintain the stress to realize material creep, and repeat step (e) to (g) to measure the permeability evolution in the creep process; (j) For multi-step creep tests, after the stabilization of the creep at the former creep step, repeat step (i) till final creep failure occurs.

Before the coupled creep tests, conventional triaxial tests were carried out in prior to determine the peak strength of the Cox argillite under different confining pressures. All the samples were tested at relative humidity of 59% corresponding to a desaturation state in the excavation damaged zones in the galleries.

Results/Discussion

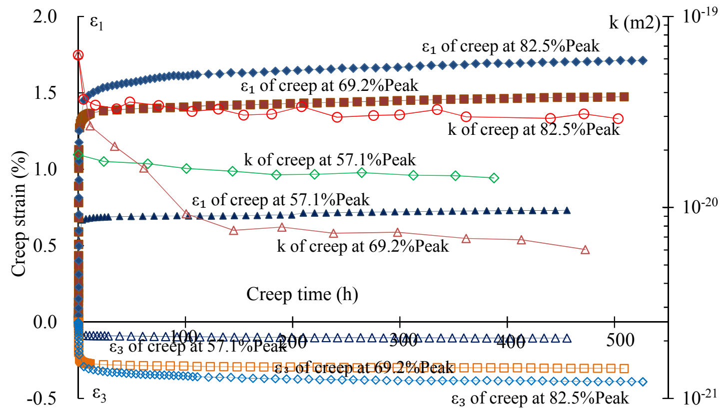

Figure 1: Strains and permeability variation of Cox argillite with deviators in perpendicular direction of bedding plans during one-step creep.

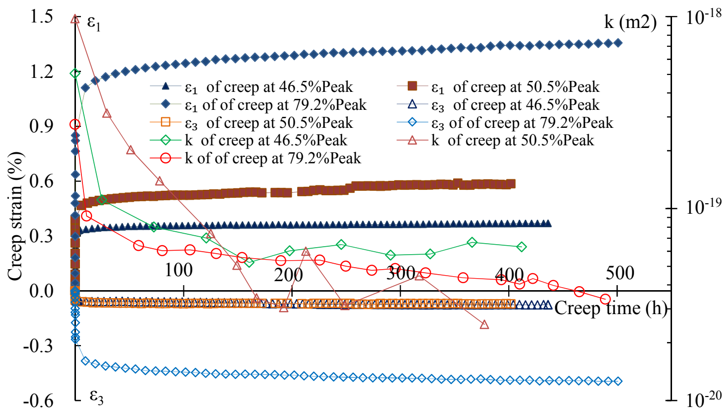

Figure 2: Strains and permeability variation of Cox argillite with deviator in parallel direction of bedding plans during one-step creep.

The results of the three coupled one-step creep tests with deviators in perpendicular and parallel directions are shown respectively in Figure 1 and Figure 2. Both the axial and radius strains as well as the permeability are given in time space. It is shown in Figure 1 or 2 that the material strains augment and the permeability decreases at a decreasing rate during the one-step creep process. As shown in Figure 1, the strains of the creep tests with deviators of 82.5% peak is much larger than those of 69.2% peak and 57.1% peak. This phenomenon indicates that the deviatoric stress can enhance the creep strains of the Cox argillite when loaded in perpendicular directions. However, the deviator shows no evident effect on the permeability evolution of the Cox argillite. Similar findings can also be found in Figure 2 for the deviators loaded in parallel direction of the bedding plans. By comparison of the material strains in Figure 1 and 2, one can find the strains of the Cox argillite are much larger when deviators are loaded in perpendicular directions than in parallel directions.

Thus, the creep deformations of the Cox argillite can be enhanced by the deviatoric stress and they exhibit an anisotropic effect when deviators loaded in different directions. However, the deviatoric stress shows no evident effect on the permeability evolution of the Cox argillite during creep process.

The strains and permeability evolution of the three multi-step creep tests with Pc=2, 6, 12MPa are shown in Figure 3. The corresponding loading paths of the tests are given in Figure 4 in which the permeability is also shown in axial strain space. It is shown evidently in Figure 3 and 4 that the strains are importantly enhanced and the permeability is greatly reduced by the confining pressure (mean stress). The permeability in multi-step creep tests experiences firstly a decreasing phase when deviatoric stress is low and secondly an increasing phase when the deviatoric stress surpasses a certain level. Since gas permeability is very sensitive to the creation and development of micro-cracks in the rocks, one can deduce that the turning point of permeability from decreasing to increasing corresponds to the creation of new micro-cracks in the Cox argillite during the creep process.

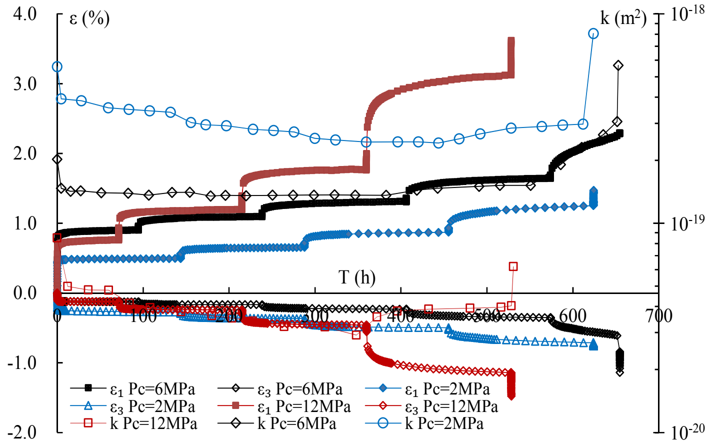

Figure 3: Strains and permeability variation of Cox argillite during multi-step creep.

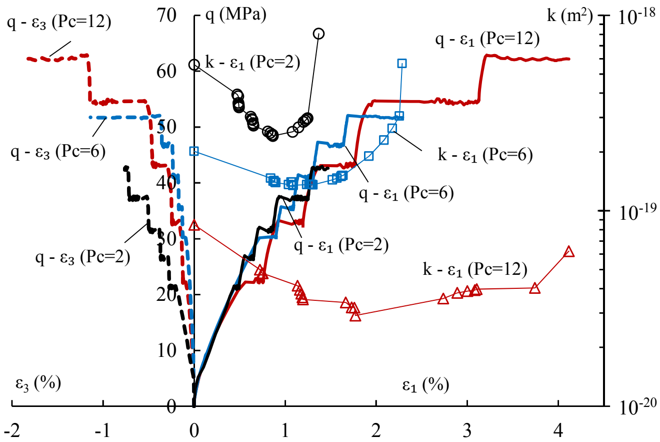

Figure 4: Stress and strains relations and permeability variation in axial strain space.

Conclusion

Both deviatoric stress and mean stress can enhance the creep deformations of the Cox argillite. Deviatoric stress in one-step creep exhibits no evident effect on the permeability evolution while the mean stress can induce an important reduce of permeability. Creep strains show a structural anisotropic effect but the permeability not. Permeability keeps decreasing in one-step creep, and it experiences firstly a decreasing phase when deviatoric stress is low and secondly an increasing phase when the deviatoric stress surpasses a certain level corresponding to the creation of new micro-cracks in the Cox claystone.

Acknowledgments

Supports from the French “Agence National Déchets Radioactive” (Andra) are gratefully acknowledged.

References

[1] Liu Z, Xie S, Shao J, Conil N. Effects of deviatoric stress and structural anisotropy on compressive creep behavior of a clayey rock. Appl Clay Sci. 2015;114:491-6.

[2] Andra. Referentiel du site Meuse-Haute Marne. Paris: Andra; 2005.

[3] Andra. Dossier 2005: CDROM Argile – plaquettes, synthèse, tomes, référentiels et glossaire. 2005.

[4] Andra. Recherche et développement à l’Andra pour les projets de stockage. Paris: Andra; 2012.

[5] Liu ZB, Shao JF, Hu DW, Xie SY. Gas Permeability Evolution with Deformation and Cracking Process in a White Marble Under Compression. Transp Porous Media. 2016;111:441-55.

Experimental and digital characterisations of the hydro-mechanical behaviour of a heterogeneous powder/pellet bentonite material

Agustín Molinero Guerra[1,2], Nadia Mokni[2], Yu-Jun Cui[1], Anh Minh Tang[1], Pierre Delage[1], Patrick Aimedieu[1], Frédéric Bernier[3], Michel Bornert[1]

[1]*Ecole des Ponts ParisTech, Laboratoire Navier, Marne La Vallée, France*
[2]*Institut de Radioprotection et de Sûreté Nucléaire (IRSN), Fontenay-aux-Roses, France*
[3]*Agence Fédérale de Contrôle Nucléaire (AFCN), Belgique*

Abstract

The MX80 powder/pellets mixture is one of the candidate sealing plugs used in deep radioactive waste disposal because of its swelling properties and operational advantages (lower compaction effort, reduced gaps between the rock and the seal). The present work focuses on the microscopic scale of the material, which is studied using several techniques (MIP, µ-CT and SEM observations). From MIP results, a typical bimodal distribution was found for both pellet and powder. However, a shifting of the mean size diameter of pores of the pellet was observed at lower suctions. From µ-CT observations, a heterogeneity was revealed in the internal structure of the pellet: heterogeneous density distribution of the clay minerals and presence of several high density elements.

Introduction

In situ compacted MX80 powder/pellets mixture is one of the candidate sealing materials for deep underground repositories, not only because of its low permeability, high swelling capacity and high radionuclide retardation properties but also for its operational advantages (lower compaction effort, reduced gaps between the rock and the seal). Once installed in the repository, these sealing materials will be subject to coupled hydro-mechanical loadings: hydration due to the infiltration of pore water from the natural barrier and mechanical confinement resulting from the engineered barriers. It is therefore essential to understand their behaviour under such loadings when assessing the overall repository safety.

In this context, the French Institute of Radiation protection and Nuclear Safety (IRSN) has launched the SEALEX project (SEALing performance Experiments) to which this work is related. SEALEX is dedicated to (i) test the long-term hydraulic performance of sealing systems in normal conditions for different core compositions (MX80 bentonite pellets/powder or sand/MX80 mixtures) and conditionings (pre-compacted blocks or in-situ compacted), (ii) quantify the impact of intra core geometry (construction joints) on the hydraulic properties of sealing systems, and (iii) quantify the effect of altered conditions (decrease of swelling pressure caused by the failure of the concrete confining plugs) on the performance of the sealing system. The current work focuses on the mixture of MX80 bentonite powder and pellets with a proportion of 20/80 in dry mass used in the last two SEALEX in-situ tests.

It is well documented that the macroscopic behaviour of expansive soils is related to its microstructure (e.g. [1]). For this reason, several investigations have been carried out on the microstructure of bentonite-based materials by several methods [2], including mercury intrusion porosimetry (MIP) and scanning electron microscopy (SEM, ESEM). [3] carried out several MIP tests on samples of pellets of FEBEX bentonite under different conditions. For a single pellet (ρ_d = 1.95 Mg/m^3), a bimodal distribution was observed.

These common techniques require a preliminary dehydration of the samples, often by freeze-drying. Moreover, they provide local observations of a part of milimetric samples. These results may be complemented by the use of microfocus X-ray computed tomography (µ-CT). This non-destructive 3D technique provides high-resolution observations of samples at a representative scale without pre-treatment. Interactions in the microfabric of a 50/50 pellet/powder mixture of FoCa clay at a dry density of 1.36 Mg/m^3 were observed during hydration under constant volume conditions by [4] using microfocus X-ray computed tomography. The evolution of the dry density of the sample was studied, but the scale considered was not suitable for investigating the microstructure of a pellet of bentonite.

This paper deals with an experimental investigation aimed at studying microstructural features of the pellet/powder mixture. µ-CT observations were carried out, together with the MIP and SEM results for further microscope investigation of the material.

Materials and methods

Investigated material

The studied soil is a powder/pellets MX80 bentonite mixture with a proportion of 20/80 in dry mass. The bentonite comes from Wyoming, USA, with high smectites content (80%) and some inclusions of non-clayey minerals. Pellets were produced by compacting the powder of MX80 bentonite (as extracted in-situ) in a mould of 7 mm diameter and 7 mm high. Compaction was performed by applying an effort instantaneously. The fabrication water content is between 5% and 7% at a dry unit mass ρ_d = 1.998 Mg/m^3 - 2.12 Mg/m^3. The initial suction, *s* = 132.34 MPa, was measured at the laboratory with a chilled mirror dew point hygrometer (Decagon WP4) and the initial water content, *w* = 7.25%, was determined after drying the sample (pellet) at 105°C for 24h. The MX80 bentonite powder used for the mixture was produced by crushing pellets of bentonite. A water content of 3.17% was found after drying at 105°C during 24h. The initial suction, *s* = 190.9 MPa, was measured with the chilled mirror dew point hygrometer (Decagon WP4).

Methods

The microstructure of the material was studied by several techniques: mercury intrusion porosimetry (MIP), scanning electron microscopy combined to energy-dispersive X-ray spectroscopy (SEM + EDS) and microfocus X-ray computed tomography (µ-CT observations). Firstly, the pore size distribution of both pellet and powder of MX80 bentonite was obtained on freeze dried samples. Then, several µ-CT observations were carried out on a pellet of bentonite at initial state and after swelling at 9 MPa of suction. Samples were scanned using 1440 projections on 360°. After the reconstruction, 1298 horizontal slices were obtained (16 bit images; 1644x1292 pixels; voxel size of 4.41 µm). Finally, SEM combined to EDS was performed on freeze dried specimens in order to carry out a chemical characterization of a pellet of bentonite at initial state.

Results/Discussion

A pellet of bentonite was observed by X-ray computed tomography (µ-CT) at its initial state (*s* = 132.4 MPa of suction, *w* = 7.25% of water content, ρ_d = 2.12 Mg/m^3 of dry density). Figure 1a presents two horizontal slices taken at different positions. Different grey levels are related to the absorption coefficient of the material, which depends on the density and the atomic number. Black level corresponds to void and white to high densities. Several elements of high density are observed everywhere (corresponding to white pixels). Moreover, several fissures are observed in the section corresponding to the upper part of the pellet (I). Another pellet of bentonite at 9 MPa of suction was analysed (this value of suction was imposed by vapour transfer from the initial state of the pellet). During wetting under free swelling conditions, the pellet experiences swelling deformation of 52% (ρ_d = 1.33 Mg/m^3). The purpose was to study the evolution of the internal structure after hydration. Two horizontal sections (III, IV) can be observed in Figure 1b. A lot of fissures are observed due to free swelling in addition to the existence of several elements of high density.

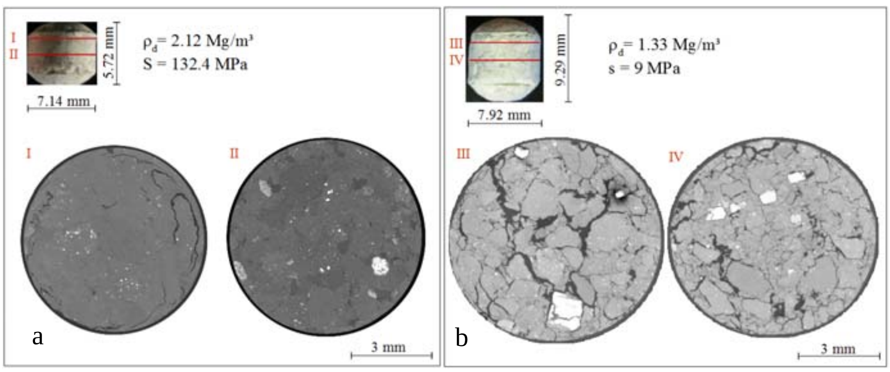

Figure 1: Microfocus X-ray computed tomography (µ-CT) observations of a pellet of bentonite at initial state (a) and after wetting at 9 MPa of suction (b).

The µ-CT observations of a single pellet of bentonite were complemented using the SEM technique combined to EDS in order to further investigate the heterogeneous structure of the material and to identify the higher density elements observed in a pellet of bentonite. An inclusion of pyrite is observed in Figure 2 (based in a high sulphur-iron concentration). It has to be noted that the dimensions of this inclusion is not negligible compared to the size of the pellet.

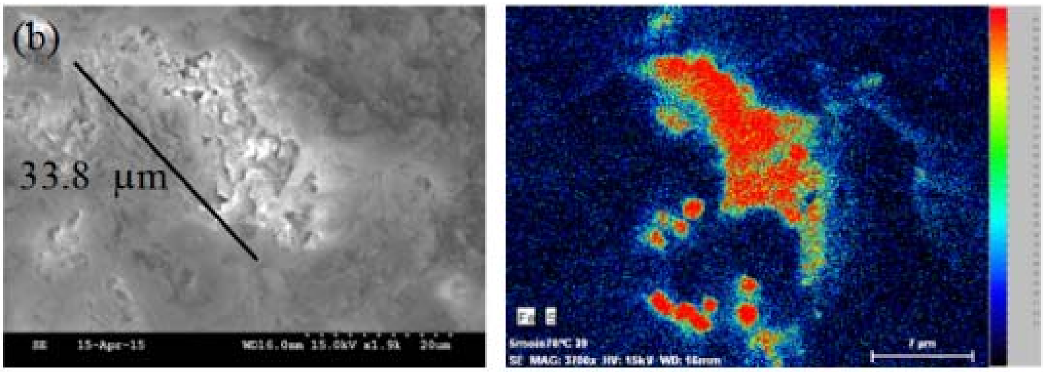

Figure 2: SEM picture taken on a pellet of bentonite at initial state (132.4 MPa of suction) + EDS results. Mineral inclusion pyrite.

In order to complete the investigation of the microstructure of the material, several MIP tests were carried out on powder at initial state and pellets of bentonite equilibrated at different suctions (under free swelling conditions by vapour transfer technique from the initial state, s = 138.4 MPa). The cumulative curves are presented in Figure 3a. The final values of intruded mercury void ratio are lower than the soil total void ratio. Figure 3b shows the pore size distribution curve, where a typical bimodal porosity is observed for a single pellet of bentonite. Two structural distributions can be defined: (i) intra-aggregate pores (micro-pores) having a mean size of 0.015 µm for suctions higher than 9 MPa and (ii) inter-aggregate pores (macro-pores). For 1 MPa, a shifting of micropores mean size is observed. The bimodal curve obtained for powder of bentonite at initial state is comparable to that of pellets.

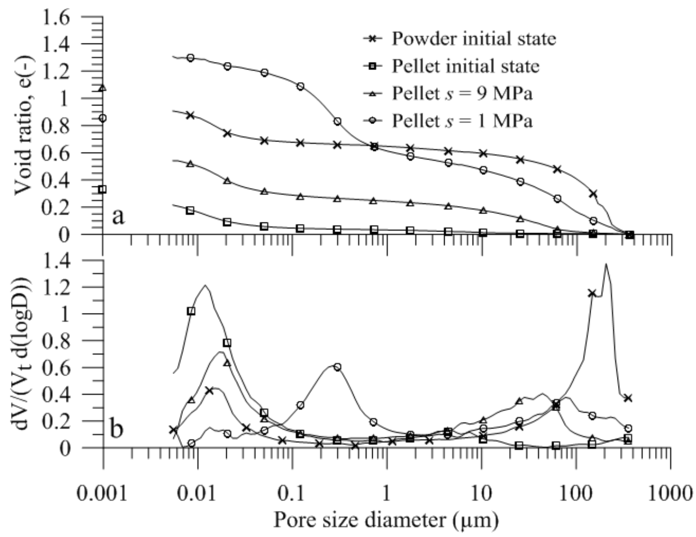

Figure 3: Cumulative porosity curves (a) and pore size distribution curve (b) for powder and pellets of bentonite at different suctions.

Conclusion

The µ-CT investigation of the microstructure of a pellet of bentonite provided complementary features that could not have been identified by MIP and MEB observations. A heterogeneity was revealed in the internal structure of the pellet, consisting in a heterogeneous density distribution of the clay minerals and presence of high density elements. From the pore size distribution curve, a typical bimodal distribution was obtained for both pellets and powder, which was an expected result due to the fact that powder is fabricated by crushing pellets of bentonite. New investigations are been conducting to study the hydro-mechanical behaviour of the mixture at a macroscopic scale.

References and Citations

[1] E. E. Alonso, E. Romero, and C. Hoffmann, "Hydromechanical behaviour of compacted granular expansive mixtures: experimental and constitutive study," Géotechnique, vol. 61, no. 4, pp. 329–344, 2011.

[2] S. Saba, J.-D. Barnichon, Y.-J. Cui, A. M. Tang, and P. Delage, "Microstructure and anisotropic swelling behaviour of compacted bentonite/sand mixture," J. Rock Mech. Geotech. Eng., vol. 6, no. 2, pp. 126–132, 2014.

[3] C. A. Hoffmann Jauge, "Caracterización hidromecánica de mezclas de pellets de bentonita. Estudio experimental y constitutivo." Universitat Politècnica de Catalunya, 18-May-2005.

[4] M. Van Geet, G. Volckaert, and S. Roels, "The use of microfocus X-ray computed tomography in characterising the hydration of a clay pellet/powder mixture," Appl. Clay Sci., vol. 29, no. 2, pp. 73–87, 2005.

Transient boundary conditions in the frame of high level radioactive waste disposal at deep geological repository

Abhishek Rawat[1], Weibke Baille[1] and Tom Schanz[1*]

[1]*Chair of Foundation Engineering, Soil and Rock Mechanics, Department of Civil and Environment Engineering, Ruhr-Universität Bochum 44780, Germany*

Abstract

The deep geological disposal concept is considered as a viable option for permanent disposal for high level radioactive waste. In this concept, the waste canisters are buried in a stable geological media with multi layer engineered barriers. The functionality of each component of such engineered barrier systems must be ensured for entire design period. Compacted bentonite-sand mixture is considered as a key component of such multi layer engineered barrier system. Considerable research has been carried out to evaluate the phenomenological evaluation of compacted buffer material on field scale and laboratory scale. The main objective is to predict the material behaviour over a large time span using constitutive modeling approach. Field scale experiments have their own pros and cons. In spite of economical issues, the major drawback is to control the repository relevant boundary conditions. In this regards, a small scale column experiment setup is designed at Ruhr Universität Bochum. The novelty of the experiment set up is the ability to control the thermal and hydraulic boundary conditions in a precise manner and to capture the transient profile of key state parameters like temperature, relative humidity, swelling pressure and water content.

Long term evaluation on the groundwater chemistry due to cement materials with numerical simulation

Diego Sampietro[1](diego.sampietro@amphos21.com), Elena Abarca[1], Marti Bayer[1], Salvador Jordana[1], Jorge Molinero[1], Tatsuya Tanaka[2], Shuji Hashimoto[2], Teruki Iwatsuki[3], Hironori Onoe[3]

1 Amphos 21 Consulting, Passeig Garcia i Faria, 49-51, 08019, Barcelona, Spain

2 Obayashi Corporation, Shinagawa Intercity Tober B 2-15-2, Konan, Minato-ku. Tokyo 108-8502, Japan.

3 Japan Atomic Energy Agency, 1-64, Yamanouchi, Akeyo-cho, Mizunami-shi, Gifu, 509-6132, Japan

Introduction

The Japan Atomic Energy Agency (JAEA) is being carried out the Mizunami Underground Research Laboratory project in Mizunami city, central Japan. This laboratory is a purpose-built generic URL (Underground Research Laboratory) that is planned for a scientific study of the deep geological environment as a basis of research and development for geological disposal of high-level radioactive wastes. As part of the project, groundwater flow model has been developed using the commercial software ConnectFlow, which is capable to generate hydrogeological models but it cannot account for chemical processes. It is important to evaluate the effect of the cement materials present in the underground facility in the groundwater. Development of modelling method for understanding the temporal evolution of the concrete structures is a key process in the radioactive waste storage.

The objective of this study was to develop a reactive transport model that reproduces the evolution of the hyperalkaline plume in the bedrock, which is supposed to be generated by the concrete degradation. The precipitation of secondary minerals can reduce porosity up to the point to induce important changes on hydraulic conductivity.

Methods

The reactive transport model have been developed using iCP (interface COMSOL-PHREEQC)[1]. COMSOL[2] is a commercial software that solves a large range of different process, such as flow or conservative transport, using the finite element method. PHREEQC [3] is a well-known program which can be used as a speciation program to calculate saturation indices, the distribution of aqueous species, and the density and specific conductance of a specified solution composition.

The model developed is formed by the URL located in the middle of a “box” formed by granitic materials. The geometry and the spatial distribution of hydrogeological conditions (hydraulic conductivity and porosity fields) have been implemented in COMSOL from the ConnectFlow files (Figure 1 and Figure 2). The URL consists of two 500 m deep shafts and several galleries. In addition to concrete lining (blue area in the Figure 1), grout has been injected to minimize groundwater inflow volume. Grouted area matches with the volume in contact with concrete lining in this model (Figure 1).

iCP uses COMSOL[2] to solve the flow and the transport. The chemical part is solved by PHREEQC. The groundwater flow model has been implemented using the Darcy’s law physics and the transport process is implemented using a custom physics interface named as Molal Solute Transport.

The chemical composition of the grout is half of the portlandite and half of the CSH (1.67). This is a simplified composition taking into account the principal components involved in the alkalinity. The chemical composition of the groundwater has been obtained from Iwatsuki et al.[4]. Basically, this groundwater is in equilibrium with granites and has a pH of about 8.5.

A total time of 10,000 years of reactive transport simulations have been performed.

Results

Results of the model show that the high pH plume caused by dissolution of portlandite and CSH extends downstream. High values of pH (pH>11) extend less than 100 m downstream (Figure 3).

The mixing between the grout and the natural groundwater produces the precipitation of three minerals with a specific order. The first phases are CSH(0.83) and the hydrotalcite. The precipitation of hydrotalcite consumes most of the OH^- of the water and buffers the pH to about 10.5. The last mineral that precipitates is calcite, covering a larger extension in the rock and buffering the pH up to natural values.

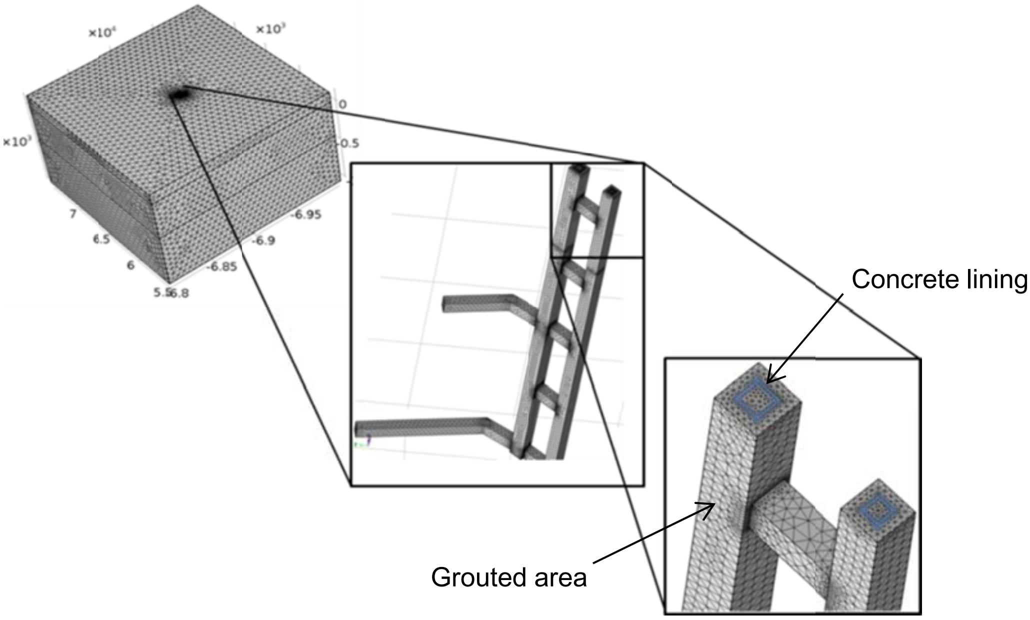

Figure 1: Detail of the URL geometry and the mesh employed in the groundwater flow model. The domain size is (2000x2000x1150 meters) and it is formed by 1,134,449 tetrahedral elements.

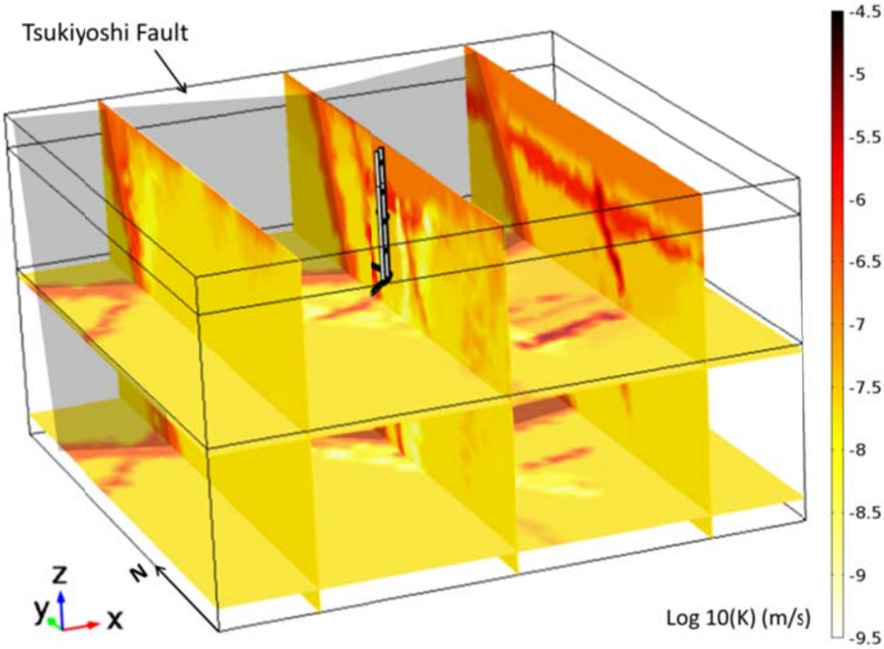

Figure 2: Hydraulic conductivity field of the rock domain implemented in COMSOL.

Discussion

Portlandite degradation is higher in the laboratory zone located upstream (northern border) and in areas where the water pore velocity is higher. The highest portlandite degradation rates are located about 200 meters of depth below the sedimentary rocks.

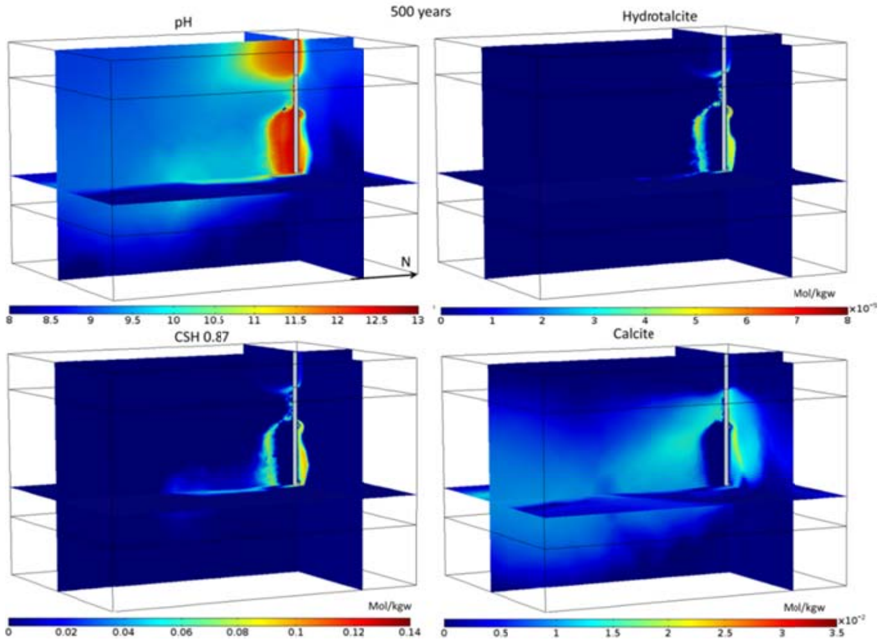

Figure 3: Groundwater pH and different mineral precipitation for a simulation time of 500 years. Groundwater flows southwards.

The high pH plume caused by dissolution of portlandite and CSH extends towards the downstream direction, but its extension is limited and buffered. High values of pH (pH > 11) extend less than 100 meters downstream. The high extension of the pH values > 11 are located in two areas characterized by low values of pore velocities. In these two areas, the mixing between the "grout water" and the native water is smaller, as a result produce less dilution.

The mixing between the grout water and the native groundwater produces precipitation of following three main minerals (CSH(0.83); hydrotalcite and calcite), occupying a larger extension and buffering the pH to almost the natural initial values.

The hydraulic shadow area located downstream the laboratory, which presents pH higher than 11, not present precipitation of mineral phases. The same effect is also observed for the sedimentary rock domain.

This study shows that iCP is a flexible and powerful tool for quantitative integration of hydrogeology and geochemistry. iCP allows to incorporate geochemical processes in 3D large scale COMSOL models and for long-time simulations.

References and Citations

[1] A.Nardi, A.Idiart, P.Trinchero, L.M.de Vries and J.Molinero, ""Interface Comsol-PHREEQC (iCP), an efficient numerical framework for the solution of coupled multiphysics and geochemistry*", Computers & Geosciences*, doi:10.1016/ j.cageo. 2014.04.011. 2014.

[2] COMSOL. COMSOL Multiphysics Reference Guide. Version 5.2. Burilington, MA: COMSOL Inc.2015a.

[3] D.L.Parkhurst and C.A.Appelo. Description of Input and Examples for PHREEQC Version 3—A Computer Program for Speciation, Batch-Reaction, One-Dimensional Transport, and Inverse Geochemical Calculations. *Chapter 53 of Section A, Groundwater book 6, Modeling Techniques* U.S. Geological Survey Water-Resources. 2013.

[4] T. Iwatsuki, R. Furue, H.Mie, S.Ioka and T.Mizuno," Hydrochemical baseline condition of groundwater research laboratory (MIU)". *Applied Geochemistry*, 20, 2283-2302. 2005.

Characterization of microbial communities in raw and homogenized bentonite samples

Rojina Shrestha[1,2], Jana Steinová[2], Lukáš Falteisek[2], Denisa Vlková[1], Alena Ševců[1,2]

(1) Faculty of Mechatronics, Informatics and Interdisciplinary Studies, Technical University of Liberec, Studentská 2, 461 17 Liberec (2) Institute for Nanomaterials, Advanced Technologies and Innovation, Technical University of Liberec, Bendlova 7, 461 17 Liberec, Czech Republic

Abstract

World-wide appreciated strategy for the management and treatment of high level and long lived radioactive waste is to dispose it in a deep and stable geological formation. Microbial community present in the host or buffer material may compromise the effective performance and safety of waste disposal system. In the Czech Republic, bentonite from Černý vrch locality is planned to be used as a buffer material. Therefore, microbial community was analysed in two bentonite samples (homogenized and raw bentonite) from this source.16S rRNA gene was amplified targeting the variable V4 region and sequencing was performed using Ion Torrent platform. Both bentonite samples were inhabited by relatively similar bacteria. Beta and Alpha-proteobacteria dominated both samples. Moreover, chemolithotrophs including *Thiobacillus*, *Gallionella* and *Nitrosomonas* capable of oxidising NH_3, Mn^{2+}, Fe^{2+} and S^{2-} were also present.

Introduction

The globally accepted strategy for the management and treatment of high level and long lived radioactive waste is to dispose of the waste in a deep and stable geological formation. The concept of the containment is based on a multi barrier system with different materials such as a metal container, bentonite and the host rock. The microbial community of the host rock or buffer material for the deep geological repository may compromise the effective performance and the safety of the radioactive waste disposal system [1]. Therefore, emphasis has been given to understanding the activity and diversity of microorganisms existing in repository. In the Czech Republic, bentonite from Černý vrch is planned to be used as a buffer material in the waste repository, however nothing is known about its microbial diversity. Therefore, our study is the first attempt made to investigate the structure of microbial community of the Czech bentonite.

Methods

Bentonite samples

Czech Mg-Ca bentonite originated from Černý vrch locality. Raw bentonite was unhomogenized and has of a very rough texture. Homogenized bentonite was commercially obtained from Keramost a.s.; the product is called “Bentonite a montmorillonite” BaM”.

Molecular analysis

Genomic DNA was extracted from 10 g of bentonite. SDS was used to lyse the cells. Furthermore; lysis was combined with precipitation of extracted DNA with polyethylene glycol followed by the purification step using AXG-100 cartridges [1-2].Qubit 2.0 or Agilent 2200 tape station was used for the quantification of genomic DNA. 16S rRNA gene was amplified using primers 530F [3] and 802R [4] targeting the variable V4 region. Same primers carrying Ion Torrent adaptor sequences and unique Tag barcodes were used for the amplicon preparation.We used Ion Torrent platform for amplicon sequencing. The process consists of following steps: i) emulsion PCR, ii) enrichment, iii) sequencing carried out on a 314 chip using the Ion Torrent personal genome machine system, New-generation Sequencing (NGS) technology.

Data analysis

Sequence data were analysed by the pipeline SEED v. 1.2.3 [5]. Sequences with insufficient quality or mismatches in tags were removed from the dataset. All sequences with minimal read length 275 bp were clustered into operational taxonomic units (OTUs) and chimeric sequences were removed using UPARSE implementation in USEARCH 7.0.1090 [6] with a 97% similarity threshold. The consensus from each OTU was constructed from an MAFFT alignment [7] based on the most abundant nucleotide at each position. The OTUs were identified and their environmental requirements were assessed by megaBLAST and BLASTn algorithms against GenBank nt/nr database.

Result/Discussion

The homogenized bentonite (BaM) and the raw bentonite samples from Černý vrch were more similar than we expected in terms of the microbial community structure based on OTU. Most OTUs were shared between the two samples.Out of 126 shared OTUs with a frequency higher than 10, only 18 of them had a very asymmetric distribution (the ratio between the two samples 1:10 or 10:1).

Beta- and Alphaproteobacteria dominated in both bentonites. Chemolithotrophic bacteria with a possible corrosion capability were present as well, though in lower abundances (Table 1).Typical soil bacteria, including *Massilia*, *Bradyrhizobium*, *Lysobacter*, *Methylocapsa*, *Microbacteriacea*, *Acidobacteria* were also present.These bacterial taxa are also known to inhabit oligotrophic environments.

Interestingly, chemolithotrophs that could utilize NH_3, Mn^{2+}, Fe^{2+}, S^{2-} as electron donors were present in relatively high abundances in both bentonite samples. Regularly it was *Thiobacillus*, *Gallionella*, *Rhodobacteraceae* and *Nitrosomonas*. This could be explained by slow and long-term adsorption of reduced compounds onto bentonite from the upper layers of soil in the Černý vrch mine and the consequent establishment of oxidative conditions during mining.

Table 1: Results of the NGS amplicon analysis showing selected OTUs. Numerical Value represents the number of respective microorganism present.

sample type / OTU	"BaM" homogenized bentonite	raw bentonite	determination
1	454	98	*Thiobacillus* sp.
7	19	68	*Gallionella* sp.
26	88	47	*Rhodobacteraceae*
28	112	57	*Arthrobacter* sp.
34	1	772	*Phreatobacter* sp.
44	5	211	*Aquabacterium* sp.
45	398	47	*Xanthomonadaceae*
63	81	227	*Nitrosomonas* sp.
67	395	1	*Beijerinckiaceae*
68	315	44	*Lysobacter* sp.
81	135	82	*Microbacteriaceae*
89	67	71	*Comamonadaceae*
95	23	72	*Acidobacteria*
98	62	13	unclassified
114	58	58	*Nocardioides sp.*
157	67	10	*Bacteroidetes*
214	75	3	*Bradyrhizobiaceae*

Conclusion

The microbial communities in the bentonite samples were relatively similar in both samples, although the first one was homogenized commercial material and the second one was raw bentonite sampled directly in the mine; in other words homogenization caused only small differences in the bacterial community structure. Beta- and Alphaproteobacteria dominated in both bentonite samples. *Thiobacillus*, *Gallionella*, *Rhodobacteraceae*, and *Nitrosomonas* capable of oxidizing NH_3, Mn^{2+}, Fe^{2+}, S^{2-} were present in both samples.

Acknowledgements

This work supported by the Euratom research and training programme 2014-2018 under grant agreement No. 661880 (Microbiology in Nuclear Waste Disposal - MIND).

References and Citations

[1] M. Lopez-Fernandez, A. Cherkouk, R. Vilchez-Vargas, R. Jauregui, D.Pieper, N. Boon, Sanchez-Castro and M.L. Merroun, “Bacterial diversity in bentonites, engineered barrier for deep geological disposal of radioactive wastes”, *Environmental Microbiology*.DOI 10.1007/s00248-015-0630-7, 2015.

[2] S. Selenska-Pobell, G. Kampf, K. Flemming, G. Radeva and G. Satchanska, “Bacterial diversity in soil samples from two uranium waste piles as determined byrep-APD, RISA and 16Sr DNA retrieval”, *Antonie van leeuwenhoek,* vol.*79*, pp. 149-161, 2001.

[3] S.E. Dowd, T.R. Callaway, R.D. Wolcott, Y. Sun, T. McKeehan, R.G. Hagevoort and T.S. Edrington, “Evaluation of the bacterial diversity in the feces of cattle using 16S rDNA bacterial tag-encoded FLX amplicon pyrosequencing (bTEFAP)”, *BMC Microbiology*, *8*, 125, 2008.

[4] M.J. Claesson, Q. Wang, O. O’Sullivan, R. Greene-Diniz, J.R. Cole, R.P. Ross and P.W. O’Toole, “Comparison of two next-generation sequencing technologies for resolving highly complex microbiota composition using tandem variable 16S rRNA gene regions”, *Nucleic Acids Research,* vol.*38, No.*22, e200, 2010.

[5] T. Větrovský and P. Baldrian, “Analysis of soil fungal communities by amplicon pyrosequencing: current approaches to data analysis and the introduction of the pipeline SEED”, *Biol Fertil Soils*, vol.49, pp.1027–1037, 2013.

[6] R.C. Edgar, “ UPARSE: Highly accurate OTU sequences from microbial amplicon reads” *Nature Methods*, vol.10, pp. 996-998, 2013.

[7] K. Katoh, G. Asimenos and H. Toh, “Multiple alignment of DNA sequences with MAFFT”, *Methods Mol Biol,* vol*.* 537, pp.39–64, 2009.

Thermo-hydro-mechanical behaviour of compacted MX80 bentonite at 150°C

P. Stratos

Cardiff University, Geoenvironmental Research Centre (GRC)

Abstract

This paper presents the behaviour of compacted MX80 bentonite specimens when they are subjected at thermal and thermohydraulic gradients. The purpose of this work is to develop an improved understanding of heat and moisture movement in unsaturated clay barriers at temperatures above 100°C. Each specimen was statically compacted at 1.65 Mg/m^3 and has dimensions of 300mm height and 100mm diameter. With the aid of a thermohydraulic column cell it was possible to apply boundary conditions that imitate the conditions in an underground repository. For the two on going tests undertaken in this study the applied temperatures were 25°C and 150°C at the top and bottom of each specimen. For applying the hydraulic gradient, water injected from the top of the specimen at a pressure of 600kPa. The test results show that, the temperature along the depth of the specimen stabilized in about 3-10 days whereas the relative humidity did not equilibrate. The exposure of the specimen at thermohydraulic gradient manifested a greater axial stress than that of the thermal gradient.

Introduction

The current concepts for engineered barriers in high-level radioactive waste (HLW) repositories suggest the usage of unsaturated compacted bentonite blocks as a buffer material. Main functions of the buffer are to protect the waste containers from rock movements by being ductile and retard the migration of ground water and radio nuclides in a repository [1]. Bentonite has been widely considered as an engineered buffer material for deep geological disposal of radioactive wastes because of its low permeability, good swelling capacity, chemical buffering capability, etc. The hydrothermal conditions in the repository can trigger physical/chemical processes that affect the favourable properties of the buffer and can decrease its effectiveness to isolate the waste canisters from the biosphere [2].

In order to investigate the behaviour of compacted bentonite when it is subjected at high temperatures and hydraulic pressures a multidisciplinary research programme commenced called SAFE Barriers project (a Systems Approach For Engineered Barriers). The experimental investigation of the thermal, hydraulic, mechanical and chemical behaviour of the bentonite when it is exposed at high thermal and hydraulic gradients and the improvement of existing numerical models for temperatures above the 100°C have been studied at Cardiff University.

Properties of the MX80 bentonite

Laboratory tests were performed on an industrial MX80 bentonite from Wyoming, US acquired by the TOLSA group. MX80 bentonite has a montmorillonite content around 85%. The initial water content of the bentonite was found to be 15.2% at ambient laboratory conditions. The liquid and plastic limits are 439% and 62% respectively.

Experimental device

The thermal and thermohydraulic tests were conducted in a column thermos/hydro/mechanical (THM) test device. The tests were carried out on compacted bentonite specimens. The experimental device used (Fig.1) is able to facilitate both thermal and hydraulic gradients. Three types of measurements can be taken during the testing period. Five relative humidity and temperature probes bored along the depth of the cell made possible to measure the humidity and the temperature along the depth of the bentonite specimen. The generated axial pressure can be measured at the top of the column device with the aid of a load cell and a plunger attached to it.

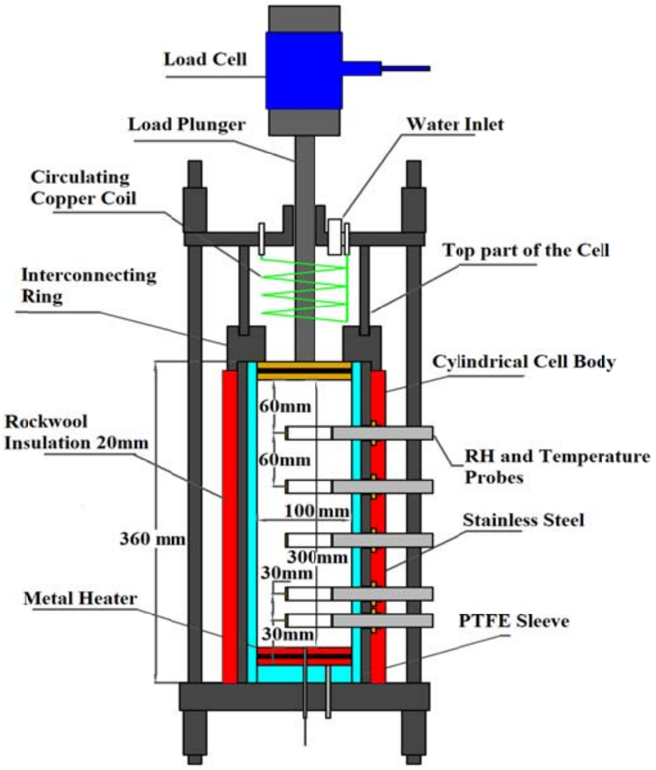

Figure 1: Schematic representation of the thermohydraulic column cell

Figure 2: Experimental set-up

Application of the cell

At first the raw bentonite powder was statically compacted to form specimens with 300mm height and 100 mm diameter. The compaction process took place in the same cell body which was used for the thermal and thermohydraulic tests. The possible extraction and reinsertion of the specimen in a different apparatus could cause rebound effects that would alter the desirable dry density. For the first ten days only thermal gradient applied at both tests. A constant temperatures of 150°C at the bottom end of the specimen applied with the aid of a steel heater. At the top end a constant temperature of 25°C sustained with the aid of a circulating copper coil connected to a heated circulating bath. For the tests subjected to hydraulic gradient, deionized water injected at the top of the specimen with a pressure of 600kPa.

Results and Discussion

Figures. 3, 4 and 5 show the effects of thermal and thermohydraulic gradients on the compacted bentonite specimens. Two tests are described in this section, a thermal and a thermohydraulic test. Both tests subjected on thermal gradient (25 °C at the top end and 150 °C at the bottom end of the specimens) for the first 10 days. The temperature equilibrated along the depth of the specimen within 96 hours. The achieved temperatures were 112, 90, 72, 59 and 49°C at 40, 60, 120, 180 and 240mm from heater respectively. The increased temperature led to an immediate increase of the specimens' relative humidity along their full length. Additionally at the areas closer to the heater (40, 60, and 120 mm from the heater) the relative humidity decreased after 4 days. With the application of thermal gradient the axial pressure at the top end of the specimens increased to a value of 1943 kPa for the thermal test within 21 days and further decreased to non-equilibrate values yet. After 10 days of thermal loading deionized water injected at the top of one of the specimens with a pressure of 600 kPa. The water supply decreased the temperatures within the specimen. The final temperatures were 110, 88, 70, 56 and 45°C at 40, 60, 120, 180 and 240mm from the heater. After a testing period of 80 days the relative humidity hasn't equilibrate yet except of the area at 240mm from heater were due to the water intrusion the relative humidity reached the 100%. The hydraulic gradient increases the axial pressure to a value of 2,386 kPa. The axial pressure equilibrate after 60 days at a value of 2,267 kPa.

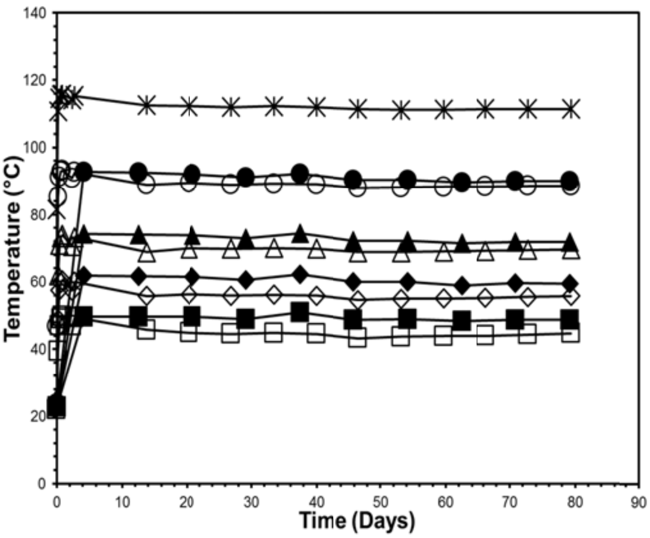

Figure 3: Effects of thermal and thermohydraulic gradients. Temperature variations at specified depths versus time

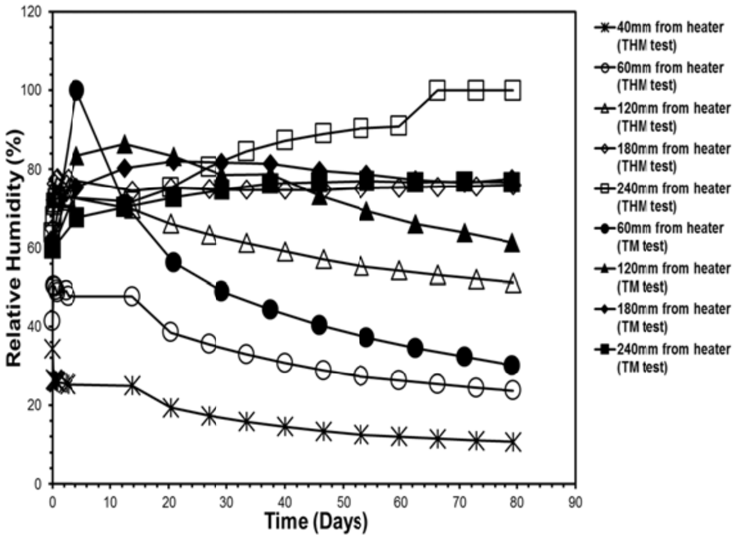

Figure 4: Effects of thermal and thermohydraulic gradients. Relative humidity variations at specified depths versus time

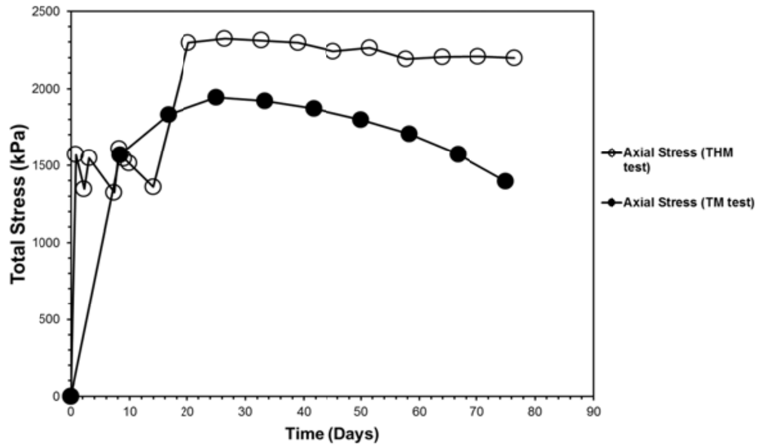

Figure 5: Effects of thermal and thermohydraulic gradients. Axial pressure development versus time.

Conclusions

The behaviour of compacted bentonite when subjected to thermal and thermohydraulic gradients were studied. Compacted MX80 bentonite specimens with dry density 1.65 Mg/m3 were used. The tests' thermal boundary conditions were 25°C at the top end and 150°C at the bottom end of the specimen. The hydraulic gradient achieved with the injection of deionized water was at the top of the specimen with a pressure of 600 kPa. The conclusion drawn from this study are: 1) The temperature in the specimen equilibrates much faster than the relative humidity. 2) Axial pressures were exhibited by both thermal and therohydraulic gradient tests. The axial pressure occurred at the latter test exceeded significantly the pressure recorded during the thermal gradient.

Acknowledgments

The financial support from Engineering and Physical Sciences Research Council (EPSRC), UK and the UK's Radioactive Waste Management Limited (RWM), is gratefully acknowledged. The work presented forms part of the author's PhD studies, supervised by Professor H R Thomas and Dr S Tripathy. Their support and academic guidance is very gratefully acknowledged.

References

[1] Xiaodong L, Prikryl R, Pusch R. THMC-testing of three expandable clays of potential use in HLW repositories. Applied Clay Science. 2011;52:419-27.

[2] Chen Y, Zhou S, Hu R, Zhou C. Estimating effective thermal conductivity of unsaturated bentonites with consideration of coupled thermo-hydro-mechanical effects. International Journal of Heat and Mass Transfer. 2014;72:656-67.

Experimental study of mechanical behaviour of compacted Czech Bentonite 75

Haiquan Sun, David Mašín, Jan Boháč

Institute of Hydrogeology, Engineering geology and Applied Geophysics, Faculty of Science, Charles University in Prague

Abstract

Compacted bentonite is often planned as an engineered barrier material between host rock and canister in nuclear waste disposal repositories thanks to its favourable swelling characteristics and low permeability. This study deals with the effects of initial dry density and vertical stress on the swelling behaviour of compacted bentonite under distill water infiltration. Conventional oedometer tests were carried out on bentonite from Czech Republic named Czech bentonite 75 (B75). One-dimensional swelling tests were performed on compacted bentonite with various initial dry densities to explore the influence of vertical stress and initial dry density on swelling strain. Results show that, for all the swelling deformation tests, the swelling strain decreases with increase of vertical load and decrease of initial dry density. The coefficient of primary and secondary swelling decrease with the increase of vertical stress. The swelling pressure determined by the swell-consolidation method is higher than that by constant volume method.

Introduction

The commercial Czech B75 bentonite extracted from the Cerny vrch deposit (north-western region of the Czech Republic), was used in this study. It is a calcium magnesium bentonite with a montmorillonite content around 60% and initial water content about 10%. Table 1 lists its physical parameters. The plastic limit, liquid limit, specific density of solid soils is 65%, 229%, and 2.87, respectively.

Table 1: The physical parameters of B75 (Stastka et al., 2015)[1]

Property	Description
Montmorillonite (%)	60
Liquid limit (%)	229
Plastic limit (%)	65
Plasticity index Ip	164
Particle density ρs (g/cm3)	2.87

Methods

The conventional oedometer apparatus was used for measuring the swelling deformation of Czech bentonite 75. The compacted bentonite was performed in the standard fixed stainless steel ring, 50 mm inside diameter and 20 mm height. Silicone grease was applied to the inner wall of the stainless steel ring to reduce friction between the specimen and the wall. The filter papers were placed at top and bottom of specimen, and then following the porous stone. Once the compacted bentonite was introduced in the stainless steel ring, the prescribed vertical stress was applied immediately last for several hours until the deformation changed no more than 0.001mm in two hours. Then the distilled water was supplied to the specimen. The vertical deformation and time required from the start of water supplied were recorded. For saturated oedometer test, the loading and unloading test continued after the swelling deformation tests. Eventually, the water content of the specimen was measured. The ASTM D2435/D2435M [2] standard recommends that the oedometer test data should be corrected for oedometer apparatus compressibility. The deflection of the apparatus was measured by substituting a smooth hard steel disk for the soil specimen before the experiment for all the test conditions. The detailed stress paths performed in the experiments presented in Fig.1.

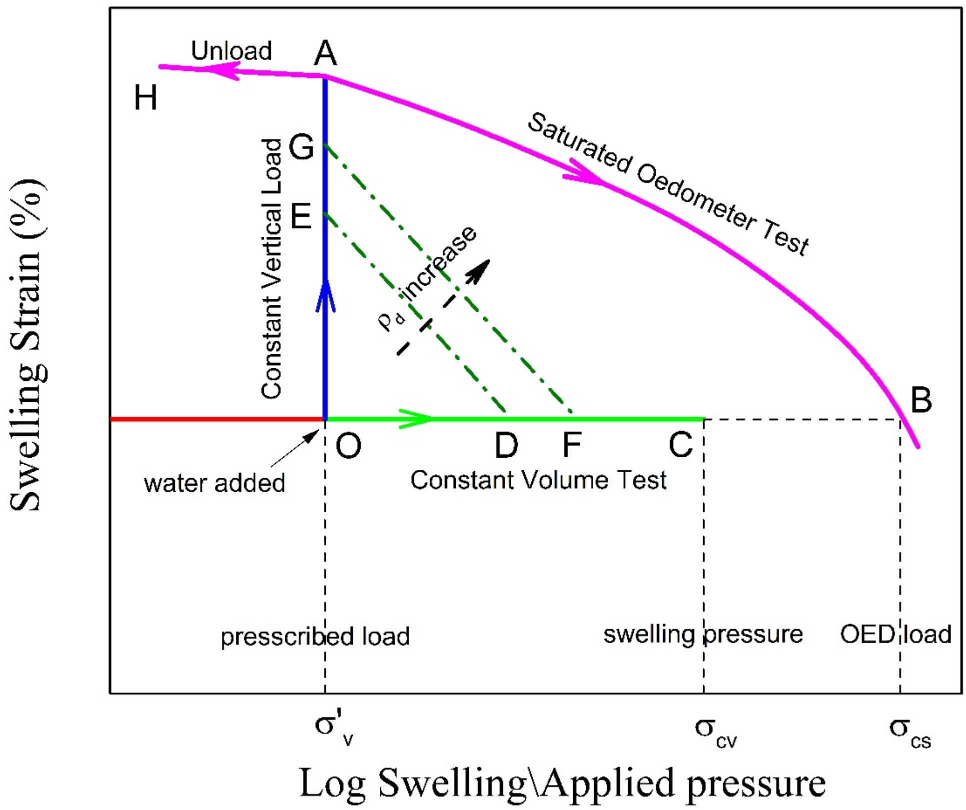

Figure 1: Stress path of various experimental methods used in this research

Results/Discussion

The swelling strain is defined by

$$\varepsilon = \frac{\Delta H}{H_0} \times 100\%$$

Where ε is the swelling strain(%) under prescribed load, ΔH is the measured vertical swelling deformation and H_0 is initial height of specimen before distilled water soaked.

Fig. 2 followed by the method (Sridharan and Gurtug (2004))[3] presents the swelling strain vs. log of time for compacted Czech B75 with initial dry density of 1.25g/cm^3. For all the tests, it can be observed the primary swelling phase starts after about 0.1-0.2h of distill water infiltration. It can be seen that the swelling strain increased rapidly at the initial stages, and it reached the asymptotic level eventually. For dry density ρ_d = 1.25 g/cm^3 with 0.98KPa vertical load (load only with top plate nearly equals to free swell), it will take about 100 hours to reach equilibrium. For 50 KPa, it will need 50 hours. The higher the prescribed load, the shorter is the time required to the equilibrium state.

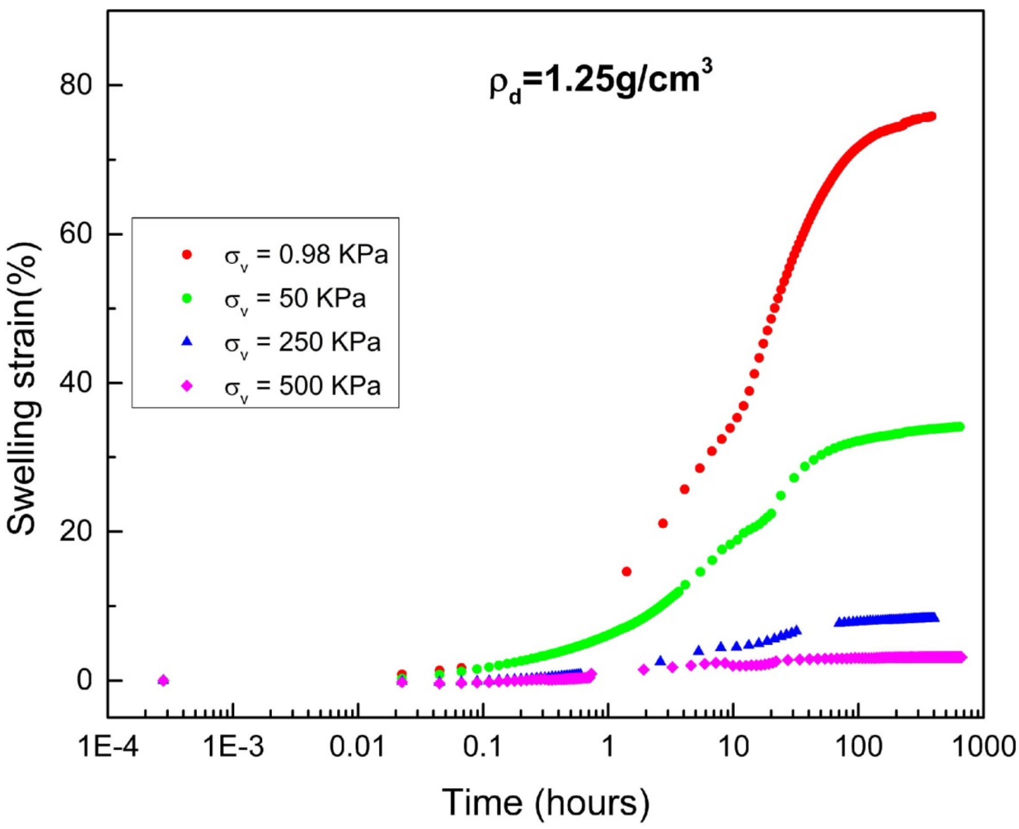

Figure 2: Swelling strain vs. log of time for compacted Czech B75 with initial dry density of 1.25g/cm^3

Conclusion

(1) The swelling strain decreases with increase of vertical load, and increases with increase of initial dry density. The relationship of maximum swelling strain and applied pressure shows a linear function, which position depends on the initial dry density.

(2) The swelling process of an initial stage, primary swelling, and a small secondary stage were observed for all the tests. The coefficient of primary and secondary swelling decrease with the increase of vertical stress.

Acknowledgments

Financial support by the research grant No. 846216 of Charles University Grant Agency is greatly appreciated.

References and Citations

[1] Jan Smutek, 2015, Experimental works with bentonite pellets at the CEG, LUCOEX conference and workshop

[2] ASTM D2435/D2435M-11. 2011. “Standard Test Methods for One-Dimensional Consolidation Properties of Soils using Incremental Loading.” ASTM International: West Conshohocken, PA.

[3] A. Sridharan, Y. Gurtug Swelling behaviour of compacted fine-grained soils Eng. Geol., 72 (1) (2004), pp. 9–18

Sorption of Uranium on Polyamide and Graphen Oxide Composite Material

Z. Tomášová[1], V. Brynych[1], J. Pospěchová[1], P. Ecorchard[2], J. Tolasz[2]

[1]ÚJV Řež, a. s. Waste Management & Fuel Cycle Chemistry Division

Hlavní 130, 250 68 Husinec-Řež, Czech Republic

[2]Department of Materials Chemistry, Institute of Inorganic Chemistry AS ČR v.v.i,

Husinec-Řež č.p. 1001, 250 68 Řež, Czech Republic

Abstract

The new synthesized material has been tested as a potential sorbent of uranium for the purpose of treating the liquid radioactive waste. The sorption batch-experiments were performed on polyamide material. The experiments revealed the ability of polyamide-GO to uptake uranium from the solution.

Introduction

The safe treatment and disposal of uranium, the key element for nuclear energy, is a worldwide environmental concern. Sorption is one of the important methods for treatment of liquid radioactive waste, produced in the nuclear industry. Through sorption processes it is possible to transfer the radioactive contaminants from the liquid into a small volume of solid which can be than handled and disposed as a solid waste [1]. One of the potential solutions is using composite materials based on graphen oxide which previously confirmed their ability to remove radionuclides from solution [2,3]. In the presented study, the new nanocomposite material, polyamide-graphen oxide has been tested for potential use as a sorbent of uranium in radioactive liquid waste.

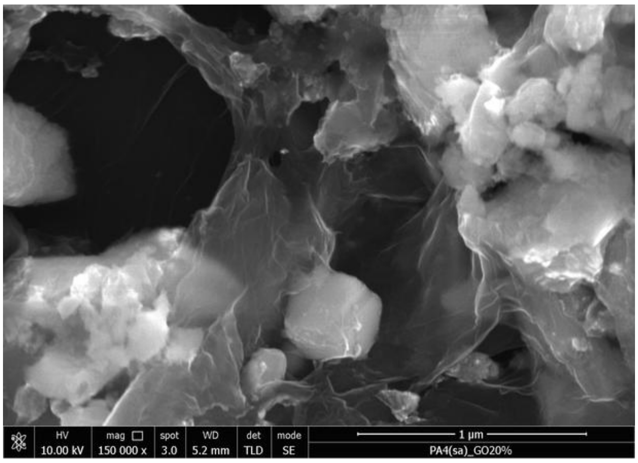

Figure 1: SEM image of synthesized polyamide-GO.

Methods

Preparation of the material

Graphen was prepared from natural graphite by exfoliation in ethylene glycole in high intensity cavitation field and pressure of 5 bar. Graphen sheets were subsequently cleansed by dialysis in destilled water and oxidised to graphen oxide (GO) by modified Hummers method which consist of reaction of graphen with H_2SO_4 H_3PO_4 a H_3PO_4 [4].

For the preparation of the composite polyamide-GO a polyamide PA66 from Sigma-Aldrich s.r.o. was used The commercial PA66 was modified before the reaction with GO in the mixture isopropanol/water in autoclave for 24 hours and the GO water suspension was added at room temperature and mixed for 48 hours. The final product was characterized by scanning electron microscopy (Fig. 1).

Sorption experiments

Batch sorption experiments were performed on polyamide-GO in order to evaluate the sorption properties of the synthesized material. The sorption kinetic was tested by reaction of 1.5 ml of $UO_2(NO_3)_2$ solution with 0.01 g of sorbent for various contact time.

Experiments for determining the sorption isotherms were carried out for defined time, being previously determined using sorption kinetic experiments. 1.5 ml solution volume was shaken in the closed vessels with 0.01 g of the studied material. After stirring, the supernatant was analyzed for U remaining in solution by means of UV spectrophotometry, using Arsenazo III method [5].

Sorption behavior was characterized by distribution coefficient K_d, defined by following relationship

$$K_\mathrm{d} = \frac{C_\mathrm{mass}}{C_\mathrm{volume}} \cdot \frac{V}{m} [\mathrm{mL/g}],$$

where c_{mass} is the concentration of the sorbate adsorbed onto the solid phase, c_{volume} is the concentration of the sorbate in solution, V [mL] is the volume of the liquid phase and m [g] is the mass of the sorbent.

The data were fitted to the Langmuir isotherm as follows:

$$q_\mathrm{e} = \frac{K_\mathrm{L} \cdot q_\mathrm{max} \cdot c_\mathrm{e}}{1 + K_\mathrm{L} \cdot c_\mathrm{e}},$$

where q_{max} is the maximum sorbate uptake [mg/g], K_L is the coefficient [L/mol], c_e is the equilibrium concentration of the solute [mg/L] and q_e is the adsorbed amount of the sorbate on the sorbent [mg/g].

Freundlich isotherm is defined as

$$q_\mathrm{e} = K_\mathrm{F} \cdot c_\mathrm{e}^{\frac{1}{n}}, [\mathrm{mg/g}],$$

where K_F and n are the characteristic constants.

Results/Discussion

The adsorption of uranium on the polyamide-GO occurs during the first few minutes. Fig. 2 (left) shows the dependence of percentage adsorption on contact time for U(VI). On the basis of previous results, a contact time of 24 h was set for subsequent experiments.

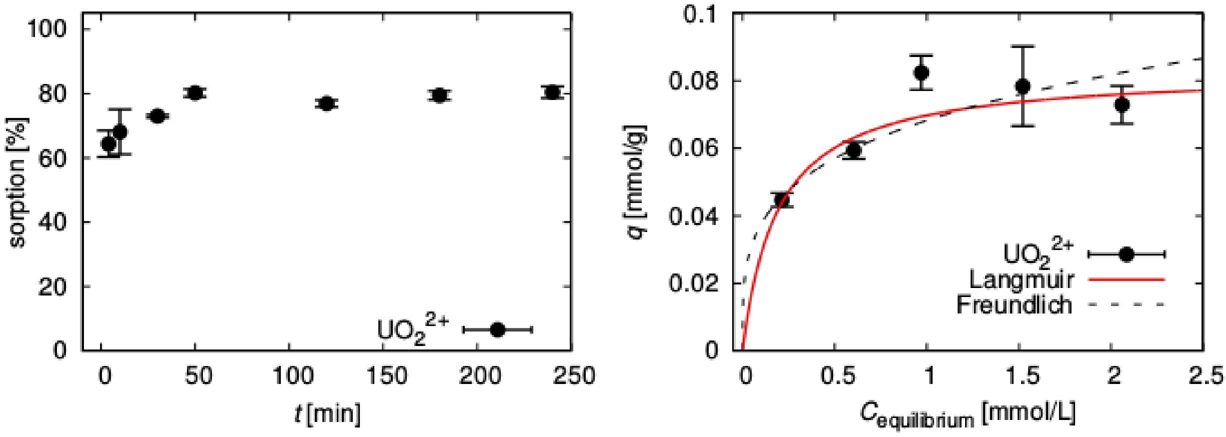

Figure 2: Uranium sorption onto polyamide-GO, sorption kinetics (left), Langmuir and Freundlich isotherm models (right).

The relationship between initial solution concentration and adsorbed amount of uranium is presented in Fig. 2 (right). Sorption of uranium to polyamide-GO is better described by Langmuir model (χ^2 =9.4) then by Freundlich (χ^2 =12). The parameters of the isotherm models are shown in the Table 1. Maximum sorbate uptake calculated from the Langmuir model corresponds to 21.8 mg/g. The distribution of sorbate between the solid phase and solution is described by distribution coefficient K_d 733.9 ml/g.

Table 1: Characteristics of Langmuir and Freundlich isotherm models.

Langmuir		Freundlich	
q_{max}	0.083	n	3.8
K_L	5.3	K_F	0.068

Conclusion

The new synthesized nanocomposite material has been tested as a potential sorbent for uranium. The sorption batch-experiments were performed on polyamide-GO to determine the sorption kinetics and isotherms. The sorption occurs during the first few minutes. The maximum sorbate uptake was calculated from the Langmuir equation and corresponds to 21.8 mg/g.

Acknowledgments

We thank for support from TAČR project no. TA04020222.

References and Citations

[1] International Atomic Energy Agency (IAEA), “Application of Ion Exchange Processes for the Treatment of Radioactive Waste and Management of SpentIon Exchangers”, IAEA Technical Reports Series No. 408, Austria, 2002.

[2] Z. Zhao, J. Li, T. Wen, C. Shena, X. Wang, A. Xu, “Surface functionalization graphene oxide by polydopamine for high affinity of radionuclides”, Colloids and Surfaces A: Physicochemical and Engineering Aspect, No. 482, pp 258-266, 2015.

[3] L. Chen, S. Lu, S. Wu, J. Zhou, X. Wang, “Removal of radiocobalt from aqueous solutions using titanate/graphene oxide composites”, Journal of Molecular Liquids, No. 209, pp. 397-403, 2015.

[4] V. Stengl , “Preparation of Graphene by Using an Intense Cavitation Field in a Pressurized Ultrasonic Reactor”, Chem. Eur. J. 2012, 18, 14047 – 14054

[5] V. I. Kuznecov and S. B. Savin, “Radiokhimiya”, Vol. 2, No. 6, 1960.

Damage model contribution on shape and extension of failure zone in quasi-brittle rocks

Ahmad Pouya[1], Edoardo Trivellato[1,2], Minh Ngoc Vu[2]

[1]: Laboratoire Navier, UMR 8205, École des Ponts, IFSTTAR, CNRS, UPE, Champs-sur-Marne, France
[2]: Andra, Direction de la R&D, 1/7, rue Jean Monnet, 92298 Châtenay-Malabry cedex, France

Abstract

The aim of this work is to investigate the contribution of an elastic-damage model to describe the evolution and asymmetries sometimes noticed in the failure zone around tunnels. The numerical simulations for deep tunnels excavated in the Callovo-Oxfordian claystone showed that a damage mechanics model can explain certain phenomena regarding the localised shape and extension of this excavation-induced failure zone.

Introduction

The excavation of deep tunnels or wells in quasi-brittle rocks creates a damaged area whose shape and extension are important to determine the mechanical and hydraulic properties of the material around these structures. In general, the extension of this zone is estimated from a stress field calculated in elasticity or based on an elastic-plastic calculation ([1], [3]); if the first method does not take into account the redistribution of stresses due to irreversible phenomena, the conventional elastoplasticity modelling seems insufficient to explain the geometry of the failure zone encountered in some cases of deep structures in quasi-brittle rocks. Observations suggest that the phenomena of softening damage are crucial to the development of this zones and must be considered for geotechnical simulations. Even if the parameters of both models can be calibrated to reproduce the same stress-strain curves under load in monotonous compression, these models can lead to different results. Therefore, the near field response around a tunnel is investigated comparing elastoplastic and damage models.

Andra (the French National Radioactive Waste Management Agency) is managing a feasibility study of the impact of a possible high-level and intermediate-level long lived waste disposal in the Callovo-Oxfordian claystone (COx). The Andra Underground Research Laboratory (URL) in Bure (Meuse / Haute-Marne Department, about 300 km East of Paris) is one of the tools used for this mission. Among numerous geotechnical surveys, important investigations on the failure zone around the drifted tunnels are performed. Figure 1 presents the location and plan of the Andra's URL. The in-situ stress state at the main level (-490 m) can be described as follows ([5]): a major horizontal stress σ_H is oriented at N155°E. The vertical stress σ_v is nearly equal to the horizontal minor one $\sigma_h \approx \sigma_v = \rho g Z \approx$ 12 MPa. The ratio σ_H / σ_h has an average value of 1.3.

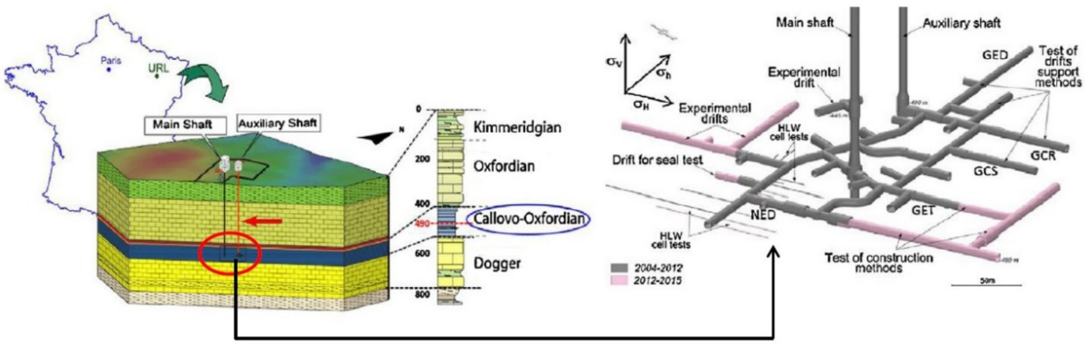

Figure 1: Meuse/Haute-Marne URL: location, geology and drifts network (grey: excavated among 2004-2012, pink: excavated among 2012-2015).

Methods

The simulations presented are performed with the numerical code *Porofis* ([4]) and executed on the geometry presented in Figure 2, representing the tunnel front plane. Firstly, the cavity was also meshed (2a) to produce the isotropic stress state reported in Table 2. Then, the material within was removed to simulate an (instantaneous) excavation (2b), adopting as input the output returned by the previous calculation, thanks to a proper tool developed in *Porofis*. The problem is simulated in plane strain ($\varepsilon_{zz} = 0$), with isotropic linear elasticity (E, ν) before the yielding occurrence, which is modelled according to the Drucker-Prager failure criterion:

$$\sqrt{3J_2} + \sin\alpha\, I_1 - h(K,\xi) = 0 \tag{1}$$

where $\sin\alpha$ and K are the shear strength parameters. In Equation 1 the stresses are expressed in terms of the invariants I_1 and J_2 and the softening law $h(K,\xi)$ varies depending on the elastoplasticity or elastodamage models. The parameters were firstly calibrated by monotonic compression data provided by Andra reproducing the uniaxial compression model in Figure 3.

Results and Discussion

Firstly, a significant overview on the difference among the elastoplastic and the damage model is provided (Figure 2). A localised extension of the failure zone along 4 preferential directions, or *lobes*, is shown for the damage model (4b), compared to the classical circular extension of the plastic zone in the framework of elastoplasticity (4a). Other two simulations are presented adding, in the boundary conditions, the out-of-plane stress σ_{zz} = -16 MPa (according to the in-situ stress state previously described [5]) and introducing a constitutive matrix which allows the damage to develop only in the tunnel front plane and does not affect the excavation axis (out-of-plane direction z) and the variable σ_{zz}. The results obtained (Figure 5) show a non-uniform damage distribution at the tunnel walls (5a), already reported by in-situ observations ([2]). Then, if the problem is modelled with a weaker material, the damage variable may further develop assuming a localised extension and asymmetries (Figure 5b), according to, in principle, the result in Figure 4b.

Table 2: initial stress state before the tunnel excavation.

σ_{xx} [MPa]	-12.0
σ_{yy} [MPa]	-12.0

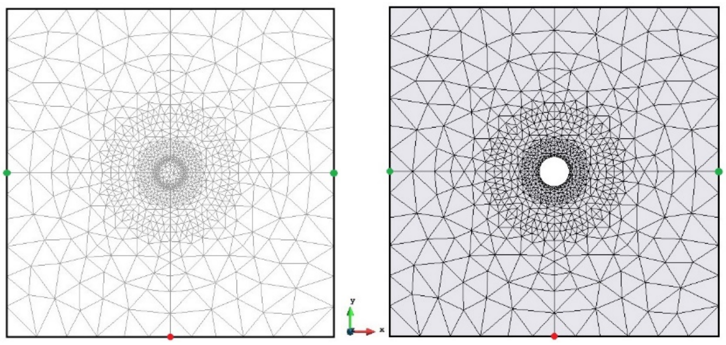

(a) **(b)**

Figure 2: (a, white) mesh adopted for the in-situ stress simulation (pre-excavation stage) and (b, grey) for the tunnel drifting and unloading stage. The red dots represent null displacements along x, the green along y. An isotropic normal stress σ = -12.0 MPa is imposed at the boundaries.

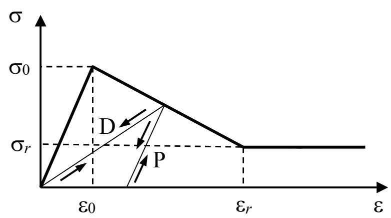

Figure 3: uniaxial stress-strain curve for the elastoplastic (unloading path P) and elastodamage softening model (unloading path D).

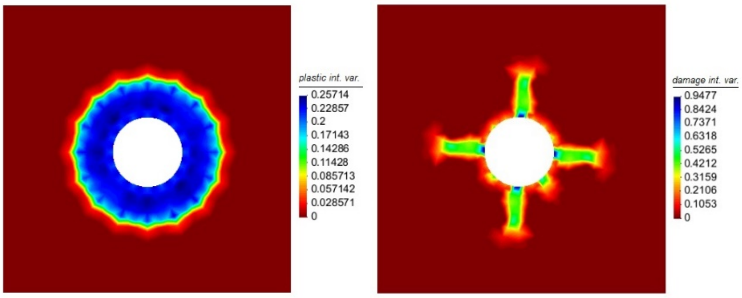

(a) (b)

Figure 4: comparison between the internal variable extension and values for the elastoplastic (a) and damage (b) softening models.

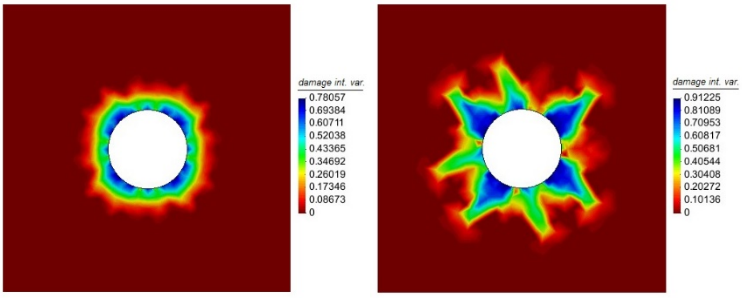

(a) (b)

Figure 5: damage variable extension and values for the elastic-damage configuration with only in-plane damage softening; effects of material weakening from (a) to (b).

Conclusion

The contributions of a damage model are presented to describe the shape and extension of the failure zone around tunnels for brittle rocks, which stress-strain curve under uniaxial compression is modelled with a softening plus residual (constant) function. A first approach to this problem with an elastodamage model leads to different results than those predicted with the traditional elastoplastic framework, taking into account dissymmetry phenomena caused by instability due to softening damage. This is intended as the evolution of a mechanical system where several developments are possible solutions under the effect of the same external load. Some solutions may correspond to stable responses induced by small perturbations, some others may not; this is the same notion of instability deeply studied for the buckling of beams or cylindrical pipe linings. These phenomena occurring for elastic structures can also occur for structures in a geological material with dissipative processes like damage. Nonetheless, other aspects, such as the fabric anisotropy of the material, will be taken into account as further developments of the current research work.

References and Citations

[1] Alonso, E., Alejano, L. R., Varas, F., Fdez-Mańin, G., Carranza-Torres, C., "Ground response curves for rock masses exhibiting strain-softening behaviour", *International Journal for Numerical and Analytical Methods in Geomechanics,* Vol. 27, No. 13, pp.1153-1185, 2003.

[2] Armand G., Noiret A., Zghondi J., Seyedi D.M.,"Short- and long-term behaviors of drifts in the Callovo-Oxfordian claystone at theMeuse/Haute-Marne Underground Research Laboratory", *Journal of Rock Mechanics and Geotechnical Engineering*, Vol. 5, No. 3**,** pp. 221-230, 2013.

[3] Chen R., Tonon F., "Closed-form solutions for a circular tunnel in elastic-brittle-plastic ground with the original and generalized Hoek-Brown failure criteria", *Rock Mechanics and Rock Engineering*, Vol. 44, No. 2, pp.169-178, 2011.

[4] Pouya A., "A finite element method for modelling coupled flow and deformation in porous fractured media", *International Journal for Numerical and Analytical Methods in Geomechanics*, Vol. 39, No.16, pp.1836–1852, 2015.

[5] Wileveau Y., Cornet F.H., Desroches J., Blumling P., "Complete in situ stress determination in an argillite sedimentary formation", *Physics and Chemistry of the Earth*, Vol. 32 , No. 8-14 , pp. 866–878, 2007.

Radiological characterization of graphite from thermal column of VVR-S research reactor in view of intermediary storage

V. Fugaru, C. Postolache, C. Tuca*, M. Dragusin, E. Ionescu and R. Deju

National Institute for Physics and Nuclear Engineering "Horia Hulubei",
30, Reactorului str., RO-077125, P.O.Box: MG-6, Magurele (Ilfov), Romania,

E-mail: vfugaru@nipne.ro

Abstract

Our paper aims to presents the experiments which were performed in order to determine the ^{14}C and ^{3}H accumulation during the functioning time of about 50 years in the thermal column of VVR-S reactor. A new facility and method for determination of tritium (^{3}H or T) and radiocarbon (^{14}C) in incinerable solid wastes are described. The protocol consists of oxidation in two steps of the samples in oxygen atmosphere, HTO and $^{14}CO_2$ kept separately and determination of T and ^{14}C activities at Liquid Scintillation Counter.

Introduction

Isotopes of interest:
^{3}H (pure β^- emitter E_{max} 18 keV) and ^{14}C (pure β^- emitter E_{max} 156 keV);
Secondary target group:
^{36}Cl (β^- E_{max} 708.6 keV/ e^- capture transition X, e^- Auger abundance <2%),
^{63}Ni (pure β^- emitter E_{max} 65.9 keV),
^{55}Fe (γ /X 6 keV (~25% abundance) 7 keV (~3%) e^- Auger 5.2 keV);

Schematic diagram of the experimental set up for ^{14}C and ^{3}H determination in irradiated graphite

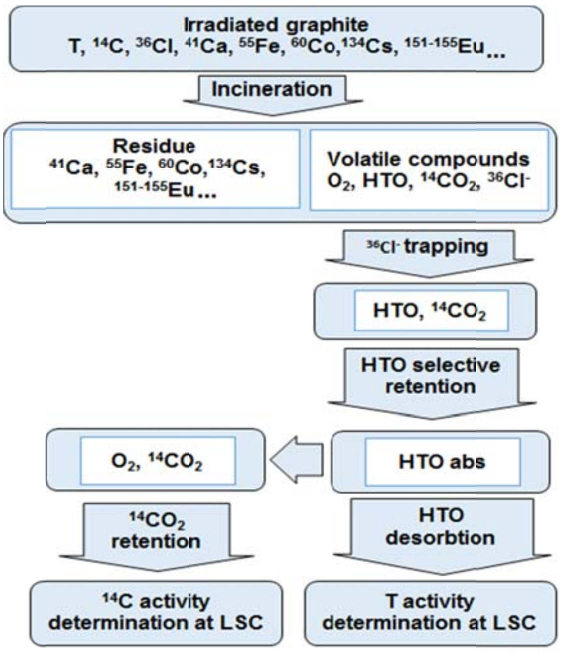

Figure 1: Experimental method for simultaneous determination of ^{3}H and ^{14}C in irradiated graphite

Equipment

The equipment used in the experiment consists in:
- Pressure oxygen tub with pressure regulator and flow control Rota meter
- 2 tube furnace with temperature controller (RT 50-250/11 Nabertherm type), one for graphite oxidation (at 800^0 C temperature) and secondary for catalytic oxidation of resulted gases at water and carbon dioxide. ($700\text{-}800^0$ C in presence of CuO wires or ~ 450^0C in presence of Pt/Alumina catalysts)
- Cooling units for flue gases with two-stage cooling, first with air and secondary using a recycling cooler DLK 40 Lauda type coupled at a Proline thermostat.
- Trapping unit for retention of tritiated water over sicative $CaCl_2$
- Trapping unit for retention of carbon dioxide using Carbo-sorb E+
- Radioactive gas monitor (RGM) with Ionizing Chamber Overhoff type

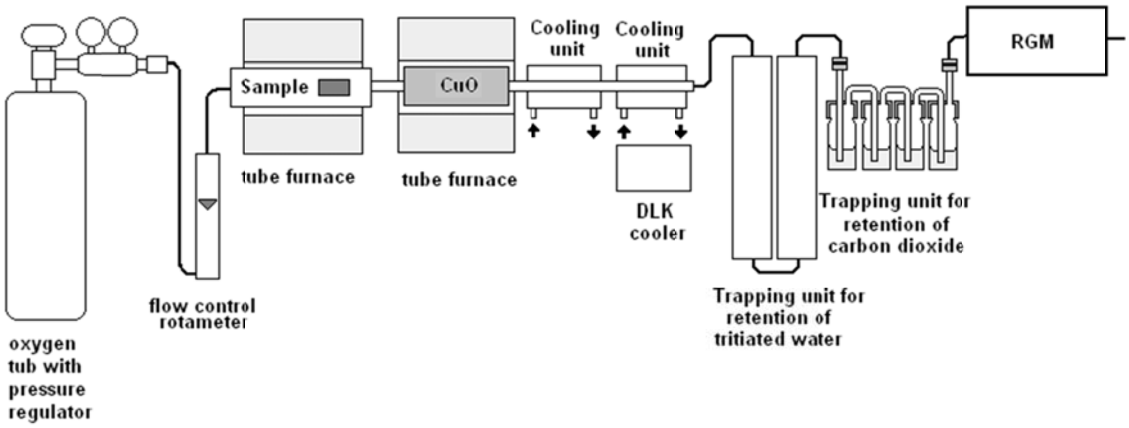

Figure 2: Facility for determination of total T and ^{14}C inside of graphite

Conclusion

An apparatus based on silica gel/ $CaCl_2$ column and oxidation at high temperature over a CuO catalyst, was designed and built for T and ^{14}C determination in irradiated graphite. A preliminary experimental protocol for the combustion of irradiated graphite and retaining separate of T and ^{14}C was established. The retention yield of the oxidation compounds was 98%. T and ^{14}C specific activity distribution in the thermal column of the VVR-S reactor were determined. The first disc of the thermal column of the VVR-S reactor, located near the reactor core, contained over 90% of the total activity of T and ^{14}C.

References and Citations

[1] X. HOU, Radiochemical analysis of radionuclides difficult to measure, for waste characterization in decommissioning of nuclear facilities, J. Radioanal. Nucl. Chem. 273, 43–48 (2007)

[2] X. HOU, Rapid analysis of ^{14}C and ^{3}H in graphite and concrete for decommissioning of nuclear reactor, Appl Rad Izot, 62, 871–882 (2005)

[3] D. ANCIUS and colab., Evaluation of the activity of irradiated graphite in the Ignalina Nuclear Power Plant RBMK-1500 reactor, NUKLEONIKA, 50 (3), 113-120 (2005)

[4] V .Fugaru, C. Postolache, M.R. Ioan, M. Dragusin, ^{14}C determination in irradiated graphite from thermal column of the VVR-S reactor- The 8th Annual International Conference on Sustainable Development through Nuclear Research and Education- May, 27-29,2015, Pitesti, Romania

Radiological characterization of radioactive waste produced in particle accelerators

B. Zaffora[1] and M. Magistris[1]

CERN, European Organization for Nuclear Research, 1211 Geneva 23, Switzerland

Abstract

The operation of high-energy particle accelerators and the associated maintenance and dismantling campaigns lead to the unavoidable production of radioactive waste. Radioactive waste must be characterized radiologically to ensure appropriate disposal in the final repositories. Waste characterization includes establishing the complete list of radionuclides produced, called the “radionuclide inventory”, and a quantitative estimate of their activity. We describe here the process adopted at CERN to characterize low-level radioactive waste.

The characterization process includes:

1. the quantification of Easy-to-Measure (ETM) nuclides, such as gamma-emitters, via nuclear non-destructive analysis,
2. the evaluation of Difficult-to-Measure (DTM) nuclides, such as beta-emitters, using radiochemical and statistical techniques,
3. the estimation of Impossible-to-Measure (ITM) nuclides using Monte Carlo simulations and numerical approaches, where ITM means the measurement of their activity would require unjustified costs and effort.

We support the description with an example of characterization of radioactive waste generated at CERN.

Introduction

In the present summary we briefly describe how to establish a radionuclide inventory and how to quantify the specific activity of significant radionuclides which are produced by activation in particle accelerators. To achieve this goal we developed a statistical method based on the so-called Scaling Factors [1] and Correlation Method [2]. A simplified workflow of the characterization procedure is given in Figure 1.

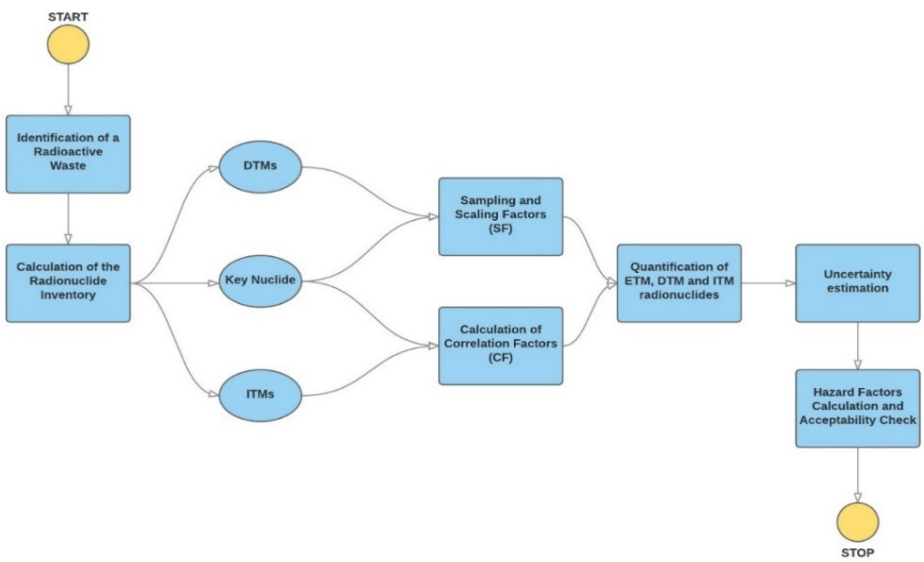

Figure 1: Flow diagram of the characterization process.

The next section introduces the various stages of the characterization process. A waste population of activated Copper is used as an example to illustrate the procedure in the results section.

Methods

At CERN, the first link in the chain leading to the disposal of radioactive waste is the identification of a batch of waste to be eliminated (waste population). We collect the relevant information (waste history and material composition) to build a radionuclide inventory based on potential activation scenarios. An activation scenario is a combination of the chemical composition of the activated material, the beam energy, the position of the waste inside the accelerator tunnel and an irradiation and decay time.

From the radionuclide inventory calculated we extract the list of measurable nuclides, including the reference gamma emitter (KN, Key Nuclide) and identify the nuclides which are Impossible-to-Measure.

The correlation between the activity of a KN and DTMs is assessed by sampling the waste population, by measuring the specific activities of both Key Nuclide and DTMs and by calculating the experimental ratio of their activities: this ratio is called Scaling Factor SF [1] [3]. The correlation between a KN and ITMs is studied using the analytical tool Actiwiz [4], which is based on Monte Carlo simulations performed with Fluka [5] [6]. The calculated ratios of the activities of a KN and ITMs are called Correlation Factor CF [2].

We tested and compared multiple techniques to estimate representative SFs and CFs. The evaluation of Scaling Factors is performed using classical statistical methods such as linear regression or best average content estimators, based on the underlying distribution of SFs. Amongst the available statistical learning methods to estimate representative CFs, we focused on multiple linear models, regression trees and bootstrap aggregation [7]. We finally combined classical and statistical learning approaches to quantify the uncertainty of the overall characterization process.

Results and Discussion

We applied the new characterization approach to activated Copper, packaged in 87 drums (the weight of the waste population is ~8520 kg). The Copper was recovered from signal and power cables dismantled at CERN. After the Copper core was separated from the insulating layers, it was shredded and collected in drums for temporary storage. Limited information was available on the waste's history.

We considered a large number of activation scenarios to estimate the radiological inventory and the distributions of Correlation Factors. The scenarios considered include 14 chemical compositions, 6 beam energies (from 160 MeV of Linac 4 up to 7 TeV of the Large Hadron Collider), 7 locations inside the tunnel of the accelerators (from a position close to the beam line to points beyond shielding walls) and irradiation and decay times spanning from a fraction of the year up to 40 years. This choice is justified by the number of activation mechanisms which are common at CERN, including spallation, thermal neutron reactions and high-energy nuclear reactions with hadrons [8]. Table 1 presents the radionuclides inventory of the waste population, the experimental Scaling Factors and the calculated Correlation Factors.

Table 1: Radionuclide inventory, average SFs and CF of the activated Copper population.

	Half-life (years)	ETM	DTM	ITM
H-3	12.312		0.31 [0.19, 0.50]	
Na-22	2.603	✓		
Ti-44	58.9	✓		
Fe-55	2.73			0.24 [0.22, 0.26]
Co-60	5.271	✓		
Ni-63	100		0.57 [0.24, 1.34]	
Ag-108m	437.7	✓		
Sb-125	2.757	✓		

Amongst the expected ETM, we identified the Co-60 as KN because this nuclide is a gamma-emitter, it is systematically detected on all packages and its half-life is long with respect to the characterization process. The DTMs H-3 and Ni-63 were measured combining radiochemical analysis and liquid scintillation. Table 1 gives the value of the experimental SF calculated as a geometric mean of the measurements above the detection limits. The use of the geometric mean is justified by the log-normal distribution of Scaling Factors. In parenthesis we give the confidence interval at k=1. The DTMs activity $a_{DTM,i}$ in the package *i* is calculated as the product:

$$a_{DTM,i} = SF \times a_{KN,i}$$

where $a_{KN,i}$ is the specific activity of the KN in the package *i*.

The only ITM identified, the Fe-55, is estimated using calculations. Samples were collected to quantify the activity of Fe-55, but its activity was below the detection limits. An alternative technique to estimate ITMs is the Mean Activity Method [1], which consists of applying the average measured activity of Fe-55, including values below the limit of detection, to each waste package.

Table 2 shows a summary statistics of the specific activities of measured ETM (Co-60), calculated DTMs (H-3 and Ni-63) and calculated ITM (Fe-55). The standard errors are used to estimate the overall uncertainty of the characterization process.

Table 2: Specific activities of ETM, DTMs and ITM in the Copper waste population.

	H-3 (mBq/g)	Fe-55 (mBq/g)	Co-60 (mBq/g)	Ni-63 (mBq/g)
Minimum	1.4	1.1	4.6	2.6
Maximum	96.1	74.4	310	176.7
Mean	13.6	10.5	43.9	25.0
Standard Error of Mean (k=1)	1.2	0.9	3.9	2.2

Conclusion

We developed a general method for the radiological characterization of waste produced in particle accelerators, based on the well-known scaling and correlation factor techniques, which are widely used in nuclear power plants. The method consists of:

1. estimating the list of radionuclides produced via Monte Carlo simulations or calculations
2. establishing correlations between a gamma-emitter and difficult or impossible to measure nuclides
3. quantifying the activity of nuclides either by measurement or by using scaling and correlation factors.

The procedure is presently used at CERN to characterize low-level radioactive waste for its disposal towards the French low-level waste repository managed by the French National Agency for Radioactive Waste Management.

The method proposed is of general validity and can easily be extended to other particle accelerators or research centres, where the activation mechanisms are comparable to the ones occurring at CERN.

References and Citations

[1] International Organization for Standardization. ISO 21238, “Nuclear energy - Nuclear fuel technology - Scaling factor method to determine the radioactivity of low- and intermediate-level radioactive waste packages generated at nuclear power plants,” Geneva, 2007.

[2] International Organization for Standardization. ISO 16966, “Nuclear energy - Nuclear fuel technology - Theoretical activation calculation method to evaluate the radioactivity of activated waste generated at nuclear reactors,” Geneva, 2013.

[3] IAEA. Tech. Report No. NW-T-1.18, “Determination and use of scaling factors for waste characterization in nuclear power plants,” Vienna, 2009.

[4] C. Theis and H. Vincke. “Actiwiz - Optimizing your nuclide inventory at proton accelerators with a computer code,” in *ICRS12 Conference*, Nara (Japan), 2012.

[5] G. Battistoni, S. Muraro, P. Sala, F. Cerutti, A. Ferrari, S. Roesler, A. Fasso' and J. Ranft. “The FLUKA code: Description and benchmarking,” in *Proceedings of the Hadronic Shower Simulation Workshop*, Fermilab, 2006.

[6] A. Fasso', A. Ferrari, J. Ranft and P. Sala. “FLUKA: a multi-particle transport code,” CERN-2005-10, INFN/TC_05/11, SLAC-R-773, Geneva, 2005.

[7] T. Hastie, R. Tibshirani and J. Friedman. “The elements of statistical learning: Data Mining, Inference and Prediction,” Stanford, Springer-Verlag, 2009.

[8] M. Barbier. “Induced radioactivity,” North-Holland Publishing Company, Amsterdam, 1969.

PETRUS

EURATOM

European Commission

TU Delft

OPERA